

ABSTRACT

Title of dissertation: ENTANGLEMENT DYNAMICS IN
ATOM-FIELD SYSTEMS

Nicholas I. Cummings, Doctor of Philosophy, 2011

Dissertation directed by: Professor Bei-Lok Hu
Department of Physics

We consider the time evolution of quantum entanglement in the context of interactions between atoms and the electromagnetic field. We explore the influence of interatomic separation and the degree to which this can change the qualitative character of those dynamics, including entanglement generation, protection, and sudden death (SD). We find that the qualitative features of entanglement dynamics can be changed entirely in few-mode models when atomic spacing is varied, allowing for particular choices of configuration that are favorable for maintaining entanglement.

We also examine the inaccuracies introduced by the use of common approximations: We characterize unexpected errors that result from using perturbative master equations as well as those that result from using the rotating-wave approximation (RWA). We find that in dissipative systems the errors introduced by these approximations can lead to an incorrect picture of late-time dynamics. Standard perturbative master equations using the RWA are constrained to predict that late-time SD occurs to only some initial states at zero temperature, but this is merely an artifact of those approximation and generally not correct. The same master equa-

tions predict that at finite temperature all states are separable asymptotically at late times and must undergo SD. In fact a proper accounting of environmentally-induced corrections to the steady state of the system shows that for low temperatures it is possible to have asymptotic entanglement in some cases. We derive a master equation for two atoms interacting with the free field without using the RWA and solve it to obtain the dynamics, including the effects of distance. From these dynamics we find that, in fact, all initial states of atoms separated by any positive distance undergo SD even at zero temperature, though there are sub-radiant states that can be quite long-lived for closely spaced atoms.

ENTANGLEMENT DYNAMICS IN
ATOM-FIELD SYSTEMS

by

Nicholas Immanuel Cummings

Dissertation submitted to the Faculty of the Graduate School of the
University of Maryland, College Park in partial fulfillment
of the requirements for the degree of
Doctor of Philosophy
2011

Advisory Committee:
Professor Bei-Lok Hu, Chair/Advisor
Professor J. Robert Anderson
Professor Christopher Davis
Professor Wendell T. Hill III
Professor Luis Orozco

© Copyright by
Nicholas Immanuel Cummings
2011

Acknowledgments

The path that leads to the end of a dissertation is a long one, so that it's not really possible to thank everyone who has played a role. Here I will mention only a few of those people.

First I owe thanks to my adviser Prof. Bei-Lok Hu, whose dedication to and support of his students is truly exceptional. I thank him for his many years of guidance and support. Many thanks also go to Prof. Luis Orozco, who has provided many opportunities to me during my studies and always treated me with kindness and consideration as though I were one of his students. I offer my gratitude also to the rest of my committee, Prof. J. Robert Anderson, Prof. Christopher Davis, and Prof. Wendell T. Hill III for taking time out of their very busy schedules to serve on the committee and help me improve my work.

I would also like to express my immense appreciation for my collaborators on some of the work presented here, since the results presented represent our combined efforts: My great thanks to Chris Fleming for his clear thoughts and hard work, which was integral to the work presented here. Not only was he my collaborator on the material from chapters 4 and 5, but it was Chris' excellent work on the weak-coupling master equation that set the stage for those calculations. I am also thankful for the opportunity to work with Kanupriya Sinha, who has proved to be a quick study, a gifted physicist, and a dedicated collaborator, and who has also occasionally provided a welcome distraction when needed. Thanks also to Charis Anastopoulos for his keen insights and patient explanations in our work together.

Finally, my gratitude goes to Prof. Perry Rice for his hospitality and for all the things I learned from him when we worked together, and to Tom Shiokawa for his help and advice.

Along with my collaborators, I also owe thanks to many of my fellow students, who taught me many things during our discussions on physics, and who made the process of being a physics student a lot more fun. They include Chuck Sehman, Chris van Breen, Aaron Bodoh-Creed, Donald Engel, Chad Mitchell, Chad Galley, Mike Ricci, Dan and Beth Dakin, Patrick Hughes, Dan Zimmerman, Santiago Triana, and many others.

I would like to give thanks to the people in my personal life who have supported and believed in me. First among them is Sara Mitchell, whose love and support has gotten me through good times and bad and never faltered, and who even helped me proofread some chapters of this dissertation. I also am grateful to my parents. It was my father who first ignited my interest in physics, and both my parents have always helped and supported me through everything. Thanks to my brother Ben and sister-in-law Conner for giving me extra motivation to study by inviting me to parties where people ask physics questions. I owe an extra debt of gratitude to Conner, who was kind enough to help with proofreading. Thanks also go to John, Sally, and Grant Mitchell, who are also always quick to lend a hand or a word of encouragement. Finally, I am grateful to Shonin Anacker for giving me a distraction from work when I needed it and for lending a listening ear when I needed that.

The staff of the physics department also deserve thanks for their help, and I would especially like to extend my gratitude to Bernie Kozlowski, Linda O'Hara,

and Jane Helsing.

Lastly, I would like to thank the Laboratory for Physical Sciences, and in particular Marvin Kruger and Keith Miller. It was the generous support of LPS that made this work possible.

Table of Contents

List of Tables	vii
List of Figures	viii
List of Abbreviations	ix
1 Introduction	1
1.1 Motivation	1
1.2 Open Quantum Systems	5
1.2.1 Markovian and Non-Markovian Dynamics	8
1.2.2 Time-local and Time-Homogeneous Master Equations	10
1.2.3 The Weak Coupling Master Equation	11
1.2.4 Master Equations with Lindblad Form	17
1.3 Atom-Field Interactions	18
1.4 Quantum Entanglement	21
1.4.1 Quantifying Bipartite Entanglement	24
1.4.2 Entanglement Sudden Death	28
1.5 Overview and Summary of Major Findings	30
2 Dynamics of Entanglement Between a Single Atom and the Electromagnetic Field	33
2.1 System and Quantities Under Investigation	36
2.1.1 Hamiltonian and Initial States Considered	36
2.1.2 Methods of Solution	39
2.1.3 Dependence on Initial Conditions	42
2.2 Specific Case Study	44
2.2.1 Single Mode — The Jaynes-Cummings Model	44
2.2.2 Multiple Modes	50
2.2.3 Full Intracavity Field	56
2.3 Summary and Discussion	60
3 Two Atoms with Two Field Modes	64
3.1 The Model	66
3.1.1 Interaction Hamiltonian and Couplings	66
3.1.2 Mapping Equivalent Models and Time Evolution	68
3.2 Entanglement Dynamics	72
3.2.1 Entanglement Generation and Transfer	76
3.2.2 Entanglement Sudden Death and Protection	85
3.2.3 General Spacing and Generic Features	92
3.3 Discussion	94

4	Accuracy of the Weak-Coupling and Rotating-Wave Approximations	101
4.1	Accuracy of Solutions to the Weak-Coupling Master Equation	101
4.1.1	Indeterminacy of Solutions	103
4.1.2	Late-time accuracy	104
4.1.3	Full-time accuracy	108
4.1.4	Time non-local accuracy	110
4.1.5	Example: QBM	111
4.2	The Rotating-Wave Approximation	113
4.2.1	The rotating-wave approximation in closed systems	117
4.2.2	The post-trace rotating-wave approximation	120
4.2.2.1	Correspondence with perturbation theory	122
4.2.2.2	RWA fails when perturbation theory fails	124
4.2.2.3	Combining RWA-Lindblad Equations	126
4.2.2.4	Application to the two-level atom	128
4.2.2.5	Application to quantum Brownian motion	130
4.2.3	The pre-trace rotating-wave approximation	133
4.2.3.1	Inconsistency of approximation	133
4.2.3.2	Noise and the Markovian limit	136
4.2.3.3	Correspondence with perturbation theory	138
4.2.3.4	Non-Markovian nature of the master equation	140
4.2.3.5	Application to the two-level atom	141
4.2.3.6	Application to quantum Brownian motion	141
4.2.3.7	A multipartite example	142
4.2.4	The Effect of Finite Bandwidth	143
4.3	Discussion	146
5	Entanglement Dynamics Beyond the Rotating-Wave Approximation	154
5.1	Weak Coupling, the Rotating-Wave Approximation, and Asymptotic Entanglement Dynamics	154
5.1.1	Asymptotic State for Weak Coupling and a Thermal Reservoir	155
5.1.2	Late-time Entanglement Dynamics of Two Qubits	157
5.2	Two Atoms in a Field Common Field	162
5.2.1	Second-order master equation	164
5.2.1.1	System-environment coupling and correlations	164
5.2.1.2	Master equation form and coefficients	168
5.2.2	Second-order solutions	177
5.2.2.1	Dynamics	178
5.2.2.2	Subradiance	183
5.2.2.3	The Asymptotic State	190
5.2.2.4	Entanglement of Two Atoms and Sudden Death . . .	192
5.2.3	Discussion	195
6	Conclusion	199
	Bibliography	210

List of Tables

3.1	Qualitative classification of entanglement dynamics for two modes with symmetrical coupling ($\phi = 0$) and anti-symmetrical coupling ($\phi = \pi$) for many initial states	75
-----	---	----

List of Figures

2.1	Effect of initial conditions on entanglement	45
2.2	Bloch sphere picture of entanglement dynamics	47
2.3	The dependence of entanglement on the parameters of the single-mode Hamiltonian	49
2.4	Entanglement dynamics with detuning for two field modes	52
2.5	Entanglement dynamics with three and five field modes	55
3.1	Entanglement dynamics for a two-mode squeezed state ($ \xi, 0, 0\rangle$) in the TMSC model	78
3.2	Entanglement dynamics for a single mode squeezed states ($ \xi_s, -\xi_s, 0\rangle$) in the TMAC model	79
3.3	Comparing entanglement dynamics for a two-mode squeezed state vs a thermal state in the DJC model for an initial atomic state $ \Phi\rangle$. . .	80
3.4	Small squeezing entanglement dynamics for a two-mode squeezed state in the DJC model	81
3.5	Comparison of entanglement generation in presence of product single mode squeezed states $ \xi_{sq}, -\xi_{sq}\rangle$ for TMSC and TMAC	82
3.6	Entanglement dynamics in presence of a completely mixed initial field state in SMSC	86
3.7	Entanglement dynamics in vacuum interacting with initially entangled atomic states	87
3.8	Entanglement dynamics for a single mode thermal field interacting with an initially entangled atomic state $ \Phi\rangle$ in the TMSC model . . .	88
3.9	Comparing entanglement dynamics for the initially entangled atomic states interacting with a two-mode squeezed state	90
3.10	Entanglement generation in presence of a coherent state in SMSC . . .	91
5.1	Qualitative plot of an (unmaximized) entanglement	159
5.2	A schematic representation of the evolution in state space and entanglement.	161
5.3	Comparison of environmental kernels for scalar and vector fields . . .	166
5.4	Separation dependence of asymptotic coefficients and renormalization	172
5.5	Time dependence of renormalized coefficients	175
5.6	Decay rates versus separation	180
5.7	Decoherence rates versus separation	180
5.8	Decoherence rates versus separation	181
5.9	Maximal decay rate versus number of atoms	187
5.10	Asymptotic concurrence values versus distance and detuning	194

List of Abbreviations

2LA	two-level atom
AL	“always alive”
BMA	Born-Markov approximation
DI	“death for an instant”
DJC	double Jaynes-Cummings
EMF	electromagnetic field
EOE	entropy of entanglement
JCM	Jaynes-Cummings model
LN	logarithmic negativity
LOCC	local operations and classical communications
posT	post-trace
PPT	positive partial transpose
preT	pre-trace
QIP	quantum information processing
RWA	rotating-wave approximation
SD	sudden death of entanglement
SMSC	single mode symmetric coupling
TMAC	two mode asymmetric coupling
TMSC	two mode symmetric coupling
TMSS	two-mode squeezed state

Chapter 1

Introduction

1.1 Motivation

The last two decades have seen an explosion of interest in uniquely quantum phenomena that rely upon coherent quantum superpositions, quantum correlations, and entanglement. There have been a number of influences driving this explosion; chief among them are the quest to understand the quantum-to-classical transition through the paradigm of environmentally-induced decoherence and the development of quantum information processing (QIP). Quantum entanglement is thought to be of key importance in both these arenas, and as a result an extraordinary effort has been made to characterize entanglement qualitatively, devise methods for quantifying it, and study its dynamical evolution. The aim of this dissertation will be to add to the understanding of that last element, by considering how careful analysis may uncover effects in the dynamics of entanglement overlooked when working under the assumptions predominant in the literature.

While demonstrating correspondence between a new theoretical paradigm and the old one is in some cases relatively straightforward, understanding how classical physics can arise from quantum physics as an emergent phenomenon (or indeed even be in any way consistent) has puzzled physicists since the seminal paper of Einstein, Podolsky, and Rosen [1] and the paradox of Schrödinger's cat [118] up through the

present day. Both of those early works uncovered the unique role of what Schrödinger called Verschränkung, or entanglement. Subsequently, Bell showed [79] that there are scenarios predicted by quantum mechanics which cannot possibly be described by any theory qualitatively similar to classical mechanics (any theory satisfying the criterion of local realism), and again entanglement is central to these puzzles.

While even the modern picture is arguably not entirely complete, understanding of the emergence of classical behavior from quantum physics increased dramatically with the introduction of the paradigm of environmentally-induced decoherence [62, 142]. Under this paradigm, a particular system of interest can attain a quantum state with classical-like features through interaction with a large environment which is then traced out (i.e., ignored degrees of freedom are averaged over). Entanglement plays an important role here as well.

While these considerations are of great theoretical and philosophical interest, QIP is the focus of considerable practical interest, and again quantum entanglement seems to play a key role [95]. Interest in QIP became widespread in 1994 when Shor discovered an algorithm for a quantum computer that allows one to determine the prime factors of a number in a polynomial number of computational steps, exponentially faster than the best known classical algorithm. This was of particular practical significance because the difficulty of this problem underlies the security of public-key encryption [119]. Shor's algorithm utilizes quantum entanglement, so that in order to build a computer capable of carrying out this algorithm one must be able to reliably generate and control quantum entanglement. In addition to Shor's algorithm, quantum computers have been found to be more efficient at solving other

problems of practical interest [66, 95].

Quantum entanglement has also emerged as a key resource for quantum communication. In quantum communication one aims to transfer a quantum state of a system from one location to an identical system at another location. If one initially has a suitably entangled pair of qubits, then it is possible to use those together with classical communication between the two parties to transfer an arbitrary unknown state of another qubit to a distant location in a process known as quantum teleportation [17]. Indeed, it has been shown that any entangled state can improve the efficiency of quantum communication [73]. Among the applied uses of quantum communication is quantum cryptography, where it can be used to distribute shared encryption keys between parties via an untrusted (but authenticated) channel in a provably secure fashion [18].

Atomic systems constitute an important setting for the investigation of quantum decoherence and entanglement phenomena [113, 103] and are very promising for quantum information processing [36, 95, 88]. The physical principles underlying these systems are quite well understood, and it is possible to limit environmental influences greatly, making these systems ideal for theoretical study. This situation contrasts with, for example, solid state models; despite being both interesting and promising for QIP, the underlying mechanisms in solid state models can be much more complex and difficult to understand with environmental influences being stronger and less tractable. Atomic systems can also be controlled and measured with great precision [120, 83, 100, 84, 19, 27, 106, 48, 21, 103, 69, 130]. As a result, we will choose to focus on atoms interacting with electromagnetic fields as the basic

model where we will investigate entanglement dynamics.

Even though atomic systems are more tractable than others theoretically, one must still employ various approximations in order to make predictions about their behavior. While earlier investigations in quantum physics sought to characterize some basic — though not necessarily easily determined — features of quantum systems, such as transition rates and energy spectra, contemporary research seeks to predict much more nuanced features including quantum coherence and entanglement. Therefore, it is fitting that one examines whether the approximations habitually used in those previous calculations are still suitable for determining these details.

This dissertation will explore entanglement dynamics in atom-field systems and specifically how separation between atoms can change the behavior of entanglement. While entanglement dynamics of atoms with position dependence has been studied in the literature before (e.g., [4, 5, 6, 50, 124, 125, 49, 11, 51, 12]), we approach problems in which some usual assumptions can be discarded to get a more complete picture of this phenomenon. We find a great diversity of behavior of entanglement dynamics arising from the dependence on distance, which we examine and classify in a simple model. Moving to more complex models, we show that with low temperature environments the weak coupling master equations generally used will not have the correct late-time behavior and together with the rotating-wave approximation (RWA) they lead to predictions about entanglement dynamics that are incorrect even qualitatively. Finally we improve on previous solutions for the dynamics of two atoms interacting with a common electromagnetic field by deriving

a solution without the RWA and correctly calculate the late-time steady state and entanglement dynamics at zero temperatures, which were misrepresented in previous solutions [49] due to the effects of the weak coupling approximation and RWA.

The following sections will introduce some of the important ideas that underlie the later chapters, and then having discussed those, we will complete this chapter by describing the remaining content of the dissertation and the contributions of this work more specifically.

1.2 Open Quantum Systems

In a closed quantum system, the state of the system is represented by a density matrix (also called a density operator) χ that is a linear operator on the Hilbert space \mathcal{H}_C . The density matrix is Hermitian, positive-semidefinite, and has trace $\text{Tr}[\chi] = 1$. The equation of motion for the density matrix is the von Neumann equation

$$\frac{d}{dt}\chi(t) = -i[\mathbf{H}, \chi(t)], \quad (1.1)$$

so that there is a unitary transformation $U(t)$ giving

$$\chi(t) = U(t)\chi(0)U^\dagger(t). \quad (1.2)$$

Here and throughout this work we will assume units in which $\hbar = c = 1$.

The setting suitable for much of the later discussion is that of an open quantum system. An open quantum system is one in which there is some interaction between the system of interest and some outside environment. Theoretically, one can construct such a situation by starting with a closed quantum system that is

bipartite, composed of two subsystems. One subsystem will be considered the system of interest S , with Hilbert space \mathcal{H}_S , while the other will be considered the environment E , with Hilbert space \mathcal{H}_E , so that $\mathcal{H}_C = \mathcal{H}_S \otimes \mathcal{H}_E$. A measurement of an observable O on only the system S can be predicted using the reduced density matrix of ρ of the system S , which is obtained by coarse-graining out the environmental degrees of freedom. Mathematically, given any orthonormal product basis $|j\rangle_S \otimes |k\rangle_E$ — indexed by some labels j and k — for \mathcal{H}_C , the reduced density matrix is obtained by taking the partial trace over the system degrees of freedom.

$$\rho \equiv \text{Tr}_E [\chi] = \sum_k \langle k|_E \chi |k\rangle_E. \quad (1.3)$$

The resulting operator is independent of the basis in which the trace was taken. The expectation of the observable O is then $\langle O \rangle = \text{Tr} [O\rho]$.

Since the reduced density matrix is obtained directly from the state of the closed system, the evolution of that operator comes directly from the partial trace of Eq. (1.1). Assuming the closed total system has a Hamiltonian $\mathbf{H}_C = \mathbf{H} + \mathbf{H}_E + \mathbf{H}_I$, where \mathbf{H} acts only on S , \mathbf{H}_E on the environment E , and \mathbf{H}_I is the interaction Hamiltonian that couples them together, the equation of motion can be cast in integro-differential form as

$$\frac{d}{dt} \underline{\rho}(t) = -i \text{Tr}_E [[\underline{\mathbf{H}}_I(t), \underline{\chi}(t)]] - \int_0^t \text{Tr}_E [\underline{\mathbf{H}}_I(t), [\underline{\mathbf{H}}_I(s), \underline{\chi}(s)]] ds, \quad (1.4)$$

which is the master equation of the system in the Dirac picture (denoted by the underline). Given an initial prescribed state of the environment this equation specifies the reduced state of the system S at all later times, although the time integral implies that in general there can be memory effects. Assuming that the open-system

dynamics can be solved for a given initial state of the environment, one may define a reduced propagator \mathcal{G} super-operator such that $\rho(t) = \mathcal{G}(t)\rho(0)$.

While Eq. (1.4) in principle gives the evolution of the system's reduced density matrix, one generally seeks to write this equation in terms of the system alone, without direct reference to the total state of the closed system. Generally the details of the full closed system dynamics are unknown in any experiment involving an open quantum system. Furthermore, the setting in which this conceptual framework is most useful is one in which the environment is quite large, most often where it contains a continuum of degrees of freedom, leading to irreversible dynamics such as dissipation. In general it is not possible to find exact master equations for the dynamics of open quantum systems in terms of ρ alone; however, arbitrary-order perturbative master equations (in the system-environment interaction) can be derived in a variety of different ways [81, 25, 122] and find application in many branches of physics and chemistry [112, 32, 26, 82]. Often such derivations additionally make a Markovian approximation, neglecting the history dependence of the evolution that may arise from Eq. (1.4). A system which displays such history dependence is said to be non-Markovian.

Starting from Eq. (1.4), some authors assume an initially separable state $\underline{\chi}(0) = \rho(-) \otimes \rho_E(0)$ (where $\rho_E(0)$ represents the initial state of the environment) and then make the approximation that at later times $\underline{\chi}(s) \simeq \rho(t) \otimes \rho_E(0)$ to obtain the Redfield equation. This approximation is based on the idea that the effect of the system on the environment is small (assuming weak coupling and a large environment). In many cases, the approximation is extended further to what

is called the Born-Markov approximation (BMA) by taking the upper limit of the integral to zero and replacing $\underline{\mathbf{H}}_I(s)$ by $\underline{\mathbf{H}}_I(t-s)$, based on the idea that the only significant contribution to the integral is near $s = t$ due to short bath correlation timescales. This yields the Born-Markov master equation [26],

$$\frac{d}{dt}\underline{\boldsymbol{\rho}}(t) = -i \text{Tr}_E [[\underline{\mathbf{H}}_I(t), \underline{\boldsymbol{\chi}}(t)]] - \int_0^\infty \text{Tr}_E [\underline{\mathbf{H}}_I(t), [\underline{\mathbf{H}}_I(t-s), \underline{\boldsymbol{\rho}}(t) \otimes \underline{\boldsymbol{\rho}}_E(0)]] ds. \quad (1.5)$$

Finally, when dealing with a system bi-linearly coupled to environmental degrees of freedom, many authors make a RWA that neglects terms in the equation of motion that oscillate rapidly in the Dirac picture, which is discussed in detail in Sec. 4.2.

1.2.1 Markovian and Non-Markovian Dynamics

Before going further it is beneficial to get a clearer definition of *non-Markovian*, as the term is applied in a variety of incompatible ways in the mathematics, physics and chemistry literature. In an open quantum system perspective, the environment acts as a stochastic source of noise, of both quantum and classical (thermal) origins, influencing the system. This noise, which imparts fluctuations and dissipation, can be multiplicative when there is nonlinear interaction amongst the constituents in the environment and colored when there is temporal correlation (memory) which reflects the dynamical timescales of the environment (see e.g. [74]). When the effects of a thermal reservoir with quantum mechanical degrees of freedom may be represented by a quantum white noise source, the open quantum system's noise kernel and damping kernel (the dissipation kernel's anti-derivative) will have delta function

correlations. Noise which induces local dissipation will only necessarily have delta correlations for the damping kernel. *Non-Markovian* refers to physical processes with memories. In an open-system framework the influence of the coarse-grained environment can engender non-local noise correlations even with local dissipation *or* in the high temperature regime. White noise only enters at high temperature *and* with local dissipation.

In the *Markovian limit* the timescales of the environment are taken to be much shorter than the timescales of the system. Thus in an open-system perspective one cannot simplistically refer to an environment as Markovian or non-Markovian in isolation from the dynamics of the system which it influences but is measured in reference to. A noise may appear ‘Markovian’ only because its characteristic time scales cannot be resolved by the system. Some authors use the terminology ‘Markovian noise’ or ‘non-Markovian noise’ to describe the **nature** of the noise. We prefer to refer the nature or properties of noise simply as white or colored while reserving the terminology Markovian or non-Markovian for the description of **process** describing the system properties, without or with memory, respectively.

Another common habit is the use of Markovian in reference to the master equation itself, if it is time-local and especially if it is additionally time-homogeneous. This should more correctly be referred to as a *Markovian representation* or simply avoided. Markovian processes produce Markovian representations, but not all Markovian representations arise from Markovian processes. A master equation which arises from a non-Markovian process, even if in Markovian representation, is not sufficient to generate the dynamics of multi-time correlations. By definition,

Markovian processes are governed by the Quantum Regression Theorem in which higher order correlations can be determined from lower order correlations, and ultimately everything can be resolved via the master equation [90, 32, 26]. But with a non-Markovian process there are corrections to the Quantum Regression Theorem [123, 43].

1.2.2 Time-local and Time-Homogeneous Master Equations

A master equation for the reduced density matrix is *time-local* or *convolutionless* if the time derivative of the (reduced) density matrix at a time t is expressed only in terms of the (reduced) density matrix at that time $\rho(t)$ (as opposed to an integro-differential equation depending on the past history of ρ). For any invertible reduced propagator matrix $\mathcal{G}(t)$ such that $\rho(t) = \mathcal{G}(t)\rho(0)$, the time-nonlocal master equation

$$\frac{d}{dt}\rho(t) = \int_0^t d\tau \mathcal{K}(t-\tau)\rho(\tau), \quad (1.6)$$

can be cast as an equivalent time-local master equation

$$\frac{d}{dt}\rho(t) = \mathcal{L}(t)\rho(t), \quad (1.7)$$

where $\mathcal{L}(t) = \frac{d}{dt}\mathcal{G}(t)\mathcal{G}(t)^{-1}$ trivially, and in this case as the kernel $\mathcal{K}(t-\tau)$ is stationary, $\mathcal{G}(t)$ is given formally by a Laplace transformation and the time-local master equation is fully determined therefrom. Note that while both master equations generate equivalent dynamics, (1.7) is Markovian only in *representation*, unless the kernel $\mathcal{K}(t-\tau)$ is delta correlated, in which case \mathcal{L} is constant in time. Essentially one finds integrals over the system's history within the time-local master

equation coefficients, which manifests through their full time dependence. A brief discussion of the behaviors of the two formalisms after application of perturbation theory can be found in [24].

The class of time-dependent time-local master equations is distinguished from the class of master equations with constant coefficients (such as the familiar Lindblad master equation) on the one hand and the time-nonlocal (integro-differential) equations on the other hand. The latter form is often encountered in a projection operator formalism with little or no coarse-graining of the environment. (See, e.g. [144]). As explicitly demonstrated by the above Eqs. (1.6)-(1.7) a master equation can be time-local and generate non-Markovian dynamics. This occurs, for example, in the second-order master equation [81, 25, 122]. A well-known example is the Hu-Paz-Zhang master equation [74, 56] where the coefficients are obtained from solutions of integro-differential Langevin equations; the non-Markovian features manifest in the nonlocal dissipation arising from the back-action of the environment with colored noise on the system. While the non-Markovian nature of the master equation may not be evident in its time-local representation the non-Markovian character is encoded in the time dependence of the coefficients and should be apparent when examining multi-time correlations.

1.2.3 The Weak Coupling Master Equation

As we have said, perhaps the most common way to derive an approximate open-system master equation is by assuming the system-environment coupling to

be weak. Systems weakly coupled to an environment, where dissipation and decoherence may be consequently weak, are a natural context to examine the coherent quantum phenomena that we are interested in. As we have mentioned, there are many different approaches to deriving a weak-coupling master equation [81, 25, 122]. We will follow the systematic approach of Fleming [31] for its clarity and also the attention to issues of accuracy and late-time stability, and we will rely heavily on the many useful and general results about open quantum system dynamics from that work. We now state some main results of that general framework.

First define a Dirac picture in terms of the free (i.e., uncoupled) evolution propagator \mathcal{G}_{CF} for the closed system, so that the propagator for the full, closed system becomes

$$\underline{\mathcal{G}}_{\text{C}}(t) = \mathcal{G}_{\text{CF}}^{-1}(t) \mathcal{G}_{\text{C}}(t), \quad (1.8)$$

and the portion of the Liouvillian of the closed system due to the interaction Hamiltonian

$$\mathcal{L}_{\text{CI}}\chi \equiv -i[\mathbf{H}_I, \chi] \quad (1.9)$$

becomes

$$\underline{\mathcal{L}}_{\text{CI}}(t) = \mathcal{G}_{\text{CF}}^{-1}(t) \mathcal{L}_{\text{CI}}(t) \mathcal{G}_{\text{CF}}(t). \quad (1.10)$$

Given that

$$\frac{d}{dt} \underline{\mathcal{G}}_{\text{C}}(t) = \underline{\mathcal{L}}_{\text{CI}}(t) \underline{\mathcal{G}}_{\text{C}}(t), \quad (1.11)$$

one may take the partial trace over the environment and write a Neumann series

$$\underline{\mathcal{G}}(t) = \mathbf{1} + \int_0^t d\tau_1 \text{Tr}_E [\underline{\mathcal{L}}_{\text{I}}(\tau_1)] + \int_0^t d\tau_1 \int_0^{\tau_1} d\tau_2 \text{Tr}_E [\underline{\mathcal{L}}_{\text{I}}(\tau_1) \underline{\mathcal{L}}_{\text{I}}(\tau_2)] + \dots, \quad (1.12)$$

for the Dirac-picture reduced-system propagator $\underline{\mathcal{G}}(t)$ that is perturbative in the system-environment coupling. For the reduced system we have $\mathcal{L}(t) = \left[\frac{d}{dt}\underline{\mathcal{G}}(t)\right] \underline{\mathcal{G}}^{-1}(t)$, so that Eq. (1.12) leads to a perturbative series for $\mathcal{L}(t)$. Assuming the odd moments of the bath vanish (as with Gaussian noise), the odd orders of the perturbative expansion vanish, and one has

$$\mathcal{L}(t) = \mathcal{L}_{[2]}(t) + \mathcal{L}_{[4]}(t) + \dots \quad (1.13)$$

with

$$\mathcal{L}_{[2]}(t) = \int_0^t d\tau \text{Tr}_E [\underline{\mathcal{L}}_{\text{CI}}(t) \underline{\mathcal{L}}_{\text{CI}}(\tau)] , \quad (1.14)$$

assuming a stationary reservoir and time-independent Hamiltonian.

Given a stationary system Hamiltonian and stationary bath correlations, Gaussian noise distributionals (e.g. noise generated via linear coupling to an environment of harmonic oscillators) *may* allow the master equation to have a stationary late-time limit [53]

$$\mathcal{L}(\infty) = \lim_{t \rightarrow \infty} \mathcal{L}(t) , \quad (1.15)$$

so that the late-time and weak-coupling limits commute; otherwise perturbation theory cannot be used for long durations of time. Gaussian noise processes are categorized by their second-order noise correlation, and whether or not the master equation will have a stationary limit is dependent upon how localized this noise correlation is. Well-localized noise correlations (e.g., Gaussian or exponential) can lead to a very well-behaved master equation, whereas long-ranged noise correlations (e.g. Cauchy) can produce a more pathological master equation which cannot be

accurately analyzed in a perturbative fashion. Exact examples of this phenomena are given in Ref. [56] in the context of quantum Brownian motion with Ohmic and sub-Ohmic couplings. Moreover, the exact solutions $\boldsymbol{\rho}(t)$ can be very well-behaved even if $\mathcal{L}(t)$ is not. Markovian representations (and, more generally, effective equations of motion) are not always suitable.

Having a perturbative expansion for the Liouvillian and Eq. (1.14) gives the lowest-order correction to the uncoupled dynamics, which is second order in the system environment coupling. We will call this second-order master equation the weak-coupling master equation. Assume that the system-environment interaction Hamiltonian takes the form

$$\mathbf{H}_I(t) = \sum_n \mathbf{L}_n \otimes \mathbf{l}_n, \quad (1.16)$$

with Hermitian system coupling variables \mathbf{L}_n coupled bilinearly to collective environment coupling variables \mathbf{l}_n . Without loss of generality, these variables can be assumed to have vanishing diagonals in the energy basis of the free system, since any diagonal portion of the coupling would commute with the free bath Hamiltonian and could be effectively absorbed into the free system Hamiltonian at second order.

With these assumptions, the second-order master equation can be expressed

$$\mathcal{L}_{[2]} \boldsymbol{\rho} = \sum_{nm} [\mathbf{L}_n, \boldsymbol{\rho} (\mathbf{A}_{nm} \diamond \mathbf{L}_m)^\dagger - (\mathbf{A}_{nm} \diamond \mathbf{L}_m) \boldsymbol{\rho}], \quad (1.17)$$

where in the basis of energy states of the uncoupled system $|\omega_i\rangle$

$$\langle \omega_i | \mathbf{A}_{nm} \diamond \mathbf{L}_m | \omega_{i'} \rangle = \langle \omega_i | \mathbf{A}_{nm} | \omega_{i'} \rangle \langle \omega_i | \mathbf{L}_m | \omega_{i'} \rangle, \quad (1.18)$$

with the \mathbf{A}_{nm} operator defined

$$\langle \omega_i | \mathbf{A}_{nm} | \omega_{i'} \rangle \equiv A_{nm}(\omega_{ii'}) , \quad (1.19)$$

$$A_{nm}(t; \omega) = \int_0^t d\tau \alpha_{nm}(t, \tau) e^{-i\omega(t-\tau)} , \quad (1.20)$$

and $\omega_{ii'} = \omega_i - \omega_{i'}$. If the correlation function is sufficiently localized in time, then these coefficients will have a stationary limit.

One can try to solve the weak-coupling master equation exactly, but given that it is of only perturbative accuracy, an equally accurate answer can be obtained by solving the open-system master equation in a perturbative fashion. To do this one seeks a solution to the eigenvalue problem

$$\mathcal{L} \mathbf{o} = f \mathbf{o} , \quad (1.21)$$

where \mathbf{o} is a Hilbert-space eigen-operator and f is its corresponding eigen-value. We already know the zeroth-order solutions

$$\mathcal{L}_{[0]} |\omega_i\rangle\langle\omega_j| = -i\omega_{ij} |\omega_i\rangle\langle\omega_j| . \quad (1.22)$$

We then have the perturbative expansions

$$\mathcal{L} = \mathcal{L}_{[0]} + \mathcal{L}_{[2]} , \quad (1.23)$$

$$\mathbf{o}_{ij} = |\omega_i\rangle\langle\omega_j| + \mathbf{o}_{ij}^{[2]} + \dots , \quad (1.24)$$

$$f_{ij} = -i\omega_{ij} + f_{ij}^{[2]} + \dots . \quad (1.25)$$

An important point in thinking about solving the master equation perturbatively is that for an N -dimensional Hilbert space the problem is always (at least) N -fold degenerate, since $\omega_{jj} = 0$ for all j . Perturbation theory tells us that the

second-order corrections to all eigenvalues and eigenoperators of \mathcal{L} outside the degenerate subspace — these operators will be purely off-diagonal in the energy basis at zeroth order — are given by:

$$f_{ij}^{[2]} = \langle \omega_i | \mathcal{L}_{[2]} \{ |\omega_i\rangle\langle\omega_j| \} | \omega_j \rangle , \quad (1.26)$$

$$\langle \omega_{i'} | \mathbf{o}_{ij}^{[2]} | \omega_{j'} \rangle = \frac{\langle \omega_{i'} | \mathcal{L}_{[2]} \{ |\omega_i\rangle\langle\omega_j| \} | \omega_{j'} \rangle}{-i(\omega_{ij} - \omega_{i'j'})} . \quad (1.27)$$

As is usual in degenerate perturbation theory, to compute corrections to eigenvalues and eigen-operators from the degenerate subspace, we must diagonalize \mathcal{L} in the degenerate subspace. The associated characteristic equation can be written

$$\mathbf{W} \vec{\sigma} = f \vec{\sigma} , \quad (1.28)$$

$$\llbracket \vec{\sigma} \rrbracket_i \equiv \langle \omega_i | \mathbf{o} | \omega_i \rangle , \quad (1.29)$$

where $\vec{\sigma}$ denotes the degenerate-subspace projection of \mathbf{o} represented as a vector, i.e. diagonal entries of the eigen-operator while in the free energy basis, and \mathbf{W} if defined as

$$\llbracket \mathbf{W} \rrbracket_{ij} = \langle \omega_i | \mathcal{L} \{ |\omega_j\rangle\langle\omega_j| \} | \omega_i \rangle , \quad (1.30)$$

which is the degenerate-subspace projection of \mathcal{L} — i.e., master-equation super-operators which map diagonal entries to diagonal entries — represented as a matrix. Thus, \mathbf{W} in essence gives the Pauli master equation [32]. It will turn out that computing the $\mathbf{o}^{[2]}$ for the degenerate subspace is problematic, which we explore later in Sec. 4.1. Once we have solved the eigensystem perturbatively, however, the solution to the master equation is merely

$$\rho(t) = \sum_{ij} c_{ij} \sigma_{ij} e^{f_{ij}t} , \quad (1.31)$$

with the constants c_{ij} determined by $\boldsymbol{\rho}(t)$.

1.2.4 Master Equations with Lindblad Form

When the environment in an open system can be represented by a quantum white noise the master equation has time-local coefficients and assumes a *Lindblad form*:

$$\frac{d}{dt}\boldsymbol{\rho} = -i[\mathbf{H} + \mathbf{V}, \boldsymbol{\rho}] + \mathcal{D}\{\boldsymbol{\rho}\}, \quad (1.32)$$

$$\mathcal{D}\{\boldsymbol{\rho}\} \equiv \sum_{nm} \mathcal{D}_{nm} \left(\mathbf{e}_n \boldsymbol{\rho} \mathbf{e}_m^\dagger - \frac{1}{2} \{ \mathbf{e}_m^\dagger \mathbf{e}_n, \boldsymbol{\rho} \} \right), \quad (1.33)$$

where \mathbf{H} is the Hamiltonian of the free system and \mathbf{V} is a correction introduced by the environment, not necessarily to be renormalized in its entirety as it may contain nontrivial features such as diffusion components. \mathcal{D} is the “dissipator” super-operator: \mathcal{D}_{nm} is a positive-definite and Hermitian coefficient matrix and \mathbf{e}_n denotes a particular (operator) basis of representation for the dissipator.

Lindblad’s theorem categorizes the algebraic generators \mathcal{L}_a for all completely-positive maps $e^{s\mathcal{L}_a}$, wherein $s > 0$ parameterizes the semi-group [93, 65]. Such algebraic generators and the dynamics arising when the Liouvillian appearing in the master equation has Lindblad form have been extensively studied [87, 40, 41, 42, 7, 3, 14, 76, 94, 132]. In general, however, the time-translation generator \mathcal{L}_t that appears in the master equation is not constant in time, so that it is not equivalent to the algebraic generator. In this case the dynamical maps are given by time-ordered products of the exponentials $e^{dt\mathcal{L}_t}$, and not necessarily of the Lindblad form. But following the generalization of Choi’s theorem on merely Hermitian-preserving maps

[34], one can quickly prove that any Hermitian and trace-preserving master equation of analogous time-local form must have a *pseudo-Lindblad form*, i.e. the form of Eq. (1.33) but with merely Hermitian \mathcal{D}_{nm} .

Therefore the Lindblad equation classifies all completely-positive master equations without any time dependence in their coefficients; completely positive master equations which are merely asymptotically constant in time are not restricted to Lindblad form, even in the weak (but non-vanishing) coupling limit. See [74, 56] for a specific example, both exactly and perturbatively. Furthermore, a Markovian representation of the master equation, i.e. a time-local \mathcal{L}_t , does not necessarily indicate Markovian dynamics, as expanded upon in Sec. 1.2.2.

1.3 Atom-Field Interactions

Given that atomic physics is a good context in which to study coherent quantum phenomena, we will repeatedly discuss the quantum physics of a set of atoms interacting with a quantized electromagnetic field. We will work in the setting of non-relativistic quantum field theory. The simplest way to formulate this approach is to imagine the field confined to some volume V . Then, subject to the boundary conditions, the field may be decomposed into normal modes. Second quantization transforms these modes into a set of quantum harmonic oscillators.

Atomic physics is attractive to the theorist in part because the interaction between light and matter is so well studied and understood. However, as with most problems in Physics a full treatment of the exact model would be intractably com-

plex. So we will follow much of the literature and adopt a relatively simplistic model of the atom as a two-level system. This two-level atom (2LA) represents two energy levels of the atom, which have an associated energy splitting given by the frequency Ω . Modes of the electromagnetic field (EMF) will significantly excite a transition between these levels provided that they have a similar frequency; thus, although the atom may have many levels, the others can be neglected provided they are not excited initially and none of the field modes resonant with those transitions are excited. Additionally, we will make the dipole approximation, in which the spacial extent of the atom is assumed to be small compared to the resonant wavelength, in which case the interaction will be dominated by the electric dipole moment associated with the transition. The basis of these approximations has been extensively treated [6, 38].

We will consider the interaction between a collection of 2LAs and an EMF decomposed in terms of normal modes with the aforementioned approximations. We will additionally assume throughout that the center of mass of each atom does not move significantly, and the j^{th} atom can be considered to have a fixed location \vec{R}_j . This will be a reasonable model in situations where the atoms are strongly confined (compared to the resonant wavelength). To simplify calculations somewhat we will also assume that the atomic transition in each atom will produce linearly polarized photons (i.e., both ground and excited state are eigenstates of some component of angular momentum with the same eigenvalue).

The free Hamiltonian for the atom-field system is

$$\mathbf{H}_0 = \left(\sum_j \Omega_j \boldsymbol{\sigma}_{+j} \boldsymbol{\sigma}_{-j} + \sum_{q,s} \varepsilon_{q,s} \mathbf{a}_{q,s}^\dagger \mathbf{a}_{q,s} \right). \quad (1.34)$$

where Ω_j is the transition frequency of the j^{th} atom, $\boldsymbol{\sigma}_{+j}$ and $\boldsymbol{\sigma}_{-j}$ are the raising and lowering operators for the two-level system representing that atom, and $\varepsilon_{q,s}$ is the frequency of the q^{th} normal mode with polarization indexed by s . With all of the approximations specified, the atom-field interaction Hamiltonian becomes

$$\mathbf{H}_I = \sum_j \sum_q \boldsymbol{\sigma}_{x_j} (g_{j,q,s} \mathbf{a}_{q,s} + g_{j,q,s}^* \mathbf{a}_{q,s}^\dagger), \quad (1.35)$$

where $\boldsymbol{\sigma}_{x_j}$ is the Pauli matrix for the j^{th} atom. The coupling constants $g_{j,q}$ are defined by

$$g_{j,q} \equiv -i d_j \vec{e}_{d,j} \cdot \vec{f}_{q,s} \left(\vec{R}_j \right) \frac{\Omega_j}{\sqrt{2\epsilon_0 \varepsilon_{q,s} V}}, \quad (1.36)$$

where d_j is the complex dipole matrix element for the transition in the j^{th} atom, the dipole moment has a direction $\vec{e}_{d,j}$, and $\vec{f}_{q,s}(\vec{r})$ is the classical electric field mode function for the q^{th} normal mode [6, 47].

In addition to the approximations already made, very often in atomic physics one makes the RWA. As we will discuss in Ch. 4, there are, in fact, two distinct forms of the RWA in use [6], but perhaps most common in atomic physics discussions is the form in which the interaction Hamiltonian is cast in the Dirac picture and the rapidly oscillating terms are neglected. If $\boldsymbol{\sigma}_{x_j}$ is written in terms of $\boldsymbol{\sigma}_{+j}$ and $\boldsymbol{\sigma}_{-j}$, then the terms containing $\boldsymbol{\sigma}_{+j} \mathbf{a}_{q,s}$ and $\boldsymbol{\sigma}_{-j} \mathbf{a}_{q,s}^\dagger$ will oscillate with frequency $\Omega_j - \varepsilon_{q,s}$ while the terms containing $\boldsymbol{\sigma}_{-j} \mathbf{a}_{q,s}$ and $\boldsymbol{\sigma}_{+j} \mathbf{a}_{q,s}^\dagger$ will oscillate with frequency $\Omega_j + \varepsilon_{q,s}$. For modes close to resonance $|\Omega_j - \varepsilon_{q,s}| \ll \Omega_j + \varepsilon_{q,s}$. On that basis, the terms with

$\sigma_{-j} \mathbf{a}_{q,s}$ and $\sigma_{+j} \mathbf{a}_{q,s}^\dagger$ (often called the counter-rotating terms) are dropped, leaving one with the perhaps more familiar interaction Hamiltonian

$$\mathbf{H}_I = \sum_j \sum_q g_{j,q,s} \sigma_{+j} \mathbf{a}_{q,s} + g_{j,q,s}^* \sigma_{-j} \mathbf{a}_{q,s}^\dagger. \quad (1.37)$$

Physically, the meaning of this approximation lies in the fact that it ensures that the free and interaction Hamiltonians commute, so that the energy according to the free Hamiltonian is still conserved in the interacting theory. For this reason, the dropped terms are also sometimes referred to as energy-non-conserving terms.

1.4 Quantum Entanglement

As we have already mentioned, entanglement is a unique property of quantum systems, which can be used as a resource for certain sorts of tasks. We will now give a brief overview of its properties, which can be found in more depth in, for example, [73]. For pure states, entanglement is relatively easily defined: any quantum state of a multipartite system — comprised of several subsystems — that cannot be factorized into a tensor product of states for the individual subsystems is called entangled. For example, the state

$$|\Psi\rangle = \frac{1}{\sqrt{2}} (|\psi\rangle_A \otimes |\phi\rangle_B + |\xi\rangle_A |\zeta\rangle_B) \quad (1.38)$$

for systems A and B will be entangled so long as $|\psi\rangle$ is linearly independent from $|\xi\rangle$ and $|\phi\rangle$ is linearly independent from $|\zeta\rangle$. If a state is not entangled then it is said to be separable and can be cast in the form

$$|\Psi\rangle = |\psi\rangle_A \otimes |\phi\rangle_B. \quad (1.39)$$

For separable pure states the outcomes of any measurements on the two subsystems are statistically independent, while for an entangled state they will have correlations. Classically there would have to be a probability distribution describing an ensemble of possible states of the system in order for there to be correlations, but in the quantum context the correlations can exist even when the global state of the system is specified uniquely.

The predominant way of thinking about quantum entanglement has become the paradigm of local operations and classical communications (LOCC) [95, 111, 73]. The physical picture appropriate to this approach is one of several distant laboratories attempting to accomplish various tasks using quantum operations performed locally in each laboratory individually, classical communications between laboratories to coordinate, and some shared multipartite quantum states. The entanglement of that shared state is then assessed as its utility as a resource for performing tasks that could not be performed by LOCC alone, which are sometimes referred to as “nonclassical tasks”. From this perspective, it then becomes clear how to generalize the definition of entanglement to mixed states.

Given initially uncorrelated systems A and B , LOCC can be used to produce only states of the form

$$\rho = \sum_j p_j \rho_j^A \otimes \rho_j^B. \quad (1.40)$$

These form the set of separable mixed (unentangled) states, since they can be synthesized through LOCC and are, therefore, not a useful resource. Any state outside this set is trivially a resource, because at the least it can be used to produce that

same non-separable state, which cannot be done by LOCC alone. Thus, any state that cannot be expressed in the form of Eq. (1.40) is entangled. In fact, entangled states can be used as a resource in many less trivial ways [95, 73]. One important task is quantum teleportation, where a general unknown quantum state can be transferred from one laboratory to another by using shared entangled states and classical communication [17, 23]. Another task of considerable import is quantum key distribution, where shared entangled states are used to distribute encryption keys among remote parties in a secure fashion [18, 16].

Having developed a notion of what constitutes entanglement, one may easily wonder whether some states can be established as being more entangled than others. In fact, the LOCC paradigm gives a natural partial order on the set of entangled states: if a state ρ can be converted to a state σ by LOCC, then ρ can be said to be unambiguously more entangled than σ (since any task that can be accomplished with σ and LOCC can obviously be done with ρ and LOCC). It also follows that if any state ρ can be converted to a state σ using only local unitary operations, then the two states must be equally entangled, since this is a reversible local operation. This ordering is only partial, however, because there are some pairs of states where neither can be converted to the other via LOCC. One can, however, further order the set of entangled states (and even quantify entanglement) under additional assumptions.

1.4.1 Quantifying Bipartite Entanglement

Now we shall restrict our attention to quantifying entanglement between two subsystems, though there has been considerable work on multipartite entanglement as well [9, 73]. While in general there are entangled states that cannot be interconverted between by LOCC, for two d -level systems the state

$$|\Phi_d^+\rangle \equiv \frac{1}{\sqrt{d}} \sum_{j=1}^d |\phi_j\rangle |\chi_j\rangle \quad (1.41)$$

can be converted to any other bipartite pure state via LOCC and is, therefore, maximally entangled. Altering the problem slightly, however, one can say much more. One may consider asymptotic convertibility, the question of whether n copies of ρ can be converted to m copies σ in the limit $n \rightarrow \infty$. One can define the entanglement cost as

$$\mathcal{E}_C(\rho) \equiv \inf \left\{ r : \lim_{n \rightarrow \infty} \left(\inf_M \left\| \rho^{\otimes n} - M \left(|\Phi_2^+\rangle \langle \Phi_2^+|^{\otimes rn} \right) \right\| \right) = 0 \right\}, \quad (1.42)$$

where M is any LOCC manipulation and the norm $\|\bullet\|$ may be the trace norm or any other topologically equivalent norm. This gives the proportion of copies of the state ρ that can be created from maximally entangled qubits in the asymptotic limit. Conversely, one can define the distillable entanglement

$$\mathcal{E}_D(\rho) \equiv \sup \left\{ r : \lim_{n \rightarrow \infty} \left(\inf_M \left\| M(\rho^{\otimes n}) - |\Phi_2^+\rangle \langle \Phi_2^+|^{\otimes rn} \right\| \right) = 0 \right\}, \quad (1.43)$$

which is the proportion of maximally entangled qubits that can be obtained from many copies of ρ via LOCC in the asymptotic limit. Because maximally entangled qubits can be used to perform, for example, quantum teleportation, the distillable entanglement indicates the usefulness of a given quantum state for that purpose.

On pure states the entanglement cost and distillable entanglement are equal (implying that such conversions are asymptotically reversible), and that common value is also given by the entropy of entanglement (EOE)

$$\mathcal{E}_{EOE}(|\Psi\rangle) \equiv S(\text{Tr}_B[|\Psi\rangle\langle\Psi|]) \quad (1.44)$$

in terms of the von Neumann entropy

$$S(\rho_r) \equiv -\text{Tr}[\rho_r \log_2(\rho_r)], \quad (1.45)$$

where ρ_r is the reduced density matrix of one of the two subsystems after the other has been traced over. The existence of a Schmidt decomposition for the total, bipartite state ensures that the eigenvalues of the reduced density matrix of either subsystem are the same, so the EOE does not depend on which subsystem is traced over. Though entanglement cost and distillable entanglement are equal for pure states, for mixed states they are in general different, with $\mathcal{E}_C(\rho) \geq \mathcal{E}_D(\rho)$. This suggests that for mixed states there may not be a unique way to quantify entanglement, and the usefulness of a particular state for carrying out non-classical tasks may depend upon the task.

While the entanglement cost and distillable entanglement both have direct meaning, they both involve taking a quite non-trivial infimum [129, 73]. Indeed, it is known that the problem of determining whether an arbitrary state of a bipartite quantum system is separable falls in the NP-hard complexity class [67], so it is not surprising that entanglement measures will be difficult to compute in general. However, there are many other functions that can be defined to quantify entanglement in some way that can be more easily computed. Generally, one may define many

entanglement monotones, which are functions that vanish on separable states and are non-increasing under LOCC. If such a function is additionally equal to the EOE on pure states, then it is often referred to as an entanglement measure. While a great variety of entanglement measures and monotones exist [111], we will be chiefly concerned with four: the negativity, the logarithmic negativity, the entanglement of formation, and the concurrence.

The entanglement of formation is an entanglement measure that is in some sense a straightforward generalization of the EOE to mixed states. Given a mixed state ρ there are many possible projector decompositions of the form $\rho = \sum_j p_j |\Psi_j\rangle \langle \Psi_j|$, provided that one does not make the requirement that the projectors be orthogonal.

The entanglement of formation is then defined as

$$\mathcal{E}_F(\rho) \equiv \inf \left\{ \sum_j p_j \mathcal{E}_{EOE}(|\Psi_j\rangle) : \rho = \sum_k p_k |\Psi_k\rangle \langle \Psi_k| \right\}. \quad (1.46)$$

While the entanglement of formation is not known to be easily computed in general, it can be efficiently computed for two qubits in terms of the Wootters concurrence [134]. The concurrence is defined as

$$C(\rho) \equiv \max \left\{ 0, \sqrt{\lambda_1} - \sqrt{\lambda_2} - \sqrt{\lambda_3} - \sqrt{\lambda_4} \right\} \quad (1.47)$$

where $\lambda_1 \geq \lambda_2 \geq \lambda_3 \geq \lambda_4$ are eigenvalues of

$$\rho(\sigma_y \otimes \sigma_y) \rho^*(\sigma_y \otimes \sigma_y) \quad (1.48)$$

computed in some basis (the eigenvalues are basis independent) and

$$\mathcal{E}_F(\rho) = h \left(\frac{1 + \sqrt{1 - C^2}}{2} \right) \quad (1.49)$$

$$h(x) \equiv -x \log_2(x) - (1-x) \log_2(1-x). \quad (1.50)$$

In addition to being useful for calculating the entanglement of formation, the concurrence itself is an entanglement monotone.

Although in general determining whether a state is separable is computationally difficult, the Peres-Horodecki criterion gives a necessary (but not sufficient) condition for separability [109, 71, 72, 73]. This criterion is the mathematical condition that the density matrix of a state remain positive-semidefinite after the partial transpose operation is performed; thus it is often referred to simply as the positive partial transpose (PPT) condition. The partial transpose with respect to some product basis $B = \{|j\rangle_A |k\rangle_C\}$ is defined as

$$\rho^{T_B} = \sum_{j,k,l,m} [\langle j|_A \langle k|_C \rho |l\rangle_A |m\rangle_C] |l\rangle \langle j|_A \otimes |k\rangle \langle m|_C. \quad (1.51)$$

The resulting operator is basis dependent, however the spectrum is not. The degree to which a state violates the PPT condition can be quantified in a number of ways. One way is to take the sum of the absolute value of all the negative eigenvalues. This quantity is known simply as the negativity, which may be written

$$\mathcal{N}(\rho) \equiv \frac{\|\rho^{T_B}\|_1 - 1}{2} \quad (1.52)$$

in terms of the trace norm defined

$$\|\mathcal{O}\|_1 \equiv \text{Tr} \left(\sqrt{\mathcal{O}\mathcal{O}^\dagger} \right). \quad (1.53)$$

One can alternatively define the closely related quantity

$$\mathcal{E}_{\mathcal{N}}(\rho) \equiv \log_2 \|\rho^{T_B}\|_1, \quad (1.54)$$

known as the logarithmic negativity (LN). Both of these are entanglement monotones, and additionally the LN provides an upper bound on distillable entanglement

[129, 110]. Furthermore, each can be efficiently computed even in the general case. These are, however, only entanglement monotones and do not equal the EOE on pure states. Moreover, these measure violation of the PPT condition, which is only a necessary condition for separability. In general there exist entangled states which have positive partial transpose, known as bound entangled states, on which both entanglement monotones vanish. However, there are important special cases in which no bound entanglement exists and a state is entangled if and only if it violates the PPT condition. These cases include two qubits and two continuous variable systems in a Gaussian state.

1.4.2 Entanglement Sudden Death

Since quantum entanglement is of both fundamental importance and practical use as a resource, its time evolution is also of great interest. Just as the loss of quantum coherence through the action of environmentally-induced decoherence is of importance for both of these perspectives, the loss of entanglement is also of great interest. Entanglement, of course, is itself a product of quantum coherence. However, where much of the earlier work on decoherence had been focused on decoherence of individual degrees of freedom, examining disentanglement involves examining the loss of the quantum coherence between different degrees of freedom. So, this is sometime thought of as examining local vs. nonlocal decoherence [138].

It is common to find that quantum coherence in a system weakly coupled to an environment will decay to zero only asymptotically as $t \rightarrow \infty$, and under many

conditions it decays exponentially [62, 142, 53]. A natural question, then, is whether entanglement will also decay to zero in the same qualitative fashion, only asymptotically. Perhaps surprisingly, theoretical study showed that in many models the entanglement will vanish entirely at finite times even when local coherence decays only asymptotically [75, 114, 138, 141]. This phenomenon has been termed entanglement sudden death (SD). It has subsequently been found experimentally [8, 89]. This change in qualitative features is interesting in its own right, but it is also potentially undesirable if one seeks to use entanglement as a resource. Another feature of theoretical and practical interest is that in such models (at zero temperature) only some initial states undergo SD while others do not, suggesting that some may be better for preserving entanglement.

Much of the theoretical study of SD has been in models of atom-field interaction [138, 136, 137, 141] or mathematically similar models. In the context of open systems, these have generally been restricted to master equations of Lindblad form that arise (explicitly or implicitly) from the weak-coupling and Born-Markov approximations. However, it has not been clarified precisely how these approximations may impact predictions of this dynamical feature. Additionally, much of the work on SD uses a model where two 2LAs interact with totally separate environments. A more physical model is one in which two atoms interact with a common field as the environment. One may then expect that the limit of large separation will be the physical situation that corresponds to the abstract model of separate environments. The issue of SD with a common field environment has been studied but only under the RWA [11, 12] and also additionally under the RWA, BMA, and

assumption of weak coupling to the field [49].

1.5 Overview and Summary of Major Findings

The aim of this dissertation will be to examine the dynamics of entanglement in atom-field systems (and other open quantum systems), how entanglement dynamics can vary with atomic separation, and how predictions of those dynamics are impacted by the conventional approximations that are widely used in this context. We begin in the early chapters with some simple models and then in the later chapters move to more complicated models and make some more general statements. In Ch. 2, we examine the dynamics of entanglement between a 2LA and the EMF without the BMA or an assumption of weak coupling, though we retain the RWA. Starting with the atom-field interaction Hamiltonian obtained under the RWA (as well as the dipole and two-level approximations common to all our calculations), we use an exact solution to that Hamiltonian dynamics to find how the entanglement must evolve. In this case we are able to compute additional features of the entanglement including the effect of many modes (with a discrete spectrum) that were not previously calculated.

In Ch. 3, we compute the entanglement for a pair of 2LAs interacting with two modes of the EMF. This calculation uses the same interaction Hamiltonian as in Ch. 2 with the RWA, but the setting is sufficiently simple that the open system dynamics of the atoms can be obtained without the BMA (because the environment is finite and the close system dynamics can be used). We proceed to examine how

changing atomic separation through even a relatively small distance can greatly affect the qualitative features of the entanglement dynamics. We find SD for many initial conditions but that a judicious choice of positioning and initial field state can generate entanglement from a separable state or protect initial entanglement from decaying away, extending previous work on these systems [85, 128, 136, 137]. This also serves to connect the study of SD in separate field modes [136, 137] to the more general case of two atoms with some separation interacting with a common multi-mode field.

Having looked at some simple models, in Ch. 4 we examine the weak coupling approximation and the RWA in-depth. We find that the accuracy of solutions obtained with a weak coupling approximation is less than one might expect, with some components of the density matrix known to only zeroth order in the coupling even when the second-order master equation is used to find the solution. This limitation of weak coupling master equations seems to have thus far gone without explicit acknowledgement in the literature. In examining the RWA, we characterize the two different forms of RWA that are in use in the literature and their effect on solutions. Chief among these effects are discrepancies in the coherences between different energy states. Using the weak coupling master equation as a tool for comparison, we are able to make a detailed and general characterization of the inaccuracies introduced by the RWA, in contrast to previous work that focused on more limited, specific questions [6, 4, 5, 133, 58, 45].

With this information about the effect of approximations, Ch. 5 examines how their shortcomings may change the properties of the predicted entanglement dynam-

ics. We show that any previous calculation of the late-time steady state of an open quantum system using a weak-coupling master equation (e.g., [6, 131, 32, 26]) will be missing the correct lowest-order environmentally induced corrections at low temperature, and we discuss how these corrections may be accurately derived at zero temperature. Furthermore, the inaccuracies in solutions of the perturbative master equation limit what one can accurately predict about the dynamics of entanglement, even qualitatively, in low temperature environments. For sufficiently low temperatures, predictions about SD using any of the previously known techniques will be incorrect. We also find that the dependence of SD on the initial state of the system [138, 141] should be a generic property of zero-temperature calculations using the RWA and weak coupling but that this feature is actually simply an artifact of the approximations and in general will not be a real physical effect. Moreover, correctly accounting for the environmentally-induced corrections to the steady state of the system will even allow the possibility of asymptotic entanglement in some cases. We use the weak-coupling master equation to solve the dynamics of two atoms interacting with a common free field, obtaining a solution to the problem that surpassing the previous approaches [4, 5, 6, 50, 124, 125, 49, 11, 51, 12] by going beyond the RWA. This, together with a correct zero-temperature asymptotic state, allows us to correctly characterize the late-time entanglement dynamics for two atoms in a common field and find, in contrast to all the previous examinations, that SD is in fact universal behavior for all initial states.

Chapter 2

Dynamics of Entanglement Between a Single Atom and the Electromagnetic Field

Our first step in exploring the entanglement dynamics induced by atom-field interactions is to consider the entanglement generated between a single atom and the electromagnetic field during the process of spontaneous emission. We will treat a single two-level atom (2LA) interacting with the electromagnetic field (EMF) via an interaction Hamiltonian that assumes the dipole approximation and the rotating-wave approximation (RWA). Given that Hamiltonian, we then pursue exact solutions.

We begin with a detailed, general, and exact treatment of the dynamics of entanglement in the Jaynes-Cummings model. From there, we expand our considerations to include the effects of other nearby field modes, which can, in principle, add new features to the evolution of entanglement when coupling is strong enough. Finally, we will explore interaction between the atom and the full, infinite collection of modes in the intracavity field. In all these cases we solve for the exact dynamics induced by our chosen Hamiltonian, keeping the full unitary dynamics of the composite system, so that our treatment can capture the non-Markovian behavior of the atom (considered as a subsystem) even in the infinite-mode case. We want to adopt an approach which can best preserve the quantum coherence and entanglement of

the system and include the full interplay of the subsystems involved (or back-action from its environment, if any one such subsystem merits special attention), treated self-consistently.

Simple atom-field models, such as that of a 2LA interacting with one single electromagnetic field mode described by the Jaynes-Cummings model (JCM), have solutions in closed form. Such closed form solutions offer a good point of comparison for results involving approximations. Quantum entanglement for the Jaynes-Cummings model has been studied in depth by Pheonix and Knight [115, 28] and Gea-Banacloche [77] for initial pure states and Bose *et al.* [22] for initial mixed states. We will begin by presenting the exact time evolution of the entanglement for general, mixed initial atomic states, and we will explore the effect of detuning between the atomic transition frequency and the cavity mode frequency. This detailed and exact description of the dynamics of entanglement in the Jaynes-Cummings model is sufficiently simple that one can gain some intuition for the behavior of the entanglement there.

Moving on to more complex models, we study the case of a 2LA interacting with any finite number M of EMF modes. We present an exact solution of the time evolution of entanglement for an arbitrary, pure initial atomic state, which gives the effect of these additional modes. Using a perturbative approach we extract simpler expressions for the leading order corrections to Jaynes-Cummings dynamics from other, nearby field modes in the case of strong atom-field coupling.

Of particular interest to us is the strong-coupling regime of cavity QED. In the context of cavity QED, strong coupling is defined as the regime where the dipole

coupling between the atom and the intracavity field g is large compared to both the cavity damping rate κ or the rate of spontaneous emission γ by the atom into modes that escape the cavity. In this regime the coherent evolution of the atomic and intracavity field state is fast compared to the dissipation rates in the system, so coherent quantum effects become important [98]. In recent years experiments have begun to approach this regime in optical-frequency systems [101, 99, 13, 20] and has been achieved for some time at microwave frequencies [113, 70]. Our model is rather theoretical. Without including the dissipative processes, the quantitative predictions that could be made relevant to experiments are limited. However, our aim here is to get a general picture of the possible phenomena. When treating the closed system models with a finite number of modes, it is the strong-coupling regime that is the physical situation relevant to the mathematical model. In the strong-coupling regime, for sufficiently short times one could in principle ignore dissipation so that the dynamics will look approximately like that of a closed system.

Finally, we study the interaction of a 2LA with a cavity and its full, infinite collection of EMF modes in certain limits, going beyond a simple one- or few-mode treatment. We do not need to invoke the Born-Markov approximation (BMA) or use a perturbative approach to obtain the general solution. This solution will be applicable to the model described by the Hamiltonian even for strong atom-field couplings. Since the RWA presumes weak coupling, the applicability of these solutions to the physical model will be limited somewhat, although some results will still prove to be of physical interest.

2.1 System and Quantities Under Investigation

2.1.1 Hamiltonian and Initial States Considered

Throughout this chapter we consider a two-level atom (2LA) coupled to M electromagnetic field (EMF) modes. We adopt the dipole and rotating-wave approximations, neglecting motion of the atomic center of mass, so that we have the free Hamiltonian appearing in Eq. (1.34) and interaction Hamiltonian Eq. (1.37). If we choose our modes to be polarized such that one is always perpendicular to the dipole vector of our atomic transition, then one polarization can be neglected and that index dropped from our expressions. Thus, the total Hamiltonian for this system becomes

$$\mathbf{H} = \omega_0 \boldsymbol{\sigma}_+ \boldsymbol{\sigma}_- + \sum_{k=1}^M \omega_k \mathbf{a}_k^\dagger \mathbf{a}_k + g_k \boldsymbol{\sigma}_+ \mathbf{a}_k + g_k^* \boldsymbol{\sigma}_- \mathbf{a}_k^\dagger, \quad (2.1)$$

the sum of the atomic energy, the energy of the field modes, and the dipole interaction term, respectively. Here ω_0 is the (bare) frequency of the atomic transition, ω_k is the frequency of the k^{th} field mode, and g_k is the electromagnetic dipole coupling of the k^{th} mode to the atom. It is convenient to divide the total Hamiltonian into the sum of a free part and an interaction part so that the free Hamiltonian is

$$\mathbf{H}_0 = \omega_0 \boldsymbol{\sigma}_+ \boldsymbol{\sigma}_- + \sum_{k=1}^M \omega_k \mathbf{a}_k^\dagger \mathbf{a}_k \quad (2.2)$$

and

$$\mathbf{H}_I = \sum_{k=1}^M \delta_k \mathbf{a}_k^\dagger \mathbf{a}_k + g_k \boldsymbol{\sigma}_+ \mathbf{a}_k + g_k^* \boldsymbol{\sigma}_- \mathbf{a}_k^\dagger \quad (2.3)$$

is the interaction Hamiltonian, with $\delta_k \equiv \omega_k - \omega_0$ being the detuning of each field mode from the atomic resonance. As will be discussed in far more detail in Ch. 3,

we may choose to define the complex phase of the field operators such that all values g_k are real. With this division of the free and interaction Hamiltonians, we have that $[\mathbf{H}_0, \mathbf{H}_I] = 0$, so they have simultaneous eigenstates. Where the atom and the electromagnetic field modes in question form a closed system, the dynamics of the total system is unitary.

For the $M = 1$ case, this model is just the familiar Jaynes-Cummings model with no dissipation. We will often write state vectors in the form $|\eta_A\rangle |n_{k_1}, n_{k_2}, \dots, n_{k_N}\rangle$, where η_A denotes the atomic state with $\eta_A = 0$ the ground state and $\eta_A = 1$ the excited state, and each n_{k_j} represents the number of photons in the EMF mode k_j . In this notation any modes not explicitly assigned a photon number are assumed to be in the vacuum state. Any state that can be written as a single such vector is an eigenstate of \mathbf{H}_0 with

$$\mathbf{H}_0 |\eta_A\rangle |n_{k_1}, n_{k_2}, \dots, n_{k_N}\rangle = \omega_0 \left(\eta_A + \sum_{j=1}^N n_{k_j} \right) \quad (2.4)$$

showing that the energy levels are degenerate.

The state of the total, bipartite system at time t is described by the density matrix $\chi(t)$. We will often be concerned with the reduced density matrix of the atom ρ_A , obtained by tracing over the field degrees of freedom. At the time t this will be

$$\rho_A(t) \equiv \text{Tr}_F [\chi(t)]. \quad (2.5)$$

Throughout the chapter we will always assume at $t = 0$ the initial state is separable and has all electromagnetic field modes in the vacuum state $|0\rangle$. The initial state

can, therefore, be written as

$$\boldsymbol{\chi}(0) = \boldsymbol{\rho}_A(0) \otimes |0\rangle \langle 0|, \quad (2.6)$$

where the atom may be in an arbitrary (possibly mixed) initial state, described by the initial atomic reduced density matrix $\boldsymbol{\rho}_A(0)$. As time advances, the atom-field interaction will generally cause entanglement between the atomic and field degrees of freedom and, consequently, changes in the purity (and entropy) of the atomic reduced density matrix. It is also important to note that in the cases where $\boldsymbol{\rho}_A(0)$ is pure then so is $\boldsymbol{\chi}(0)$, and the unitary evolution of the total system implies $\boldsymbol{\chi}(t)$ is pure for all times.

The internal state of the 2LA at any time t , described by the reduced density matrix $\boldsymbol{\rho}_A(t)$, can be represented by a point in the Bloch sphere, as is well known. We will use the spherical polar parametrization of the sphere, so that $\boldsymbol{\rho}_A$ can be specified by the triple (r, θ, ϕ) , and, as usual, pure states lie on the surface of the sphere with $r = 1$. We choose $(1, 0, \phi)$ to represent the excited state of the atom $|1_A\rangle$ and $(1, \pi, \phi)$ to represent the ground state $|0_A\rangle$.

In this work we seek to quantify the bipartite entanglement between the atom and the electromagnetic field (considered as a whole). We will not look at entanglement with individual modes of the field separately, nor will we explore entanglement among the modes of the field. A local unitary operation of the form $\boldsymbol{U} = \boldsymbol{U}_{Atom} \otimes \boldsymbol{U}_{Field}$ does not change the amount of entanglement in the system [111], and the time evolution due to \boldsymbol{H}_0 , which relates the Schrödinger picture to the interaction picture, is such a local unitary operation; therefore, we may work

entirely in the interaction picture and compute the entanglement of the interaction picture state directly, as though it were the Schrödinger picture state.

2.1.2 Methods of Solution

For the single-mode case ($M = 1$) we have the Jaynes-Cummings model, and one can exactly diagonalize \mathbf{H}_I in the basis known as the dressed states (see, for example, [30, 60]). The evolution of χ in this basis is quite simple, and knowing $\chi(t)$ we can then calculate the entanglement using the logarithmic negativity (LN) in general and the entropy of entanglement (EOE) if $\chi(0)$ is a pure state. For any finite $M > 1$, one can still diagonalize the Hamiltonian in the same way. Our initial state has all the EMF modes in their vacuum, so the energy arises from the atomic state. This confines the initial state to a subspace spanned by energy eigenstates of \mathbf{H}_0 with zero-excitations (energy $E = 0$) or one-excitation ($E = \omega_0$). Since $[\mathbf{H}_0, \mathbf{H}_I] = 0$, the system will remain in this subspace. We then only need to diagonalize \mathbf{H}_I in the subspace of the degenerate one-excitation energy level of \mathbf{H}_0 . When there are M field modes, this subspace has dimension $M + 1$. While this diagonalization is straightforward numerically, doing this analytically requires the solution to a polynomial of degree $M + 1$, so for $M > 3$ there is, in general, no closed form solution. Aside from the possible necessity of this numerical root finding, this method of solution is otherwise exact, requiring no further approximations to find the evolution under the Hamiltonian of Eq. (2.1).

For a pure initial state $\chi(0)$, however, we only need the reduced density matrix

ρ_A to find the entanglement. Anastopoulos and Hu [10] found the solution for the evolution of $\rho_A(t)$ for a 2LA coupled to the EMF with the Hamiltonian and initial condition we've described in Sec. 2.1.1. Given an initial atomic state $(1, \theta, \phi)$, at time t the reduced density matrix of the atom interacting with M modes is given by

$$\rho_A(t) = \begin{pmatrix} \frac{1}{2}u^*u(1 + \cos(\theta)) & \frac{1}{2}ue^{i\phi} \sin(\theta) \\ \frac{1}{2}u^*e^{-i\phi} \sin(\theta) & 1 - \frac{1}{2}u^*u(1 + \cos(\theta)) \end{pmatrix} \quad (2.7)$$

where

$$u(t) = \mathcal{L}^{-1} \left(\frac{1}{z + i\omega_0 + \hat{\mu}(z)} \right) = \frac{1}{2\pi i} \int_{c-i\infty}^{c+i\infty} \frac{e^{zt}}{z + i\omega_0 + \hat{\mu}(z)} dz, \quad (2.8)$$

\mathcal{L}^{-1} represents the inverse Laplace transform, and

$$\hat{\mu}(z) = \sum_{j=1}^M \frac{g_j^2}{z + i\omega_j}. \quad (2.9)$$

In this solution the function $u(t)$ contains all the time evolution of the 2LA reduced density matrix, including coherently all interaction with the field (and, thus, any non-Markovian behavior the field induces in the reduced density matrix of the atom). The function $\hat{\mu}(z)$ encapsulates all the effects of the EMF on the dynamics of the atom. If one considers the propagator for the two-level system with and without the atom-field interaction, then $\hat{\mu}(z)$ can be thought of as the self-energy correction to the 2LA propagator that occurs due to the interaction with the EMF.

In the case that the total state of the system is pure, the amount of entanglement can be determined from the reduced density matrix of the atom $\rho_A(t)$. This is clear for the EOE as defined in Eq. (1.44), which depends directly on the eigenvalues of the reduced density matrix p_j . One may also show using the Schmidt

decomposition that the LN [defined in Eq. (1.54)] can be expressed

$$\mathcal{E}_{\mathcal{N}} = \log_2 \left(\left(\sum_j \sqrt{p_j} \right)^2 \right). \quad (2.10)$$

When the total state of the system is mixed, however, knowing only the reduced density matrix is not sufficient (since, for example, the reduced density matrix of a maximally entangled state is the same as when the total system is in a separable, completely-mixed state). Thus, if we wish to track the evolution of entanglement for a total mixed state, we must keep more information than just the reduced density matrix.

Having $u(t)$, we can compute the time evolution of entanglement. In fact, the entanglement only depends on $|u(t)|$. One can understand this by noting that the complex phase of u only determines the phase between the ground and excited states in the atomic reduced density matrix, so it does not affect the entropy and, thus, the entanglement. Equivalently, such a phase shift in the reduced density matrix can be achieved by a local operation on the composite system, so we know that it cannot influence the entanglement. We can calculate the eigenvalues of $\rho_A(t)$,

$$p = \frac{1}{2} \left(1 \pm \sqrt{1 - 4 \cos^4 \left(\frac{\theta}{4} \right) (|u|^2 - |u|^4)} \right), \quad (2.11)$$

which determine the entanglement. For M field modes

$$|u(t)| = \left| \sum_{j=0}^M \frac{\prod_{k=1}^M (z_j + i\delta_k)}{\prod_{l \neq j}^M (z_j - z_l)} e^{z_j t} \right| \quad (2.12)$$

with the z_j values being all the solutions to the equation

$$z \prod_{k=1}^M (z + i\delta_k) + \sum_{k=1}^M \left(g_k^2 \prod_{l \neq k}^M (z + i\delta_l) \right) = 0. \quad (2.13)$$

Using Eq. (2.11) we can compute the eigenvalues of the reduced density matrix and, thus, the EOE or the LN. From Eq. (2.7) we can see that we must have $|u(t)| \leq 1$ (in order for ρ_A to be Hermitian). From Eq. (2.11) for the eigenvalues of the atomic reduced density matrix we can see that when $|u(t)| = 0$ or $|u(t)| = 1$ we have a pure atomic state, and when $|u(t)| = \frac{1}{\sqrt{2}}$ we have a completely mixed atomic state. As a result, both the EOE and LN share the qualitative features that they are smooth functions of $|u(t)|$ on the interval $[0, 1]$ which take on minima (of zero) at the ends of the interval and a maximum value (of one) at when $|u(t)| = \frac{1}{\sqrt{2}}$ and have no inflection points. Inserting the expression for the eigenvalues into Eq. (2.10), the LN takes the particularly simple form

$$\mathcal{E}_{\mathcal{N}} = \log_2 \left(1 + 2 \cos^2 \left(\frac{\theta}{2} \right) \sqrt{|u|^2 - |u|^4} \right) \quad (2.14)$$

that readily exhibits these qualitative features.

2.1.3 Dependence on Initial Conditions

In examining the evolution of entanglement in this system, one of the primary questions is how it depends on initial conditions. We have already said that the phase of the reduced density matrix does not affect the entanglement; if at any instant two atomic reduced density matrices differ only in ϕ on the Bloch sphere, they must have the same entanglement at that time. However, one may ask whether states with different initial ϕ values will evolve under the dynamics into states of different entanglements. Given the Hamiltonian and the class of initial states we are considering, we find that the entanglement at any point in time is completely

independent of the initial value of the parameter ϕ on the Bloch sphere, because for these dynamics ϕ is just carried forward by the evolution as a phase shift in the ρ_A . This is clear for pure initial states, because the form of the solution for those states, Eq. (2.11), shows clearly ϕ only appears in the phase of the density matrix at all times. For mixed initial states, note that the unitary operator $\mathbf{U}_\phi(\alpha) \equiv e^{-i\mathbf{H}_0\alpha/\omega_0}$ acting on an initial state of the form Eq. (2.6) will simply shift the angle ϕ of the atomic state by an amount α (and add an overall complex phase). Consider two initial states, $\chi(0)$ and $\chi'(0) \equiv \mathbf{U}_\phi(\alpha)\chi(0)\mathbf{U}_\phi(\alpha)^\dagger$, which differ only in their coordinate ϕ on the Bloch sphere. Since \mathbf{H}_0 commutes with \mathbf{H}_I , we know

$$\begin{aligned}\chi'(t) &= e^{-i\mathbf{H}_I t}\mathbf{U}_\phi(\alpha)\chi(0)\mathbf{U}_\phi(\alpha)^\dagger e^{i\mathbf{H}_I t} = \mathbf{U}_\phi(\alpha)e^{-i\mathbf{H}_I t}\chi(0)e^{i\mathbf{H}_I t}\mathbf{U}_\phi(\alpha)^\dagger \\ &= \mathbf{U}_\phi(\alpha)\chi(t)\mathbf{U}_\phi(\alpha)^\dagger.\end{aligned}\tag{2.15}$$

Because $\mathbf{U}_\phi(\alpha)$ represents a local operation, we also know that the degree of entanglement in the states $\chi(t)$ and $\chi'(t)$ must be the same.

For the case where the initial state of the system is a pure state, we can additionally conclude that, while the value of the entanglement at a given time depends on the θ coordinate of the initial state, qualitative features like the times at which local maxima and minima of entanglement occur will be the same for all such initial pure states. The easiest way to see this is by looking at Eq. (2.14), since the value of $|u(t)|$ at which the LN reaches extrema does not depend on θ .

2.2 Specific Case Study

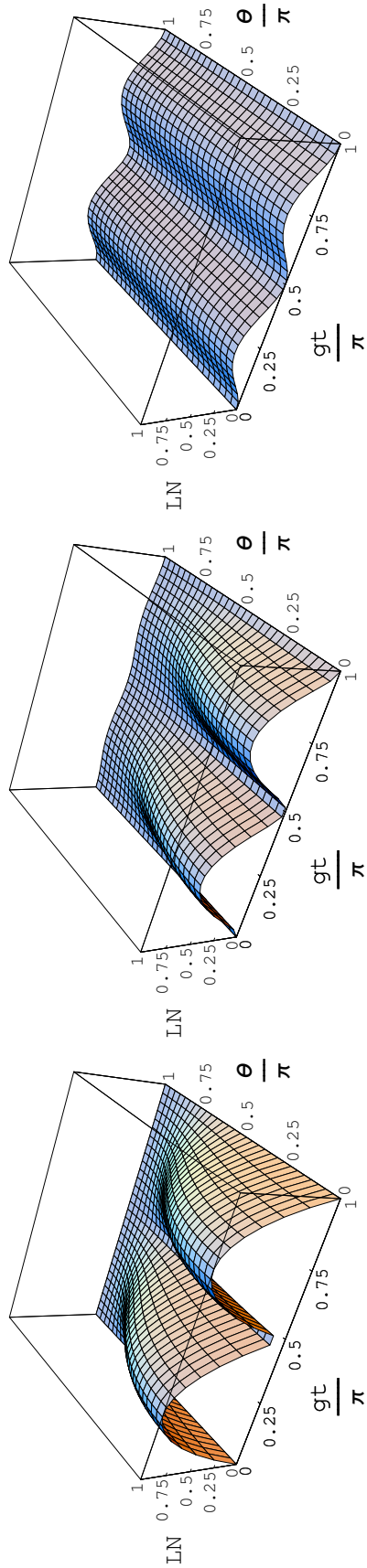
2.2.1 Single Mode — The Jaynes-Cummings Model

We begin with the case of a single mode of the field ($M = 1$) interacting with the atom, which is just the Jaynes-Cummings model. The Hamiltonian now depends only on the single atom-field coupling g , the field mode frequency ω , and the atomic transition frequency $\omega + \delta$. First, consider a system in which the atom is initially in a pure, excited state and the field mode is resonant with the atomic transition. In this case, the system undergoes Rabi oscillations between the separable states $|1_A\rangle|0\rangle$ and $|0_A\rangle|1\rangle$, passing through a maximally entangled state each way. As a result, the entanglement has relatively simple oscillatory behavior with a time scale set by g . For an initial pure state we have

$$u(t) = e^{-i(\omega + \frac{\delta}{2})t} \left[\left(\frac{\Delta\alpha + \delta}{2\Delta\alpha} \right) e^{-i\frac{\Delta\alpha}{2}t} + \left(\frac{\Delta\alpha - \delta}{2\Delta\alpha} \right) e^{i\frac{\Delta\alpha}{2}t} \right] \quad (2.16)$$

where $\Delta\alpha \equiv \sqrt{\delta^2 + 4g^2}$. For initially mixed atomic states, the full density matrix for the bipartite system may be computed using the dressed states, as discussed in Sect. 2.1.2.

The variation in the behavior of entanglement in the $\delta = 0$ case for different initial conditions is shown in Fig. 2.1.



(a) $r = 1$

(b) $r = 1/2$

(c) $r = 0$

Figure 2.1: Logarithmic negativity (LN) as a function of time t and the initial state value of θ on the Bloch sphere for states with different values of r , where g is the value of the atom-field coupling. In the last case, of course, all values of θ correspond to the same state.

As stated above, the entanglement evolution does not depend on the ϕ of the initial state, and many of the qualitative features, such as the times at which maximal and minimal entanglement occur, do not depend on θ . All plots in Fig. 2.1 show the amount of entanglement generated by the dynamics becomes small as θ increases. This is due to that fact that initial states with larger values of θ have a larger projection onto the ground state of the atom-field system, $|0_A\rangle|0\rangle$, for which no excitations and, thus, no entanglement occur. For $r \neq 1$, the initial state is a statistical mixture of one state on the surface of the Bloch sphere with coordinate θ and the antipodal state. For states with small values of θ , the antipodal states (which then have large θ) generate little entanglement, causing the total entanglement generated by the dynamics of this initially mixed state to be reduced. Conversely, for states with large θ , the mixing with antipodal states increases the amount of entanglement that occurs during time evolution. When $r = 0$ the mixture is equally weighted, and the state lies at the center of the Bloch sphere. In this case all values of θ correspond to the same state, making it irrelevant, which is reflected in Fig. 2.1 (c).

The other question is how the entanglement generated by the dynamics of the system depends on the parameters of the Hamiltonian. As is well known for the Jaynes-Cummings model, the time scale of the evolution is the vacuum effective Rabi frequency $\Delta\alpha/2$, which increases with the detuning as stated above. For an initial pure state, we can understand the time evolution of entanglement by focusing on the manifold of states composed of the degenerate one-excitation energy level of \mathbf{H}_0 , states with $\eta_A + n = 1$. This two-level system can again be mapped to the

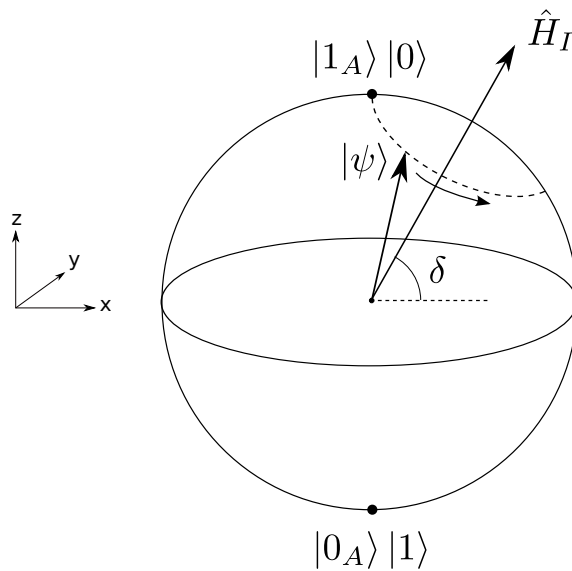


Figure 2.2: The Bloch sphere for the one-excitation manifold of \mathbf{H}_0 . The vector representing the quantum state of the system $|\psi\rangle$ precesses in a circle about the vector for the Hamiltonian \mathbf{H}_I as time advances. The vector for the state starts on the pole of the sphere (due to the initial condition) and travels around a circle centered on the Hamiltonian vector; thus, the circle of precession is a great circle when $\delta = 0$, and the circle becomes very small when $|\delta/g|$ is large.

Bloch sphere, as shown in Fig. 2.2. Any time-independent Hamiltonian acting on this system can be represented by a fixed vector, and the state's evolution under the Hamiltonian can simply be described by a precession of the Bloch vector for the state about the Hamiltonian vector. If we choose the basis to be $B = \{|1_A\rangle |0\rangle, |0_A\rangle |1\rangle\}$ where the first state lies at the top of the Bloch sphere and the second state lies at the bottom, then we have

$$\mathbf{H}_I = \begin{pmatrix} -\delta/2 & g \\ g & \delta/2 \end{pmatrix} = -\frac{\delta}{2}\boldsymbol{\sigma}_z + g\boldsymbol{\sigma}_x = (g, 0, -\frac{\delta}{2}) \cdot \vec{\sigma} \quad (2.17)$$

where $\vec{\sigma}$ is the (pseudo) vector associated with the Pauli matrices, and $(g, 0, -\frac{\delta}{2})$ becomes the vector representing the Hamiltonian. The poles at the top and bottom of the sphere represent separable states. Notice that all points along the “equator” of this Bloch sphere are maximally entangled, because they are all equivalent to $\frac{1}{\sqrt{2}}(|1_A\rangle |0\rangle + |0_A\rangle |1\rangle)$ by a local unitary operation. Entanglement of a state then decreases monotonically with its distance from the equator.

From this picture we can understand the dependence of the entanglement dynamics on the parameters of the Hamiltonian. The ratio of the detuning δ to the atom-field coupling g determines the angle the Hamiltonian vector makes with the vertical axis. When the detuning is small, the vector for \mathbf{H}_I points almost along the x-axis, and the state rotates from $|1_A\rangle |0\rangle$ nearly to $|0_A\rangle |1\rangle$ as it evolves in time, crossing the equator twice, so it passes through two maximally entangled states, one separable state, and one nearly separable state during each cycle. As $|\delta/g|$ increases the Hamiltonian vector acquires a larger z-component, so the circle along which the state precesses no longer passes as close to the bottom of the Bloch

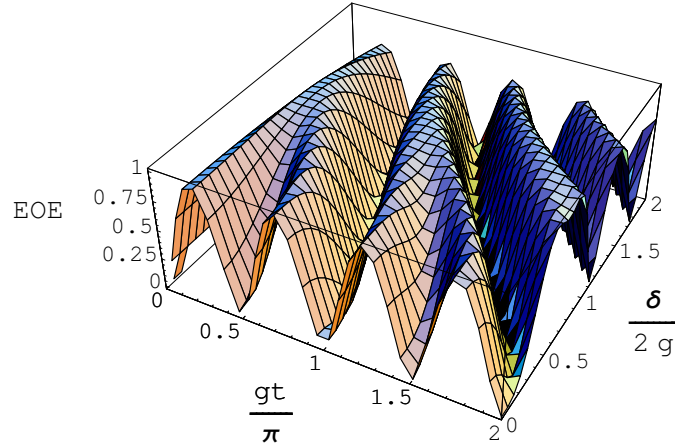


Figure 2.3: The dependence of entanglement on the parameters of the Hamiltonian, the detuning δ and atom-field coupling g . The odd numbered minima in the entanglement (as a function of time t) increase and eventually disappear as the detuning increases.

sphere; thus, the state is only separable once per cycle, and the other minimum in entanglement is significantly non-zero. When $|\delta/g| = 2$ the path of the state no longer enters the lower hemisphere so that there is now only one maximum and one minimum in entanglement each cycle, and as $|\delta/g|$ increases further the circle of precession becomes smaller and smaller, so that the maximum amount of entanglement decreases. Finally, we know from the expression given earlier for the effective Rabi frequency that the frequency of the oscillations in entanglement will increase with $|\delta/g|$, doubling when $|\delta/g| = 2$. All these features of the entanglement dynamics for the different values of $|\delta/g|$ can be seen in Fig. 2.3.

2.2.2 Multiple Modes

With additional modes of the electromagnetic field, the behavior of the system quickly becomes more complex. We already have outlined the mathematical tools necessary for solving the M mode case. For pure states we may use Eq. (2.12) and Eq. (2.13) to find the entanglement dynamics, while for the mixed state we can exactly diagonalize the Hamiltonian as described in Sect. 2.1.2. Getting a conceptual understanding of the dynamics, however, becomes much more difficult.

In the last section we laid out a clear conceptual picture of the evolution of entanglement for an initially pure, excited atomic state in the single-mode case by looking at the evolution of the state's representation on the Bloch sphere. Based on the discussion in Sect. 2.1.2, we know that the state will remain in the one-excitation subspace of \mathbf{H}_0 . With M field modes considered, this space has dimension $M + 1$, and the set of physically distinct states (i.e., normalized state vectors with the same overall complex phase) is the complex projective M -space $\mathbb{C}\mathbf{P}^M$. When $M = 1$ this is just the Bloch sphere, but for $M > 1$ this is a higher dimensional (in some cases non-orientable) surface. Also, in the single-mode case both time evolution and entanglement could be visualized simply, as precession of the state vector about some axis and as the distance from the “equator” of the sphere, respectively. In the higher dimensional case it is not at all clear how to simply visualize these things simultaneously, and such visualization seems no longer to be such a simple conceptual aid, though with enough work one can get a geometrical picture of dynamics and entanglement in $\mathbb{C}\mathbf{P}^M$ as discussed in [15].

We can gain some very rough conceptual insight into what should happen, however. If we view the problem in terms of the dressed states that diagonalize the Hamiltonian, then the initial, separable state is a superposition of these entangled dressed states. As time evolves the different energies of these dressed states cause them to evolve at different rates, changing the quantum interference between them. In the single-mode case, this interference between the two dressed states shows up as changes in entanglement on a time scale set by the difference in their energies. As more modes are added, then, there will be additional interference on other time scales based on the difference in energies between any two of the dressed states; the energy shifts between the atom and the various field modes at different rates depending on their detuning from resonance. By analogy with the single-mode case, we can surmise that the addition of far-detuned modes will give rise to additional dressed states with little entanglement. We therefore would expect modes near resonance to dominate the dynamics of the entanglement while modes further from resonance cause smaller, higher frequency fluctuations.

Let us begin the consideration of multiple-mode models with the bipartite entanglement between the atom and the EMF when the field has only two modes. First consider the “symmetric” case, where $g_1 = g_2 \equiv g$ and $\delta_1 = -\delta_2 \equiv \delta$. If the initial state is pure, then we have

$$u(t) = \frac{\delta^2 + 2g^2 \cos\left(t\sqrt{2g^2 + \delta^2}\right)}{\delta^2 + 2g^2} \quad (2.18)$$

and we can easily compute the entanglement as a function of time. The dependence on δ shown in Fig. 2.4 is somewhat more complex than in the single mode case,

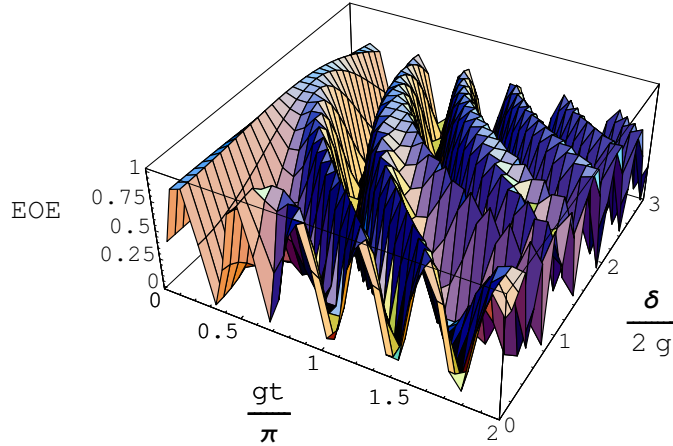


Figure 2.4: The dependence of the EOE on both time t and the detuning δ from the atomic resonance frequency for the case where there are two EMF modes.

which we can understand from the fact that in this case the initial state is now a superposition of three dressed states of different energies, rather than just two as in the single-mode case. The symmetric detuning and equal g values we have selected, however, limit the complexity considerably. As these states evolve in time, the interference between the three dressed states leads to the oscillations in entanglement. Increasing detuning causes the energy of the dressed states to be more disparate and, thus, the interference to evolve more rapidly in time. We are more interested, however, in cases where one of the field modes is very close to resonance, so a more practical case to investigate is that of three field modes.

In considering a finite number of field modes, we are primarily thinking of modeling the behavior of a resonator with a sufficiently high quality factor that

the intracavity field effectively behaves like a set of discrete modes rather than a continuum. Any physical resonator will have dissipation, however we will work for the moment with a model where the dissipation is neglected. This should at least correspond approximately to the behavior in a resonator with very low dissipation at early times.

For our cavity modes we will just consider the harmonics in one dimension (the longitudinal direction along the cavity axis). Considering the frequencies of these cavity modes, if the mode closest to resonance is detuned by an amount δ then all other modes will be detuned by an amount $\delta + k\Delta$ where Δ is the free spectral range of the cavity in angular frequency, which is $\Delta = \frac{\pi}{L}$ for a cavity of length L in our simple model. All the g_j values are proportional to each other, so if we call the value for the mode closest to resonance g , this sets the value for all the other coupling constants. Thus, we are left with only four constants whose values need be specified.

We will consider the regime where $\delta \ll \Delta$ (as is often the case in cavity QED experiments); thus, one mode is almost in resonance, and the next nearest two modes have almost the same detuning. From the single-mode model, we can expect the influence of modes on the dynamics of the atom to decrease with detuning; as a result, it will make most sense to consider odd total numbers of modes M (so that they are in pairs with comparable detuning). With this further specificity, we may rewrite the formula for $|u(t)|$. Let $M = 2Q + 1$, then using calculus of residues we

find

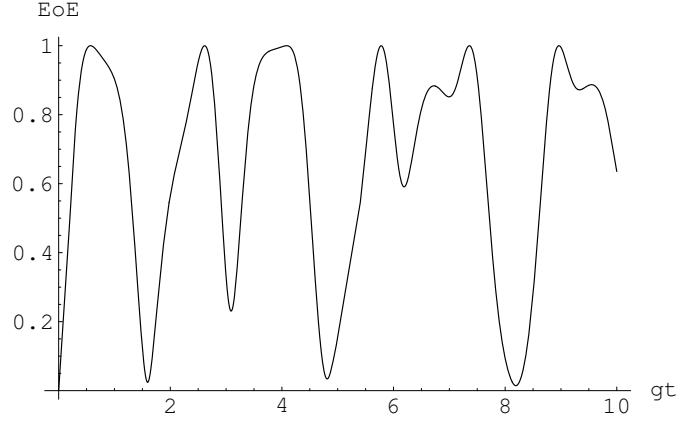
$$|u(t)| = \left| \sum_{j=0}^M \frac{\prod_{n=1}^Q (w_j^2 + n^2 \Delta^2)}{\prod_{l \neq j}^M (w_j - w_l)} e^{w_j t} \right| \quad (2.19)$$

where w_j are solutions to the equation

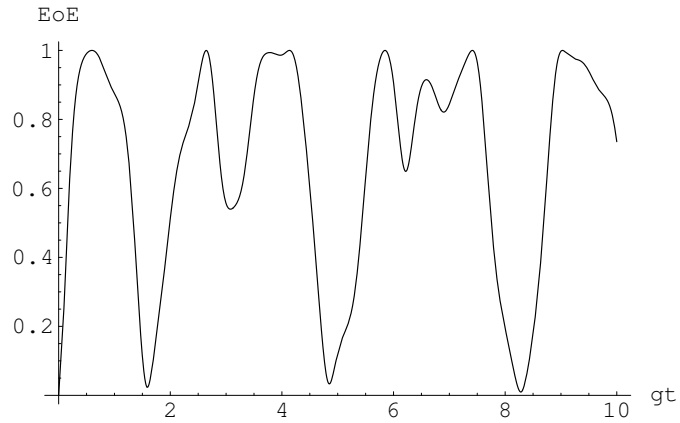
$$(w^2 - i\delta w + g^2) \prod_{n=1}^Q (w^2 + n^2 \Delta^2) + 2wg^2 \sum_{n=1}^Q \left(1 - \frac{n^2 \Delta^2}{(\omega_0 + \delta)^2}\right)^{-1} \left(w + \frac{in^2 \Delta^2}{(\omega_0 + \delta)}\right) \cdot \prod_{j \neq n}^Q (w^2 + j^2 \Delta^2) = 0, \text{ which are the location of the poles.}$$

We consider first the $M = 3$ case. When Δ is small, the time evolution behavior, shown in Fig. 2.5(a), becomes considerably more complex with the contributions of more frequency components to $u(t)$. The effect of the addition of two more modes in the $M = 5$ case is shown in Fig. 2.5(b). The clear intuitive interpretation that was present in the single mode case is not obvious in these cases.

In cavity QED experiments, for example, one is generally working in the regime where $\omega_0 \gg \Delta \gg g$ and δ is $\mathcal{O}(g)$. In this case, other cavity modes are far enough away in frequency to have little effect on the atom, and the evolution for the multi-mode models becomes nearly identical to that of the single mode case. We can calculate the solutions in this regime by writing Eq. (2.20) in terms of the dimensionless parameters g/Δ , Δ/ω_0 , and δ/ω_0 and solving it perturbatively in these small parameters. In experiments, these parameters might typically have values on the order of 10^{-4} , 10^{-3} , and 10^{-7} respectively. This perturbative analysis leads to



(a) $M = 3$



(b) $M = 5$

Figure 2.5: The evolution with time t of the EOE between an atom in an initially pure, excited state and (a) three modes or (b) five modes of the EMF. To highlight the effect of additional modes, we choose the values for the detuning δ , atom-field coupling g , and free spectral range Δ so that $\Delta/g = 5$, $g/\delta = 10$, and $\omega_0/g = 10^7$, though these are unlikely to be characteristic of experimental values.

the solutions

$$w = -\frac{i}{2} \left(\delta \pm \sqrt{\delta^2 + 4g^2} \right) \quad (2.21)$$

$$w = \pm i \left(k\Delta + \frac{g^2}{k\Delta} \right) \quad k \in \left\{ 1, 2, \dots, \frac{M-1}{2} \right\} \quad (2.22)$$

keeping up to terms linear in δ/ω_0 and terms quadratic in g/Δ and Δ/ω_0 (including terms of order g/ω_0). This is the lowest order at which the poles in Eq. (2.22) yield non-vanishing contributions to $|u(t)|$ ¹. In the sum from Eq. (2.19), the poles of the form shown in Eq. (2.21) give terms of order unity, while poles of the form shown in Eq. (2.22) yield terms of order g^2/Δ^2 , so in this regime the effects of additional modes are very small, but we have found an analytic expression for the behavior of the system for an arbitrary, finite number of modes.

2.2.3 Full Intracavity Field

Having treated the idealized cases in which there are only a finite number of EMF modes, we turn to considering the full intracavity field, including the continuum of modes present. We will use a simple cavity model consisting of two infinitely large, perfectly conducting parallel plates separated by a distance L . We will restrict our attention to initially pure states, so that (as discussed in Sect. 2.1.2) we can determine the behavior of the entanglement simply by calculating $u(t)$.

We calculate $u(t)$ via the contour integral in Eq. (2.8). This integral can be

¹If one keeps only to zeroth order in δ/ω_0 and linear order in g/Δ and Δ/ω_0 , then the resulting expression for $|u(t)|$ is identical to the single-mode case, as one may expect when all other modes are very far off resonance.

evaluated using the calculus of residues. If the integrand has isolated poles z_j then

$$u(t) = \sum_j \text{Res}(z_j) e^{z_j t}, \quad (2.23)$$

where $\text{Res}(z_j)$ is the residue arising from that pole. If z_j is a first-order pole, then $\text{Res}(z_j) = \left(1 + \frac{d\hat{\mu}(z)}{dz}\Big|_{z_j}\right)^{-1}$. The time dependence is all carried in the exponential terms of Eq. (2.23). Having already established that at all times $|u(t)| \leq 1$, we know that all the poles must have a non-positive real part, so we can say that at sufficiently late times only the terms from the poles with the largest real parts will be important, because all other will be exponentially suppressed.

It remains to find the correct expression for $\hat{\mu}(z)$ for the full intracavity field. We can begin by considering a box having a square transverse cross-section of area A and a longitudinal length L with boundary conditions such that the field vanishes on the plates at the longitudinal boundaries and is periodic on the transverse boundaries. In this case we can write $g_{\vec{k}} = \frac{\lambda}{\sqrt{\omega_{\vec{k}} LA}}$, where the dimensionless quantity λ is the strength of the coupling to the overall field. As found in [10],

$$\mu(s) = \sum_{\vec{k}} g_{\vec{k}}^2 e^{-i\omega_{\vec{k}} s} \rightarrow \frac{\lambda^2}{2\pi^2 L} \sum_{n=-\infty}^{\infty} \int_{|\frac{\pi n}{L}|}^{\infty} e^{-ik's} dk' \quad (2.24)$$

in the continuum limit where $A \rightarrow \infty$. Since this integral clearly diverges, we add an exponential cutoff by taking $s \rightarrow s - i\epsilon$ to regularize it. With this cutoff

$$\mu_{\epsilon}(s) = \frac{\lambda^2}{2\pi^2 L} \sum_{n=-\infty}^{\infty} \int_{|\frac{\pi n}{L}|}^{\infty} e^{-ik's - k'\epsilon} dk' = \frac{\lambda^2}{\pi L} \frac{1}{\epsilon + is} \frac{1 + e^{-i\pi(s-i\epsilon)/L}}{1 - e^{-i\pi(s-i\epsilon)/L}}. \quad (2.25)$$

Taking the Laplace transform yields approximately [10]

$$\begin{aligned} \hat{\mu}_{\epsilon}(z) &= \frac{-i\lambda^2}{\pi^2 \epsilon} + \frac{\lambda^2}{\pi^2} z \ln(i e^{\gamma_e} \epsilon z) \\ &\quad - \frac{i\lambda^2}{\pi L} \left[\ln\left(\Gamma\left(\frac{Lz}{i\pi}\right)\right) - \frac{Lz}{i\pi} \ln\left(\frac{Lz}{i\pi}\right) + \frac{Lz}{i\pi} + \frac{1}{2} \ln\left(\frac{Lz}{2i\pi^2}\right) \right] + \mathcal{O}(\epsilon) \end{aligned} \quad (2.26)$$

where $\ln(\Gamma(z))$ is defined such that it has a branch cut on each ray $\{-n + iy \mid n \in \mathbb{N} \& y \in \mathbb{R} \geq 0\}$, and γ_e is the Euler-Mascheroni constant. Clearly this expression depends on the cutoff ϵ , which we assume to be small. One cannot in the end take the limit of $\epsilon \rightarrow 0$ for this model, even with renormalization of the model parameters. ϵ should be regarded as a phenomenological parameter that reflects the fact that at high frequencies the approximations that underlie our model (the rotating wave approximation, the two level approximation, etc.) must give way to other physics. Inserting this result for $\hat{\mu}(z)$ into Eq. (2.8), we can now in principle obtain $u(t)$.

Unfortunately, the contour integral in Eq. (2.8) will be quite complicated in general, especially given the infinite set of branch cuts in the integrand. This does, however, reduce the problem to simply evaluating this integral, numerically if necessary. If λ is sufficiently small then we may follow [10] and use a perturbative treatment to find the pole with the greatest real part to at least get some sense of the late-time behavior. (A true solution for this behavior, however, would need to take into account the contribution of the branch cuts.) Doing a perturbative expansion in λ yields

$$z_p = -i\hat{\omega}_0 - \hat{\mu}_\epsilon(-i\hat{\omega}_0) + \mathcal{O}(\lambda^4) \equiv -i\Omega - \gamma \quad (2.27)$$

where $\hat{\omega}_0 \equiv \omega_0 - \frac{\lambda^2}{\pi^2\epsilon}$ for notational convenience. Let us further define

$$\Omega_\infty \equiv \hat{\omega}_0 - \frac{\lambda^2\hat{\omega}_0}{\pi^2} \ln(e^{\gamma_e}\epsilon\hat{\omega}_0). \quad (2.28)$$

Ω_∞ would be the value of Ω in the case of the free field and, therefore, the physically observable dressed value of the two-level transition frequency in free space. If we

rewrite our expression for z_p in terms of this dressed atomic frequency, we may write

$$\hat{\omega}_0 = \Omega_\infty + \frac{\lambda^2 \Omega_\infty}{\pi^2} \ln(e^{\gamma_e} \epsilon \Omega_\infty) + \mathcal{O}(\lambda^4), \quad (2.29)$$

so then the pole from Eq. (2.27) becomes

$$z_p = -i\Omega_\infty - \frac{i\lambda^2}{\pi L} \left\{ \ln \left[\Gamma \left(-\frac{L\Omega_\infty}{\pi} \right) \right] + \frac{L\Omega_\infty}{\pi} \ln \left(-\frac{L\Omega_\infty}{\pi} \right) - \frac{L\Omega_\infty}{\pi} + \frac{1}{2} \ln \left(-\frac{L\Omega_\infty}{2\pi^2} \right) \right\} + \mathcal{O}(\epsilon) + \mathcal{O}(\lambda^4). \quad (2.30)$$

This perturbative solution for the pole will be valid as long as λ is sufficiently small that the higher order terms can be ignored and no branch cut lies between $-i\Omega_\infty$ and the pole calculated in Eq. (2.30). Clearly, the expression will not be valid when $L\Omega_\infty/\pi$ is a non-negative integer, which is the condition for resonance.

When Ω_∞ is close to resonance or λ is large, then the perturbative solution is no longer valid and multiple poles of the integrand may become important. In this case we can attempt to find the significant poles, those with the greatest real parts, by numerically finding the zeros of the denominator of the integrand in Eq. (2.8). Having performed such numerical solutions for cases close to resonance with larger values of λ , we were able to find, as expected, the emergence of two closely spaced, significant poles, which give rise to oscillatory behavior similar to what we saw in the treatment of the cases above where only a finite number of longitudinal cavity modes were considered. Now, however, the oscillating terms are also decaying in time, due to the coupling to the continuum of transverse modes that escape from the cavity.

In examining the solution for the full intracavity field, we found, through nu-

merical solutions, the qualitative connection with models using only a finite number of modes and the new decay features arising from the continuum of modes present in the full intracavity case. With Eqs. (2.8), (2.14), and (2.25) we have the ingredients for further work on numerical solutions for the entanglement evolution in any parameter regimes that might be of specific interest.

2.3 Summary and Discussion

In this chapter we have considered the interaction between a single two-level atom and different numbers of electromagnetic field modes with the aim of gaining a detailed description and deeper understanding of the nature and dynamics of quantum entanglement between the atom and the field. Results discussed go beyond the usual single-mode Jaynes-Cummings model. They are an exact solution of the dynamics under the usual atom-field interaction Hamiltonian (derived from making the rotating wave, dipole, and two-level approximations), and we have given the complete solution of quantum entanglement in time for a system where the field is initially in the vacuum state.

On the effect of initial conditions of the atom in the general case, we find that quantum entanglement is not affected by the ϕ angle of the initial atomic state on the Bloch sphere. For initially pure atomic states, we also find that qualitative features of the time evolution of entanglement remain the same for different values of θ .

For the case where the cavity has only one dominant field mode, these cal-

culations reproduce the familiar results for the Jaynes-Cummings model obtained before [77, 78, 115]. This result shows the expected oscillations of entanglement between the atom and the field, including periodic complete disentanglement in the resonant case. We have calculated the entanglement when the initial state (and, thus, the state at all times) of the atom-field system is mixed, and we have shown the effects of detuning from resonance on the dynamics, giving a simple conceptual picture that accounts for all qualitative features.

When discussing the strong- and weak-coupling regimes of cavity QED, the meaning is somewhat different than the distinction of strong versus weak coupling made above. In the cavity QED context there is the rate g of coupling between the atoms and the intracavity field and the dissipation rates that arise from coupling to environments outside the cavity. These dissipation rates include a rate γ of emission from the atom into field modes that escape the cavity and a rate κ for cavity losses, from transmission through the mirrors for example. Thus, the strong-coupling regime of cavity QED refers to when the intracavity coupling rate dominates over the dissipation rates.

The calculations here with a finite number of field modes are neglecting coupling to any other environmental reservoirs, so if one wishes to relate this to an actual cavity QED system where losses due to spontaneous emission and cavity damping are present, our closed-system treatment will be useful exclusively in the case of strong coupling $g \gg \kappa, \gamma$ at sufficiently early times where $\kappa t \ll 1$ and $\gamma t \ll 1$, wherein dissipation is insignificant and can be ignored.

We have also treated the case of a 2LA interacting with the infinite number

of modes present in an intracavity field. We have obtained a formal solution that could be evaluated numerically or by further approximation. In this model we have assumed that the mirrors are perfectly reflecting. There are two possible approaches to applying these results to a physical cavity with damping. If the damping time scale is sufficiently longer than the other important dynamical time scales then the damping can be ignored for times $\kappa t \ll 1$, and one can apply our results directly. Alternately, one could modify the treatment we have given by constructing the field from “modes of the universe”, cavity field modes that extend through the cavity mirrors to the exterior, as would exist with partially transmitting mirrors. However, the entanglement calculated would still be with the entire field, not merely the intracavity portion.

In this chapter we have looked at the usual Hamiltonian under the RWA and derived the exact solutions for entanglement dynamics that are predicted by this model. Except where noted in Sec. 2.2.3, we have made no explicit assumption that the coupling between the atom and the field modes in the model is small. So the material in this chapter addresses the strong-coupling regime of the model described by the Hamiltonian derived in the the RWA. In Ch. 4 we will examine the RWA in more detail and the errors it introduces, and in Ch. 6 we will return to consider the applicability of these results to physical atom-field systems. More generally, while the behavior of the solutions to the RWA Hamiltonian for strong coupling may be of interest in the abstract or in relation to systems where this form of Hamiltonian may arise without approximation, we do not expect them to predict the physical behavior of atom-field interactions that, in fact, contain “counter-rotating” terms.

In Ch. 3 we will continue looking at the RWA Hamiltonian, this time in the context of examining the entanglement dynamics in two atoms interacting with a common field. In that case we will consider an environment consisting of two resonant field modes, and the RWA will be quite reasonable. Then in Ch. 5 we will return to a calculation with a continuum of modes without the RWA and take careful account of the precision of our results.

Chapter 3

Two Atoms with Two Field Modes

One of the simplest scenarios for theoretically studying the dynamics of entanglement between atoms is that of two atoms which are isolated from one another and interact with different electromagnetic fields. This is the context in which entanglement sudden death (SD) [138, 141, 8, 136, 137] was discovered. An alternative simple model for atom-field interaction in which to study entanglement dynamics is a Dicke model [44], where one assumes all atoms are grouped in a sample whose size is small compared to the resonant wavelength (resulting in identical coupling to every atom). However, such a simplistic model may miss the variety of behavior that can result when the atoms are not confined to such a small sample.

Entanglement dynamics have been shown to have a significant distance dependence when two atoms are interacting with a common field [126]. For atoms weakly interacting with a continuum of field modes in the Born-Markov approximation, it has been shown [51, 124, 124, 49] that changing the atomic separation of two atoms can affect whether there is SD and whether there is revival of entanglement, as well as modify the dynamical generation of entanglement; in short, the qualitative features are sensitive to the atomic spacing. At short inter-atomic distance non-Markovian effects associated with induced interactions between the atoms due to the quantum field may become more pronounced, and in this case the qualitative

behavior varies greatly with different classes of initial states [11]. So it is clear that distance dependence gives rise to a significant variety of behaviors, and some seemingly innocuous approximations can qualitatively alter the entanglement dynamics in unintuitive ways [12, 80].

In view of this, we seek to study entanglement dynamics in a model that is sufficiently complex to manifest some of this variety of behavior yet simple enough that the dynamics may be understood in considerable detail and obtained with fewer approximations. The simplest model one may pursue along this line would be two two-level atoms (2LA) coupled to a single mode with couplings that reflect the distance dependence; however, as we demonstrate in Sec. 3.1, one needs to include at least two field modes before any non-trivial distance dependence can arise in the problem. So we will study such a model with two field modes here.

Out of the class of Hamiltonians that can arise from distance dependence, we will focus on two special cases with the aim of illustrating the variety of different behaviors that can arise. Specifically, we will show how SD, dynamical entanglement generation, and other phenomena differ between these two cases. We will also compare with the behavior of the analogous versions of the two well-studied types of models mentioned above: For two isolated atom-field systems, we will compare with the case where each system is a single 2LA interacting with a single field mode [136, 137, 33]. In the instance of two atoms interacting with the same field, we will compare with the properties of two 2LAs interacting with a single common field mode [85, 128]. We will show that the entanglement dynamics in these models differs significantly from the model of two atoms interacting with a two-mode field,

which is our focus.

We will describe the cases where entanglement meets sudden death (SD) and identify the conditions under which entanglement can survive. Situations in which entanglement never dies (i.e., the system is never separable) we term always alive (AL). In addition to known scenarios of entanglement death, birth and revival we also encounter situations where entanglement dies only for an instant (DI). The qualitative features for all the cases we have studied are summarized in Table 3.1.

3.1 The Model

3.1.1 Interaction Hamiltonian and Couplings

We will consider a pair of identical two-level atoms (2LA) coupled via the multipolar interaction Hamiltonian to a collection of electromagnetic (EM) field modes in the dipole and rotating-wave approximation as described in Sec. 1.3. In general, the mode functions $\vec{f}_{q,s}(\vec{r}_j)$ that appear in the coupling constants of the interaction Hamiltonian can be quite complicated, and even for a single atom there can be position dependence in the dynamics arising from the boundary conditions that the mode functions obey. In order to distinguish these effects from the effect of atomic separation, we will consider mode functions of the form

$$f_q(u, v) e^{\pm ik_q w} \vec{e}_{q,s} \quad (3.1)$$

in terms of some set of coordinates (u, v, w) , with $s = 1, 2$ indexing the polarization. This form describes traveling-wave mode functions that are solutions to an EM

boundary value problem which is invariant under translations in the coordinate w . This form appears in a number of interesting physical systems, including spherical resonators [96] and toroidal resonators [13]. We will consider situations in which all atoms share the same coordinates $u = u_0$ and $v = v_0$, differing only in the coordinate w_j , so that the variation in behavior due to the atomic separation will manifest without additional position dependence arising from the boundary conditions. Let us further assume that the atoms are arranged such that the atomic transition dipole vectors are aligned with one of the mode polarizations, so $\vec{e}_{d,j} \cdot \vec{e}_{q,s} = \delta_{s,1}$. In this situation only one polarization is relevant, and all polarization labels will be suppressed. With these further assumptions we may express the coupling constants as

$$g_{j,q} = d_j f_q(u_0, v_0) e^{\pm i k_q w} \sqrt{\frac{\omega_q}{2\epsilon_0 V}}; \quad (3.2)$$

however, it turns out that without loss of generality one may study a much smaller set of Hamiltonians.

Given a particular set of complex phases for the coupling constants $g_{j,q}$, one may make a trivial basis transformation

$$\mathbf{U}_b = \prod_l e^{-i\xi_l \sigma_{z_l}/2} \prod_s e^{i\zeta_s \mathbf{a}_s^\dagger \mathbf{a}_s}, \quad (3.3)$$

which simply amounts to redefining the reference for the phases of the atoms by $\sigma_{+j} \rightarrow \sigma_{+j} e^{-i\xi_j}$ and for the fields by $\mathbf{a}_q \rightarrow \mathbf{a}_q e^{-i\zeta_q}$. After this transformation, the interaction Hamiltonian becomes

$$\mathbf{H}'_I = \mathbf{U}_b \mathbf{H}_I \mathbf{U}_b^\dagger = \mathbf{H}_I = \sum_j \sum_q g'_{j,q} \sigma_{+j} \mathbf{a}_q + (g'_{j,q})^* \sigma_{-j} \mathbf{a}_q^\dagger \quad (3.4)$$

with $g'_{j,q} = g_{j,q}e^{-i\xi_j}e^{-i\zeta_q}$, and we may obtain the solution to the original problem by using the transformed Hamiltonian:

$$|\psi(t)\rangle = e^{-i\mathbf{H}t} |\psi(0)\rangle = \mathbf{U}_b^\dagger e^{-i\mathbf{H}'t} \mathbf{U}_b |\psi(0)\rangle \equiv \mathbf{U}_b^\dagger e^{-i\mathbf{H}'t} |\psi'(0)\rangle. \quad (3.5)$$

If we consider two identical atoms, with frequencies Ω_0 and dipole strengths $|d_j| = d$ coupled to a single EM field mode, then the previous paragraph implies that it suffices to consider only a Hamiltonian where both couplings are real, and the atomic separation does not enter; thus, there can be no non-trivial distance dependence. However, if we consider the two identical atoms coupled to two field modes, then without loss of generality we can write the total Hamiltonian of the system as

$$\begin{aligned} \mathbf{H} = & \Omega_0 \left(\sigma_1^\dagger \sigma_1 + \sigma_2^\dagger \sigma_2 \right) + \omega_1 \mathbf{a}_1^\dagger \mathbf{a}_1 + \omega_2 \mathbf{a}_2^\dagger \mathbf{a}_2 + g_1 \left(\sigma_{+1} \mathbf{a}_1 + \sigma_{-1} \mathbf{a}_1^\dagger \right) \\ & + g_2 \left(\sigma_{+1} \mathbf{a}_2 + \sigma_{-1} \mathbf{a}_2^\dagger \right) + g_1 \left(\sigma_{+2} \mathbf{a}_1 + \sigma_{-2} \mathbf{a}_1^\dagger \right) + g_2 e^{i\phi} \left(\sigma_{+2} \mathbf{a}_2 + \sigma_{-2} \mathbf{a}_2^\dagger \right), \end{aligned} \quad (3.6)$$

where all distance dependence arises from $\phi = (k_2 - k_1)(w_2 - w_1)$. For simplicity, we will further assume that $\omega_1 = \omega_2 = \Omega_0$, which by implies $g_1 = g_2 \equiv g$. Our aim is to get a sense of the variety of different entanglement dynamics that can result from different separations and initial conditions. To that end, we will consider two special cases, which are arguably extreme cases of the general model, $\phi = 0$ and $\phi = \pi$.

3.1.2 Mapping Equivalent Models and Time Evolution

Since we have assumed the two field modes have the same frequency, rather than using the original modes F_1 and F_2 one could equally well choose a differ-

ent mode decomposition of the field where the two modes are replaced by linear combinations TF_1 and TF_2 with annihilation operators

$$\mathbf{A}_1 = \frac{1}{\sqrt{2}} (\mathbf{a}_1 + \mathbf{a}_2) \quad (3.7)$$

$$\mathbf{A}_2 = \frac{1}{\sqrt{2}} (\mathbf{a}_1 - \mathbf{a}_2). \quad (3.8)$$

In the case of two modes with symmetrical coupling (TMSC), where $\phi = 0$, the interaction Hamiltonian can then be written

$$\mathbf{H}_I = \sqrt{2}g \left[\sigma_{+1} \mathbf{A}_1 + \sigma_{-1} \mathbf{A}_1^\dagger + \sigma_{+2} \mathbf{A}_1 + \sigma_{-2} \mathbf{A}_1^\dagger \right] \quad (3.9)$$

in terms of these transformed modes, so that the atoms only couple to \mathbf{A}_1 and not \mathbf{A}_2 . This shows that the Hamiltonian is equivalent to the model of a single mode symmetrically coupled (SMSC) to two atoms. If we consider the evolution of the reduced density matrix of the atom $\rho_A(t)$ in the TMSC model it should be the same as in the SMSC model with a properly transformed initial state. Namely, if the total system (atoms and modes) is in an initial state described by the density matrix $\chi_{TMSC}(0)$, then the appropriate initial density matrix for the SMSC model is obtained by making the mode transformation of Eqs. (3.7) and (3.8) and tracing out the second transformed mode TF_2 . For example, if the initial state in the TMSC model is separable with the field in a product of Glauber coherent states $|\alpha, \beta\rangle$, then

$$\begin{aligned} \chi_{TMSC}(0) &= |\phi\rangle \langle\phi| \otimes |\alpha, \beta\rangle \langle\alpha, \beta| \rightarrow \text{Tr}_{TF_2} \left[|\phi\rangle \langle\phi| \otimes \left| \frac{\alpha + \beta}{\sqrt{2}}, \frac{\alpha - \beta}{\sqrt{2}} \right\rangle \left\langle \frac{\alpha + \beta}{\sqrt{2}}, \frac{\alpha - \beta}{\sqrt{2}} \right| \right] \\ &= |\phi\rangle \langle\phi| \otimes \left| \frac{\alpha + \beta}{\sqrt{2}} \right\rangle \left\langle \frac{\alpha + \beta}{\sqrt{2}} \right| = \chi_{SMSC}(0) \end{aligned} \quad (3.10)$$

is the appropriate mapping to the equivalent SMSC problem. It is important to note that, because this mapping of initial states involves a partial trace, it is a many-

to-one mapping from the TMSC problem to the SMSC problem (and this mapping does not preserve purity). In order to solve the dynamics in the SMSC model, and by extension the TMSC model, we simply compute the time evolution operator expressed in the atomic basis $\{|ee\rangle, |eg\rangle, |ge\rangle, |gg\rangle\}$ directly by exponentiation (as in, e.g. [85]):

$$\begin{aligned} \mathbf{H}_I &= \sqrt{2}g \begin{pmatrix} 0 & \mathbf{A}_1 & \mathbf{A}_1 & 0 \\ \mathbf{A}_1^\dagger & 0 & 0 & \mathbf{A}_1 \\ \mathbf{A}_1^\dagger & 0 & 0 & \mathbf{A}_1 \\ 0 & \mathbf{A}_1^\dagger & \mathbf{A}_1^\dagger & 0 \end{pmatrix} \\ \Rightarrow \mathbf{U} = e^{-i\mathbf{H}_I t} &= \begin{pmatrix} \mathbf{C}_1 & -i\mathbf{S}_1 & -i\mathbf{S}_1 & \mathbf{C}_2 \\ -i\mathbf{S}_2 & \mathbf{C}_3 & \mathbf{C}_4 & -i\mathbf{S}_3 \\ -i\mathbf{S}_2 & \mathbf{C}_4 & \mathbf{C}_3 & -i\mathbf{S}_3 \\ \mathbf{C}_5 & -i\mathbf{S}_4 & -i\mathbf{S}_4 & \mathbf{C}_6 \end{pmatrix} \end{aligned} \quad (3.11)$$

where

$$\begin{aligned} \mathbf{C}_1 &= 1 - \mathbf{A}_1 \frac{1}{\mathcal{A}} \mathbf{A}_1^\dagger + \mathbf{A}_1 \frac{\cos(\sqrt{4\mathcal{A}}gt)}{\mathcal{A}} \mathbf{A}_1^\dagger & \mathbf{S}_1 &= \mathbf{A}_1 \frac{\sin(\sqrt{4\mathcal{A}}gt)}{\sqrt{2\mathcal{A}}} \\ \mathbf{C}_2 &= -\mathbf{A}_1 \frac{1}{\mathcal{A}} \mathbf{A}_1 + \mathbf{A}_1 \frac{\cos(\sqrt{4\mathcal{A}}gt)}{\mathcal{A}} \mathbf{A}_1 & \mathbf{S}_2 &= \frac{\sin(\sqrt{4\mathcal{A}}gt)}{\sqrt{2\mathcal{A}}} \mathbf{A}_1^\dagger \\ \mathbf{C}_3 &= \frac{1}{2} (\cos(\sqrt{4\mathcal{A}}gt) + 1) & \mathbf{S}_3 &= \frac{\sin(\sqrt{4\mathcal{A}}gt)}{\sqrt{2\mathcal{A}}} \mathbf{A}_1 \\ \mathbf{C}_4 &= \frac{1}{2} (\cos(\sqrt{4\mathcal{A}}gt) - 1) & \mathbf{S}_4 &= \mathbf{A}_1^\dagger \frac{\sin(\sqrt{4\mathcal{A}}gt)}{\sqrt{2\mathcal{A}}} \\ \mathbf{C}_5 &= -\mathbf{A}_1^\dagger \frac{1}{\mathcal{A}} \mathbf{A}_1^\dagger + \mathbf{A}_1^\dagger \frac{\cos(\sqrt{4\mathcal{A}}gt)}{\mathcal{A}} \mathbf{A}_1^\dagger & \mathcal{A} &\equiv \mathbf{A}_1 \mathbf{A}_1^\dagger + \mathbf{A}_1^\dagger \mathbf{A}_1 . \\ \mathbf{C}_6 &= 1 - \mathbf{A}_1^\dagger \frac{1}{\mathcal{A}} \mathbf{A}_1 + \mathbf{A}_1^\dagger \frac{\cos(\sqrt{4\mathcal{A}}gt)}{\mathcal{A}} \mathbf{A}_1 \end{aligned} \quad (3.12)$$

When $\phi = \pi$ we have a two-mode model with asymmetrical coupling (TMAC), and we may again use the mode transformation of Eqs. (3.7) and (3.8) and write the Hamiltonian as

$$\mathbf{H}_I = \sqrt{2}g \left[\sigma_{+1} \mathbf{A}_1 + \sigma_{-1} \mathbf{A}_1^\dagger + \sigma_{+2} \mathbf{A}_2 + \sigma_{-2} \mathbf{A}_2^\dagger \right]. \quad (3.13)$$

In this case, rather than both atoms coupling to one mode we see that atom one couples only to transformed mode TF_1 while atom two couples only to TF_2 , implying that this Hamiltonian is equivalent to a model comprised of two subsystems that are totally isolated from one another, each composed of a single atom coupled to a single mode. We will call this the double Jaynes-Cummings (DJC) model. This sort of model with isolated subsystems is common to the study of entanglement sudden death [138, 141], and the DJC model specifically has been studied [33, 136, 137]. As in the previous case, the evolution of $\rho_A(t)$ for the TMAC model should be the same as given by the DJC model with the proper mapping of initial states. In this case the mapping of initial states is limited to transforming the modes according to Eqs. (3.7) and (3.8), so

$$|\phi\rangle \otimes |\alpha, \beta\rangle \rightarrow |\phi\rangle \otimes \left| \frac{\alpha + \beta}{\sqrt{2}}, \frac{\alpha - \beta}{\sqrt{2}} \right\rangle. \quad (3.14)$$

This mapping implies that there can, for example, be no dynamical generation of atomic entanglement in the TMAC model unless the DJC initial field state obtained by the mapping is entangled. In the DJC model we can write the unitary time-evolution operators for the two separate non-interacting atom-field subsystems as \mathbf{U}_1 and \mathbf{U}_2 , and then the total time evolution operator is $\mathbf{U} = \mathbf{U}_1 \otimes \mathbf{U}_2$. We

again compute the two subsystem unitary time evolution operators by direct exponentiation to obtain

$$U_1 = e^{-iH_1 t} = \begin{pmatrix} \mathbf{C}_{11} & 0 & -i\mathbf{S}_{11} & 0 \\ 0 & \mathbf{C}_{11} & 0 & -i\mathbf{S}_{11} \\ -i\mathbf{S}_{12} & 0 & \mathbf{C}_{12} & 0 \\ 0 & -i\mathbf{S}_{12} & 0 & \mathbf{C}_{12} \end{pmatrix} \quad (3.15)$$

$$U_2 = e^{-iH_2 t} = \begin{pmatrix} \mathbf{C}_{21} & -i\mathbf{S}_{21} & 0 & 0 \\ -i\mathbf{S}_{22} & \mathbf{C}_{21} & 0 & 0 \\ 0 & 0 & \mathbf{C}_{22} & -i\mathbf{S}_{21} \\ 0 & 0 & -i\mathbf{S}_{22} & \mathbf{C}_{22} \end{pmatrix} \quad (3.16)$$

with

$$\begin{aligned} \mathbf{C}_{i1} &= \cos(\sqrt{2\mathbf{A}_i\mathbf{A}_i^\dagger}gt) & \mathbf{C}_{i2} &= \cos(\sqrt{2\mathbf{A}_i^\dagger\mathbf{A}_i}gt) \\ \mathbf{S}_{i1} &= \frac{\sin(\sqrt{2\mathbf{A}_i\mathbf{A}_i^\dagger}gt)}{\sqrt{\mathbf{A}_i\mathbf{A}_i^\dagger}}\mathbf{A}_i & \mathbf{S}_{i2} &= \mathbf{A}_i^\dagger \frac{\sin(\sqrt{2\mathbf{A}_i^\dagger\mathbf{A}_i}gt)}{\sqrt{\mathbf{A}_i^\dagger\mathbf{A}_i}}. \end{aligned} \quad (3.17)$$

3.2 Entanglement Dynamics

In order to illustrate the variety of behavior that can arise among the four models we discussed in Sec. 3.1.2, we will examine the entanglement dynamics of a selection of initial states in which the atoms are separable from the fields and which are comprised of familiar atomic and field states. In each case we will select the atomic state from the set of pure states $\{|gg\rangle, |ee\rangle, |eg\rangle, |\Phi\rangle, |\Psi\rangle\}$, where $|\Phi\rangle \equiv (|ee\rangle + |gg\rangle)/\sqrt{2}$, $|\Psi\rangle \equiv (|eg\rangle + |ge\rangle)/\sqrt{2}$, and e and g label the excited and ground

states of the atom respectively. The initial field state will be either the vacuum $|00\rangle$, a product of Fock states $|n_N, m_N\rangle$, a product of Glauber coherent states $|\alpha_c, \beta_c\rangle$, a product of squeezed vacuum states $|\xi_{sq}, -\xi_{sq}\rangle$, a two-mode squeezed vacuum state (TMSS) $|\xi, 0, 0\rangle$, a thermal state ρ_{th} (with both modes having equal temperature), the pure state $|\eta_{nm}\rangle$, or the mixed state ρ_{nm} . The two-mode squeezed state is defined as the state resulting from the action of the two-mode squeezing operator $\mathcal{S}(\xi) = e^{(\xi^* a_1 a_2 - \xi a_1^\dagger a_2^\dagger)}$ on vacuum. The state $|\eta_{nm}\rangle$ is the result of mapping the state $|n_N, m_N\rangle$ in the original modes of the TMAC problem to the transformed modes equivalent to the DJC problem, with

$$|\eta_{nm}\rangle = \sum_{k=0}^n \sum_{l=0}^m \frac{{}^n C_k {}^m C_l}{\sqrt{2^{m+n} m! n!}} \sqrt{(m+n-k-l)!(k+l)!} (-1)^l |m+n-k-l\rangle |k+l\rangle, \quad (3.18)$$

and $\rho_{nm} \equiv \text{Tr}_{TF_2} [|\eta_{nm}\rangle \langle \eta_{nm}|]$ is the state in the SMSC model that gives equivalent evolution to the state $|n_N, m_N\rangle$ in the TMSC model. ${}^n C_k$ represents the binomial coefficients.

The correspondence drawn between the TMSC-SMSC leads to the essential feature that the map for the initial field states from TMSC to SMSC is many to one; the set of initial states that have the same reduced density matrix for the first transformed mode TF_1 have identical entanglement dynamics in terms of A_1 - A_2 entanglement. As a counterintuitive example of this feature we will see that a squeezed state of the form $|\xi_{sq}, -\xi_{sq}, 0\rangle$ and a thermal field in the TMSC model give the same entanglement dynamics provided the average number of photons in the thermal field corresponds to that in the squeezed state ($\bar{n}_{th} = \sinh^2 |\xi_{sq}|$).

We summarize our findings for the entanglement behavior given the various initial states considered in the four models in Table 3.1, listing the equivalent TMSC-SMSC cases and TMAC-DJC cases. When discussing entanglement sudden death, we adopt the usage of the term as in [136] in applying it only to instances where the entanglement goes to zero for some time interval of non-zero length. In the case where entanglement goes to zero only for an instant during the time evolution we refer to it as death for an instant (DI). If there is a non-zero entanglement at all times once it is generated in the system then we label it as being “always living” (AL).

Initial field State		Atomic State				
TMSC	SMSC	A. $ ee\rangle$	B. $ eg\rangle$	C. $ gg\rangle$	D. $ \Phi\rangle$	E. $ \Psi\rangle$
1. $ 00\rangle$	$ 0\rangle$	No	Yes, DI	Yes, DI	AL	DI
2. $ n_N, m_N\rangle$	ρ_{nm}	No	Yes, DI	Yes ¹ , DI/SD	SD	SD
3. $ \eta_{nm}\rangle$	$ n_N\rangle$	No	Yes, DI	Yes, SD	SD	SD
4. ρ_{th}	ρ_{th}	No	Yes, DI	Yes, SD	AL/SD	SD
5. $ \frac{1}{\sqrt{2}}(\alpha_c + \beta_c), \frac{1}{\sqrt{2}}(\alpha_c - \beta_c)\rangle$	$ \alpha_c\rangle$	Yes, AL/SD	Yes, SD	Yes, AL/SD	AL/SD	AL/SD
6. $ \xi_{sq}, -\xi_{sq}\rangle$	ρ_{th}	No	Yes, DI	Yes, SD	AL/SD	SD
7. $ \xi, 0, 0\rangle$	$ \xi_{sq}\rangle$	Yes, AL/SD	Yes,SD	Yes, AL/SD	AL	SD

Initial field State		Atomic State				
TMAC	DJC	A. $ ee\rangle$	B. $ eg\rangle$	C. $ gg\rangle$	D. $ \Phi\rangle$	E. $ \Psi\rangle$
1. $ 00\rangle$	$ 00\rangle$	No	No	No	SD	DI
2. $ n_N, m_N\rangle$	$ \eta_{nm}\rangle$	Yes ¹ , SD	Yes ¹ , SD	Yes ¹ , SD/DI	SD	SD/AL
3. $ \eta_{nm}\rangle$	$ n_N, m_N\rangle$	No	No	No	SD	SD
4. ρ_{th}	ρ_{th}	No	No	No	SD	SD
5. $ \alpha_c, \beta_c\rangle$	$ \frac{1}{\sqrt{2}}(\alpha_c + \beta_c), \frac{1}{\sqrt{2}}(\alpha_c - \beta_c)\rangle$	No	No	No	SD	SD
6. $ \xi_{sq}, -\xi_{sq}\rangle$	$ \xi, 0, 0\rangle$	Yes, SD	Yes, SD	Yes, SD	SD	SD
7. $ \xi, 0, 0\rangle$	$ \xi_{sq}, -\xi_{sq}\rangle$	No	No	No	SD	SD

Table 3.1: Entanglement dynamics for two modes with symmetrical coupling ($\phi = 0$) and anti-symmetrical coupling ($\phi = \pi$). Columns A-C list whether there is an entanglement generation in an initially separable atomic state (yes or no). The dynamical phenomena observed in columns A-E are listed as entanglement sudden death (SD), entanglement dies for only an instant (DI), entanglement remains non-zero at all times and so is “always living” (AL). A ‘/’ denotes that both kinds of dynamics are present depending on the particular initial state chosen from within the class indicated. The initial states have been explained in Sec. 3.2.

3.2.1 Entanglement Generation and Transfer

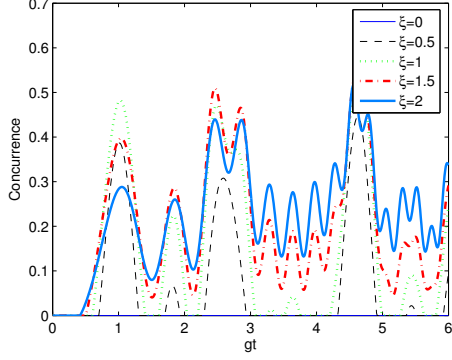
The generation of entanglement from an initially separable state by the dynamics of the system is one interesting, and potentially useful, phenomenon to examine. In the DJC model each atom interacts only with a separate field mode, so the dynamics cannot increase entanglement between the two atom-field subsystems; therefore, if the atomic state is not entangled initially then it will remain separable, unless there is an initial entanglement between the field modes that can be transferred to the atoms by the dynamics. Knowing this, we can see that any initial field state for the TMAC model that maps to a separable DJC field state will also fail to generate entanglement. The nature of the mapping means that even some entangled field states will fail to generate atomic entanglement in the TMAC model, while some separable states will map to an entangled DJC state and will generate entanglement.

This structure means that, as shown in Table 3.1, many familiar initial field states fail to dynamically generate entanglement in the TMAC model. In contrast, entanglement generation is a common feature in the TMSC model for the same selection of field states. For example, starting with a two-mode squeezed state in the field modes does not generate any entanglement in TMAC, because the corresponding field state in DJC possesses no correlations amongst TF_1 and TF_2 . On the other hand, a two-mode squeezed state in the symmetrically coupled case generates entanglement in the initially separable atomic states as can be seen in Fig. 3.1. In fact, for initial atomic states $|ee\rangle$ and $|gg\rangle$, if the field is sufficiently squeezed then

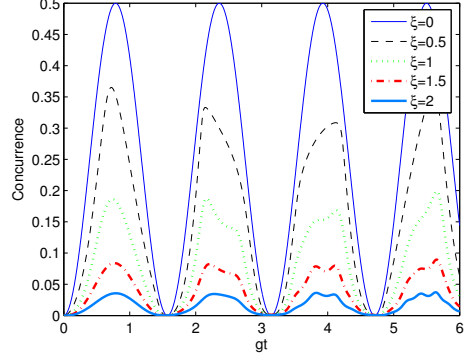
entanglement once generated sustains forever.

When considering the TMAC model with an initial field state that is a product of squeezed states $|\xi_{sq}, -\xi_{sq}\rangle$ we find that entanglement is dynamically generated as shown in Fig. 3.2. One can understand this from the fact that the state $|\xi_{sq}, -\xi_{sq}\rangle$ maps to the DJC model with an initial TMSS, so the generation of atomic entanglement occurs simply because the dynamics transfers the entanglement between the field modes to the atoms. Further, we find that there is an optimal squeezing value that generates maximal entanglement. The maxima in generated entanglement occur for values of the squeezing parameter such that the field state is close to being a maximally entangled qubit state $(\alpha_0(\xi) |00\rangle + \alpha_1(\xi) |11\rangle)$, with $\alpha_1(\xi)$ and $\alpha_0(\xi)$ being comparable. On increasing the squeezing parameter further there are contributions from higher Fock states which decrease the transfer of entanglement. We also notice some secondary peaks on increasing the squeezing parameter ξ_{sq} .

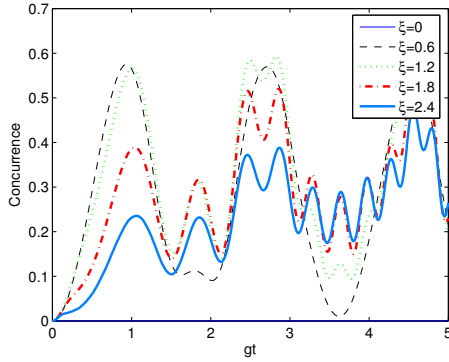
By comparing the effects of a TMSS and thermal field state in the DJC model, one can also get some insight into the role of correlations between the field modes. The reduced density matrices for individual modes correspond to a thermal state for both the cases; the difference being that in a TMSS the two field modes are strongly correlated with each other while in the thermal fields there are no correlations. One would generally expect that the correlated TMSS generates more entanglement in the atomic subsystem, which is trivially true for the case of an initially separable atomic state. This intuition generally extends to the situation of initially entangled atomic states, where we see that apart from the regular SD pattern in the absence of the field-field correlations there are spontaneously generated peaks as a result



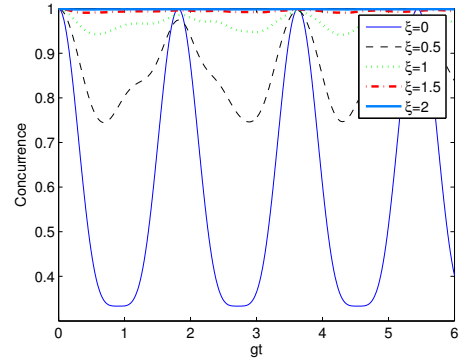
(a) $|ee\rangle$ - No SD once entanglement is generated if the state is sufficiently squeezed



(b) $|eg\rangle$ - increased squeezing destroys entanglement in this case

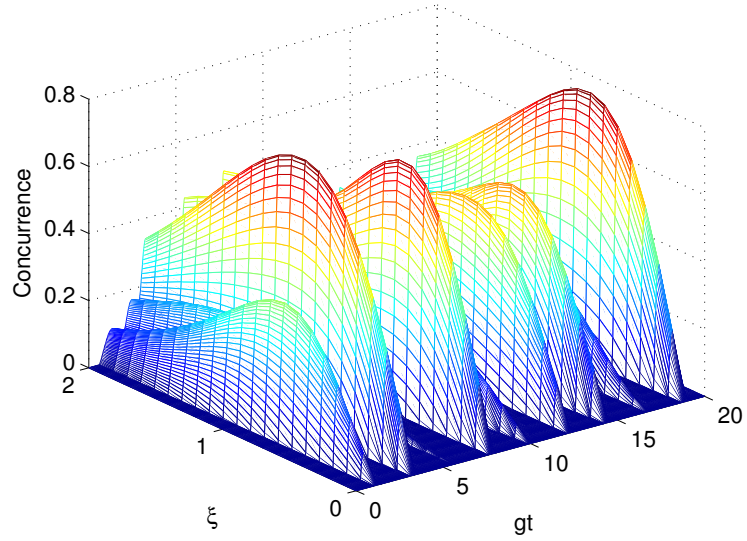


(c) $|gg\rangle$ - SD disappears on increasing the squeezing

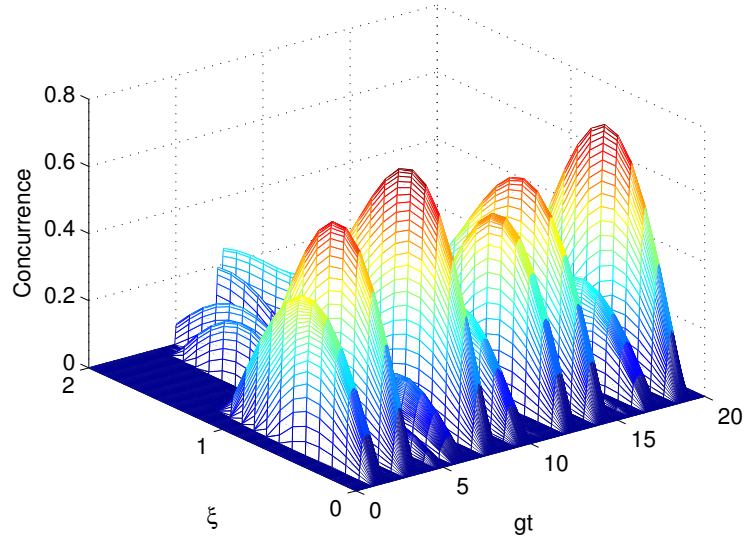


(d) $|\Phi\rangle$ - State moves towards being maximally entangled at all times as squeezing is increased

Figure 3.1: Entanglement dynamics for a single mode squeezed state ($|\xi_s\rangle$) in the SMSC model or two-mode squeezed state ($|\xi, 0, 0\rangle$) in the TMSC model interacting with different initial atomic states



(a) $|ee\rangle$ - Entanglement generation from transfer of correlations from the field, optimal squeezing can be seen $\xi \approx 1$



(b) $|eg\rangle$ - Secondary peaks in entanglement vs squeezing can be observed for $\xi \approx 1.5$

Figure 3.2: Entanglement dynamics for a two-mode squeezed state $(|\xi, 0, 0\rangle)$ in DJC or product of single mode squeezed states $(|\xi_s, -\xi_s, 0\rangle)$ in TMAC interacting with different initial atomic states

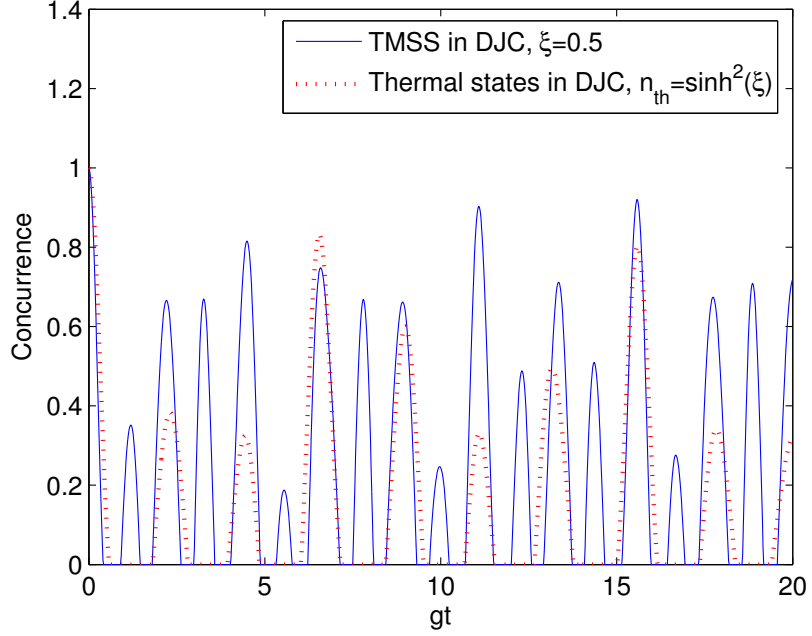


Figure 3.3: Comparing entanglement dynamics for a two-mode squeezed state vs a thermal state in the DJC model for an initial atomic state $|\Phi\rangle$

of two-mode squeezing (Fig. 3.3); however, we note as an exception that at certain instants of time the entanglement in the presence of an initial thermal field exceeds that of the TMSS. Transfer of field-field (TF_1-TF_2) correlations can be explicitly seen in a small squeezing approximation when a two mode squeezed state interacts with an initially separable atomic state $|ee\rangle$ (Fig. 3.4). Since the probability of higher photon numbers is small, by restricting to the 4-dimensional subspace of lowest energy states in the Fock basis for TF_1-TF_2 we obtain the negativities for the two subsystems as,

$$\mathcal{N}_{A_1-A_2} \approx |\min(s_1^2 c_1^2 - \xi s_1^2 c_2^2, 0)| \quad (3.19)$$

$$\mathcal{N}_{TF_1-TF_2} \approx |\min(s_1^2 c_1^2 - \xi c_1^2 c_2^2, 0)|.$$

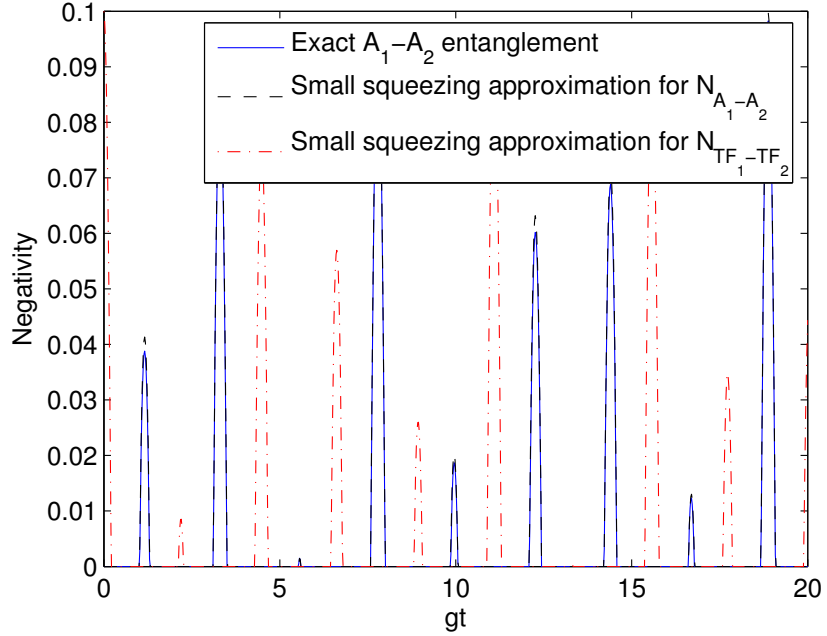
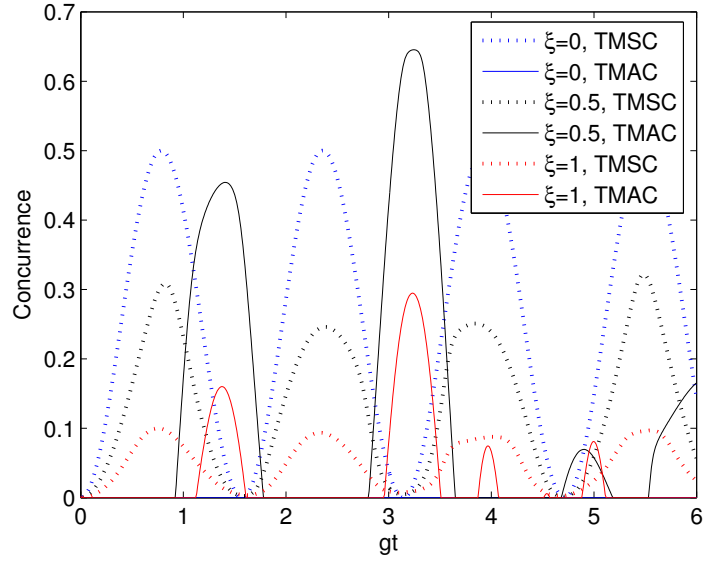


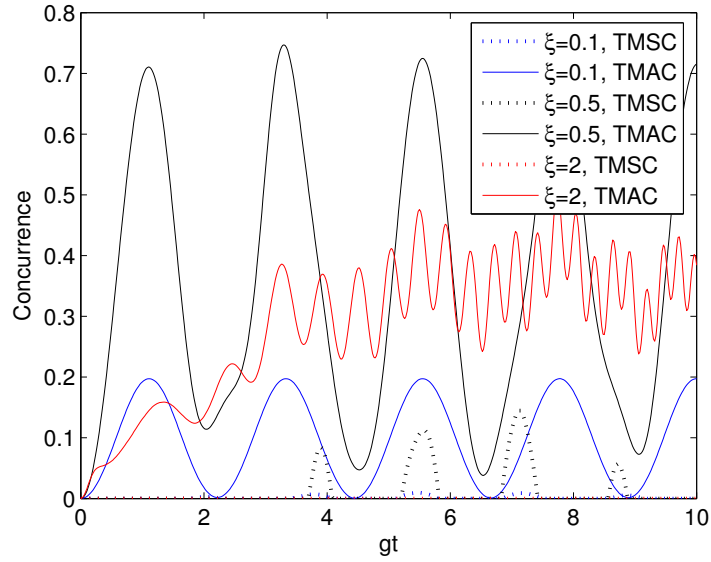
Figure 3.4: Small squeezing entanglement dynamics for a two-mode squeezed state in the DJC model interacting with an initially separable atomic state $|ee\rangle$, entanglement is generated in the atomic subsystem via transfer of field-field correlations

where $s_1 = \sin(\sqrt{2}gt)$, $c_1 = \cos(\sqrt{2}gt)$ and $c_2 = \cos(2gt)$

In the TMSC model, the same initial field state, consisting of a product of squeezed states, corresponds to having a thermal field state in the SMSC model, a situation where entanglement generation has been previously studied [85]. Comparing the entanglement behavior in Fig. 3.5 for the two different couplings, we see that for the initial atomic state $|gg\rangle$ there is more entanglement generated in TMAC than TMSC. As mentioned before, two thermal fields in TMSC also map to the same situation. This is a somewhat unintuitive situation for the generation of entanglement. There is no entanglement generation when the atoms are initially in



(a) $|eg\rangle$ - we observe the TMSC entanglement getting smaller as squeezing is increased, while the TMAC entanglement goes to an optimum value and then decreases



(b) $|gg\rangle$ - TMAC shows more entanglement than TMSC, for both the entanglement increases and then decreases on increasing squeezing

Figure 3.5: Comparison of entanglement generation in presence of product single mode squeezed states $|\xi_{sq}, -\xi_{sq}\rangle$ for TMSC and TMAC

the state $|ee\rangle$. As Figs. 3.6(c) and 3.6(d) show, for $|eg\rangle$ entanglement is generated with only instantaneous zeros, however high the temperature, and for $|gg\rangle$ there is entanglement generation and sudden death behavior with an optimal $\bar{n}_{th} \approx 1$ for the generation of atomic entanglement.

The observation that the initial atomic state $|ee\rangle$ will remain separable can, in fact, be generalized to any initial field state with a density matrix that is diagonal in the Fock basis. As had been shown in [128], in the SMSC model an atomic state $|ee\rangle$ interacting with any Fock state $|n\rangle$ in the field mode never gets entangled.¹ This then implies that the atom-atom density matrix given as $\rho^{(n)} = \text{Tr}_F [|\psi_n\rangle \langle \psi_n|]$ remains separable, where the time evolved state $|\psi_n\rangle \equiv \mathbf{U} |ee\rangle |n\rangle$. Extending to a general completely-mixed field density matrix the time evolved atom-atom density matrix given as $\rho_{12} = \text{Tr}_F [\sum_n P_n \rho^{(n)}]$ is clearly a convex sum of separable density matrices, and hence there is no entanglement generation.

Looking at the initial state $|eg\rangle |n\rangle$ in the SMSC case, we observe no SD in Fig. 3.6(a). This can be explained by considering the state as a superposition $|eg\rangle = \frac{1}{2}(|eg\rangle + |ge\rangle) + \frac{1}{2}(|eg\rangle - |ge\rangle)$, where due to the symmetry of the coupling constants the maximally entangled dark state $(|eg\rangle - |ge\rangle)/\sqrt{2}$ does not interact with the field. It is only momentarily during the evolution that the state of the system returns to being the original separable superposition $|eg\rangle$. As a result we

¹To explain this it can be observed from symmetry arguments that the time evolved atom-atom density matrix is an incoherent mixture of the states $\{|ee\rangle, |gg\rangle, |\Psi\rangle\}$ such that the contribution of the maximally entangled part $|\Psi\rangle$ in the mixture is at all times smaller as compared with the other two.

always observe some entanglement between the two atoms for an initial field density matrix diagonal in the Fock basis. The dynamics of the $|gg\rangle|n\rangle$ state in the SMSC model, shown in Fig. 3.6(b), exhibit SD in general except for the special case of $n = 1$ where because of symmetry reasons the state oscillates between the states $|gg\rangle|1\rangle$ and $|\Psi\rangle|0\rangle$, going from being separable to maximally entangled. Hence, any density matrix diagonal in the Fock basis with a high component of $|1\rangle\langle 1|$ would generate more entanglement in general.

Apart from the Fock state in the SMSC model with a thermal field, another example of having a initial field density matrix diagonal in the Fock basis is to have a Fock state $|n, m\rangle$ in the TMSC which corresponds to the SMSC density matrix

$$\rho_{nm} \equiv \frac{1}{2^{m+n}n!m!} \sum_{k,p=0}^n \sum_{l,q=0}^m \kappa_{mnkl} |m+n-k-l\rangle \langle m+n-k-l| \quad (3.20)$$

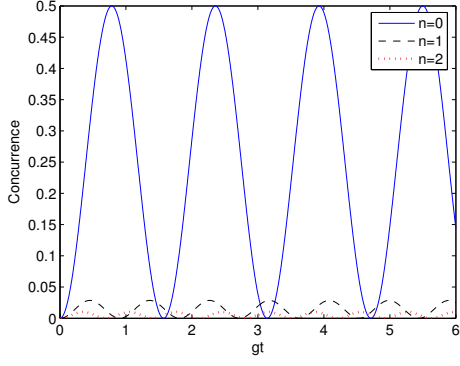
where $\kappa_{mnkl} = {}^nC_k {}^nC_p {}^mC_l {}^mC_q \delta_{k+l,p+q} (m+n-k-l)!(k+l)!(-1)^l$. For this state again we see no entanglement generation for $|ee\rangle$ and DI for $|eg\rangle$ and maximal entanglement in $|gg\rangle|10\rangle$, as shown in Figs. 3.6(e) and 3.6(f). Another point we observe is that for an initial state $|gg\rangle|n, n\rangle$ there is no entanglement generation, which is a common feature between TMSC and TMAC. A Fock state $|n, m\rangle$ in TMAC transforms into an entangled state in the DJC model, so we expect and observe entanglement generation in the system for an initially separable atomic state. As an exception we find that for $n = m$, if there is no atom-atom entanglement to begin with then the atoms remain separable evolving into a completely mixed state. This is counterintuitive in the sense that even though the field state in the DJC model is entangled to begin with, there is still no transfer to the atomic

subsystem. This feature can be explained by considering the initial field state $|\eta_{mn}\rangle = \frac{1}{2^n n!} \sum_{k=0}^n {}^n C_k (-1)^k \sqrt{2k!(2n-2k)!} |2n-2k, 2k\rangle$. If the atoms are initially in the state $|ee\rangle$ then time evolution will lead to an entanglement of atomic and field states such that detecting whether the number of photons in each mode is even or odd tells us the state of the two atoms. On tracing out the field this gives us a completely mixed atom-atom density matrix with no atom-atom entanglement. The same is true for the initial atomic states $|eg\rangle$ and $|gg\rangle$.

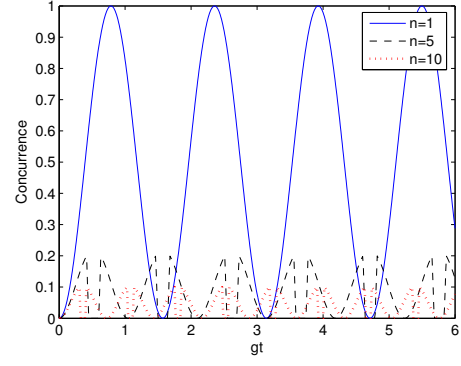
While there are more nuanced details in what we have reported in this section, generically speaking it seems that the TMSC (and SMSC) models are much more conducive to the dynamical generation of entanglement than the TMAC (and DJC) model, suggesting that atomic separation may have a strong influence on this. Particularly useful is the ability in the TMSC to dynamically generate entanglement with a thermal field state or from a squeezed state in SMSC where one can even generate atomic entanglement that is AL.

3.2.2 Entanglement Sudden Death and Protection

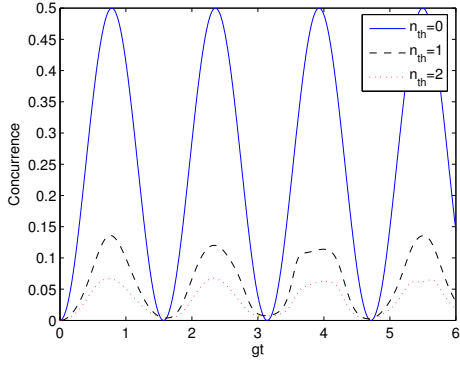
The phenomenon of entanglement sudden death has clearly provoked much theoretical interest, and it is related to another question that is both interesting from a theoretical perspective and clearly of great practical importance: how can one protect a system from disentanglement? Here we do not propose any active scheme for protecting entanglement (as in, e.g. [97]), but rather consider what initial states of the field tend to minimize the loss of entanglement or safeguard entanglement



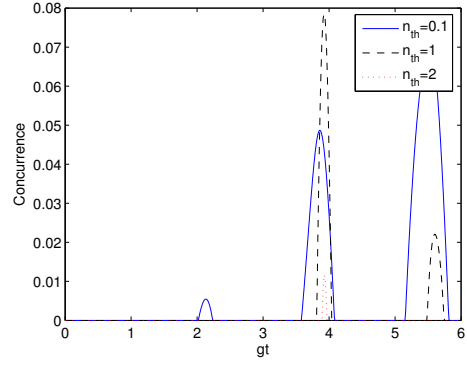
(a) $|eg\rangle$ with $|\eta_{nm}\rangle$ in TMSC or $|n\rangle$ in SMSC



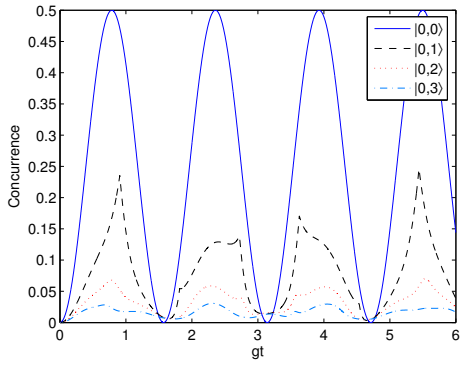
(b) $|gg\rangle$ with $|\eta_{nm}\rangle$ in TMSC or $|n\rangle$ in SMSC



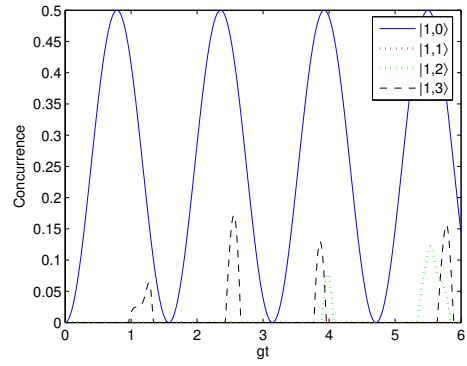
(c) $|eg\rangle |eg\rangle \otimes \rho_{th}$ in SMSC



(d) $|gg\rangle |gg\rangle \otimes \rho_{th}$ in SMSC



(e) $|eg\rangle$ with $|n_N, m_N\rangle$ in TMSC or ρ_{nm} in SMSC



(f) $|gg\rangle$ with $|n_N, m_N\rangle$ in TMSC or ρ_{nm} in SMSC

Figure 3.6: Entanglement dynamics in presence of a completely mixed initial field state in SMSC - no entanglement is seen for initial atomic state $|ee\rangle$, only DI is observed for the atomic state $|eg\rangle$ and maximum entanglement for $\bar{n} \approx 1$ for $|gg\rangle$

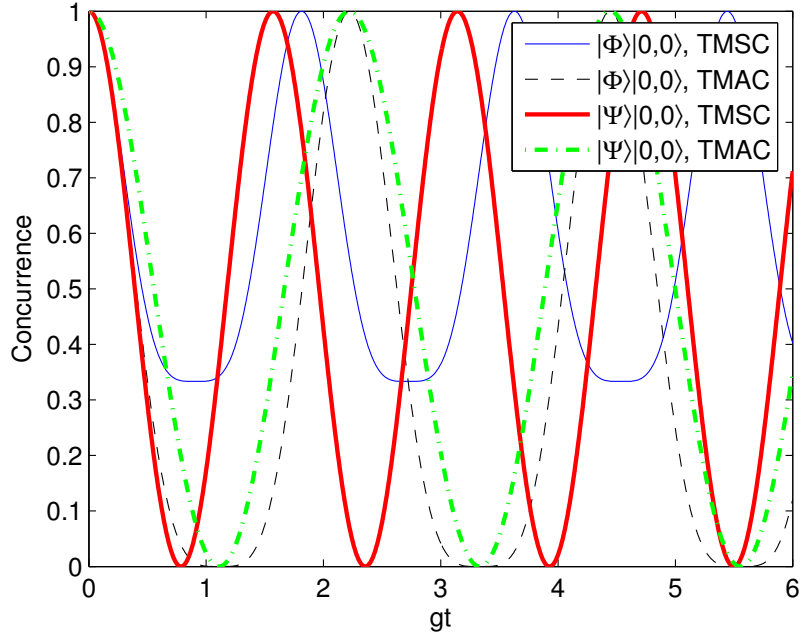


Figure 3.7: Entanglement dynamics in vacuum interacting with initially entangled atomic states $|\Phi\rangle$ and $|\Psi\rangle$ in presence of symmetric and anti-symmetric couplings

once it has been dynamically generated. Of particular interest is avoiding SD.

In terms of the effect of the initial atomic state on the entanglement dynamics, it has been discussed previously in [137] for the DJC model that the initial state $|\Phi\rangle|00\rangle$ undergoes sudden death while $|\Psi\rangle|00\rangle$ has DI of the atomic entanglement. This differentiation in behavior is common to many of the models for studying SD in which each atom interacts with a separate field [138, 141]. The same situation must occur in the TMAC case as well. In comparing these two initial states for the TMSC we find a sort of reversal of roles; as Fig. 3.7 shows, $|\Phi\rangle|00\rangle$ enjoys non-zero entanglement at all times and $|\Psi\rangle|00\rangle$ still suffers DI, so now the entanglement of $|\Phi\rangle$ is better preserved. This reversal also holds in the case of a thermal field in the

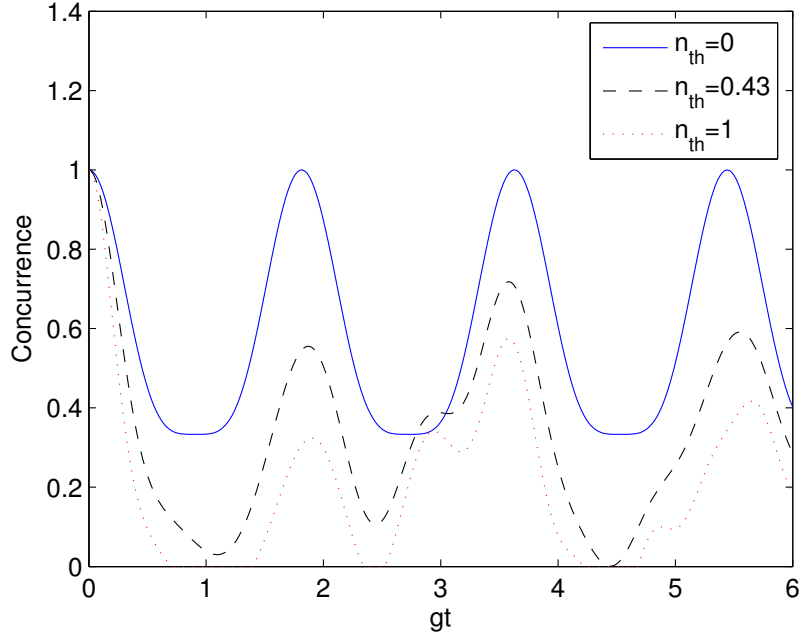


Figure 3.8: Entanglement dynamics for a single mode thermal field interacting with an initially entangled atomic state $|\Phi\rangle$ in the TMSC model. SD occurs after a certain threshold temperature.

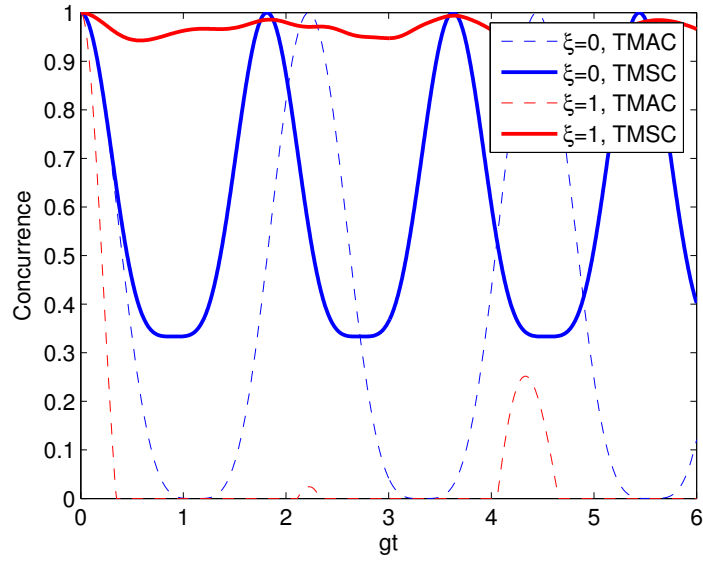
TMSC model so long as the thermal average photon number is below a threshold value $\bar{n}_{crit} \approx 0.43$ (Fig. 3.8) with the state being AL (above this critical temperature $|\Phi\rangle$ experiences SD as well).

If one considers the TMSC model with the field modes in a two-mode squeezed state, then for the separable initial atomic states $|ee\rangle$ and $|gg\rangle$, if the field is sufficiently squeezed, entanglement is dynamically generated and once generated sustains forever (whereas a Fock state or thermal state may generate entanglement but it goes to zero again at some later time). This behavior is shown in Figs. 3.1(a) and 3.1(c). If the atoms are initially in the entangled atomic state $|\Phi\rangle$, then Fig. 3.9 shows that in the TMSC model increasing squeezing raises the minimum value of

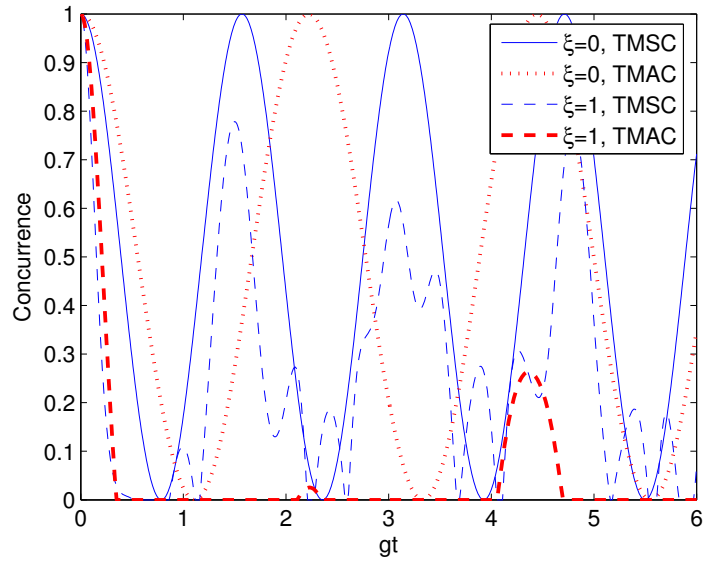
entanglement progressively towards a situation where the state is maximally entangled at all times, while for the TMAC model the system exhibits SD, and the entanglement gets destroyed in general with increasing squeezing.

A general observation that seems to fit for most of the cases considered is that a higher average number of photons in the field destroys entanglement. As an exception, however, it can be seen from Fig. 3.10(a) that in the TMSC model with the field in a product of coherent states, if the average number of photons is in a particular range then there is no SD once entanglement is generated for the states $|ee\rangle$ and $|gg\rangle$. While Fig. 3.10(b) shows that for $|eg\rangle$, the regular rule applies. In the case of the initial field being a two-mode squeezed state (Fig. 3.1), we observe that after a threshold squeezing (or average photon number) there is no sudden death of entanglement after generation in the system when the atoms are initially in the state $|ee\rangle$ or $|gg\rangle$. On the other hand, for the initial atomic state $|eg\rangle$ entanglement decreases as the average number of photons is increased.

Much as for generating entanglement, we find that the TMSC model is generically better suited to protecting entanglement from sudden death. While in the TMAC model at nonzero temperature disentanglement occurs for both entangled states considered, in the TMSC we find that below a threshold temperature entanglement of the $|\Phi\rangle$ state remains AL. In addition, we find that in the SMSC model a two-mode squeezed vacuum field can keep $|\Phi\rangle$ almost maximally entangled at all times, provided squeezing is large enough. In the TMAC sudden death is a quite generic feature, which is only escaped for an initially entangled state when the field is the vacuum or a select product Fock state.

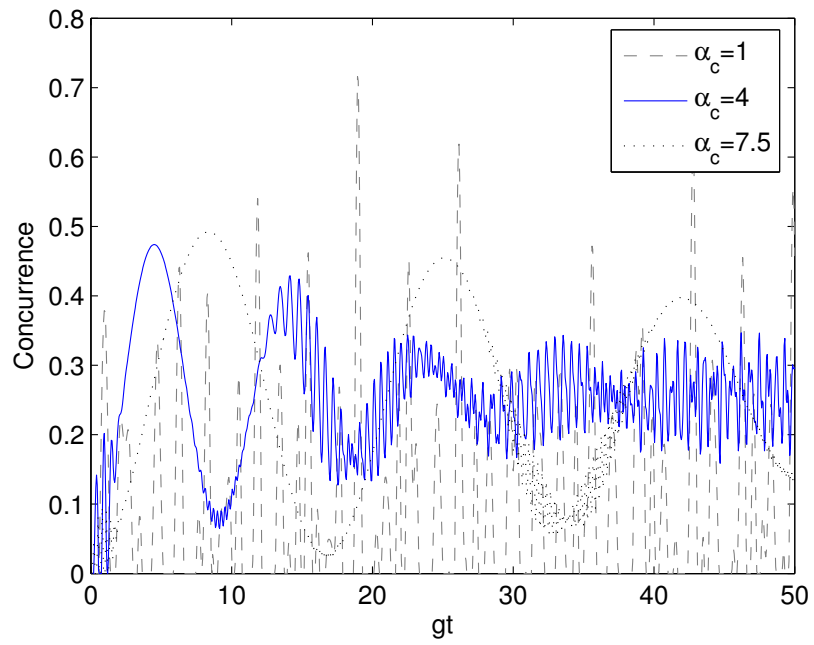


(a) $|\xi, 0, 0\rangle |\Phi\rangle$ - SD for TMAC, entanglement moves towards maximal entanglement in TMSC

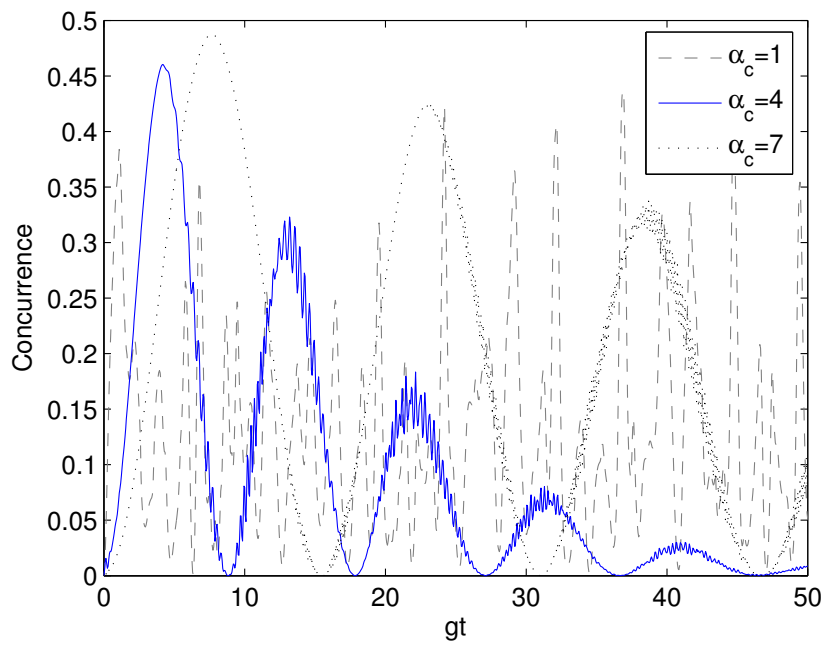


(b) $|\xi, 0, 0\rangle |\Psi\rangle$ - SD for both TMSC and TMAC

Figure 3.9: Comparing entanglement dynamics for the initially entangled atomic states interacting with a two-mode squeezed state in the TMSC and TMAC models



(a) $|ee\rangle$ - No sudden death for a range of values of α



(b) $|eg\rangle$ - Sudden death for all $|\alpha| > 0$

Figure 3.10: Entanglement generation in presence of a coherent state in SMSC

3.2.3 General Spacing and Generic Features

We have examined two special cases $\phi = 0$ and $\phi = \pi$, on the basis that they would appear likely to be extreme cases, and examining them should give an idea of the breadth of qualitative behaviors possible for the entanglement dynamics with different inter-atomic separations. In these cases we found that the field could be expressed in terms of transformed modes where the Hamiltonian is especially simple and the unitary matrix governing the time evolution can be explicitly computed by hand. For other values of ϕ , however, it is not clear that any such simple representation exists. The dynamics may always be solved, however, by exact diagonalization.

With the field modes included, the Hilbert space of our system is infinite dimensional, and diagonalization would not be easy in general. When the rotating-wave approximation (RWA) is used, however, matters become considerably simpler. In the RWA the interaction Hamiltonian commutes with the free Hamiltonian, so that they must have simultaneous eigenstates. Specifically, the eigenvalue N of the operator

$$\sum_{jk} \sigma_{+j} \sigma_{-j} + \mathbf{a}_k^\dagger \mathbf{a}_k \tag{3.21}$$

is conserved, and this may be thought of as the number of quanta of energy or number of excitations. The result of this is that the Hamiltonian can be diagonalized on each finite dimensional subspace separately. Moreover, if the number of quanta cannot increase, a state which has no probability of having more than some certain number of quanta will continue to obey that condition, restricting the state to a finite subspace. This situation is then quite amenable to exact diagonalization of

the Hamiltonian. This process will generally involve finding the roots of higher order polynomials for which no closed form exists, making symbolic expressions rather opaque; however, the problem may be solved numerically relatively simply.

We have therefore used numerical solution of the diagonalization problem to generate the unitary operator for time evolution in this system, and using that further observations about entanglement dynamics in this system can be made. We do not present a complete characterization of all those results here, however, we will note some aspects of the foregoing analysis on which light is shed by the numerical solutions. What we find when examining the same set of initial states as before for a range of ϕ values is that SD is the generic behavior. Instances in Table 3.1 where we have DI or AL invariably become SD for any intermediate value of ϕ . For example, in Sec. 3.2.2 we found that when $\phi = 0$ there is a critical temperature below which entanglement is AL. Allowing ϕ to vary, we find that there is SD for any $\phi \neq 0$. It is simply that as $\phi \rightarrow 0$ the instant at which SD occurs moves to later and later times. Similarly, the ability we observed for a squeezed field state to protect the entanglement of the state $|\Phi\rangle$ exists only at $\phi = 0$ with exactly the same transition of behavior when $\phi \neq 0$.

These observations suggest that while the two cases $\phi = 0$ and $\phi = \pi$ are extreme cases that exhibit the breadth of behavior, they are not characteristic. The special symmetry that allows easy solutions in those two cases also seems to lead to exceptional features in the entanglement dynamics. If the effects we observed in those two cases exist only on a set of measure zero in parameter space, as seems likely from our numerical investigations, one may reasonably ask to what degree

they are real physical effects. In fact they do seem to be real effects insofar as a scenario which was AL in the case $\phi = 0$ will have a very late time of SD when ϕ is a very small value. However, given the complicated nature of the solutions in many of these cases, clearly qualifying this approach to the special cases appears to be quite difficult.

3.3 Discussion

In this chapter we have analyzed the entanglement dynamics in a model consisting of two two-level atoms and two electromagnetic field modes for a variety of familiar field states and classified the various cases in terms of phenomena such as dynamical entanglement generation, entanglement sudden death. One aim of this analysis is to get a sense of the variety of different classes of entanglement dynamics that can arise from different atomic separations in a case where two atoms interact with a common EM field. It is useful to examine this question in a very simple model that can be solved with a minimum of approximations in finding solutions, since approximations can in some case introduce unphysical effects, though the Hamiltonian itself still have a number of approximations underlying it, including the RWA. We have argued that there is no non-trivial distance dependence in a single mode model, and, therefore, a two-mode model represents the simplest case for the study of distance dependence in the entanglement dynamics.

We have studied two arguably extreme cases out of the class of two-mode Hamiltonians that can arise, one in which the two modes are symmetrically coupled

(TMSC) to the second atom, and one where the two modes have asymmetric coupling (TMAC). A useful insight in understanding these models is that the atomic dynamics in the TMSC model correspond exactly to the dynamics for a model with single field mode symmetrically coupled (SMSC) to both atoms with a suitable mapping of the field state, while the atomic dynamics for the TMAC model correspond exactly to the dynamics for a double Jaynes-Cummings (DJC) model, made up of two isolated subsystems each with one atom coupled to one mode, under the proper transformation of the field state. These mappings help one understand the significant differences in behavior in the two seemingly similar models, giving a window into how significantly atomic separation can affect entanglement dynamics. Another significant implication of the mapping between the TMSC and SMSC models comes from the fact that the mapping of initial field states between those models is many-to-one (because it involves a partial trace); this shows us entire classes of field states for the TMSC model that will give exactly the same atomic dynamics. In particular, we saw that a product squeezed state can be identical to a thermal state with respect to the atomic dynamics.

In examining the dynamical generation of entanglement from an initially separable atomic state in Sec. 3.2.1, we find quite a marked contrast between the TMSC and TMAC models. While entanglement generation is a relatively common feature, present for a variety of field states, in the TMSC model, it is comparatively much more rare in the TMAC model. One aspect that highlights these differences is that in the TMAC model entanglement can be generated by a product of squeezed states or fock states, but in the TMSC model it can also be generated by more easily prepared

states including thermal states and product coherent states. This difference is not so surprising however, if one views it in terms of the mappings we have introduced to the other models. When considering that the TMAC maps to the DJC model, where the two subsystems are isolated, one would expect entanglement generation to be relatively rare; it can only exist in cases where the field state is mapped to an entangled state whose entanglement can then be transferred to the atoms. With the TMSC, by contrast, we have a mapping to the SMSC model where a single shared field mode can readily introduce entanglement between the two atoms.

When one is concerned with protecting the entanglement of two initially entangled atoms, our analysis in Sec. 3.2.2 shows that again the TMSC model is better for that purpose in most cases. In the TMAC entanglement sudden death (SD) is a fairly generic feature, with the initial state $|\Psi\rangle|00\rangle$ being one of only two classes we consider that does not show SD; the $|\Psi\rangle|00\rangle$ shows "death for an instant" (DI), where entanglement goes to zero only on a finite set of points. The TMSC shows a reversal of the fortunes of the $|\Psi\rangle|00\rangle$ and $|\Phi\rangle|00\rangle$ states, with the former experiencing DI while entanglement for the latter is AL, staying non-zero for all times. Moreover, the DI property of the dynamics of the $|\Psi\rangle|00\rangle$ state in the TMAC model is fragile, in the sense that it is destroyed by even the smallest departure from the vacuum to, for example, a finite temperature field, while for the TMSC model the AL feature of the dynamics of the $|\Phi\rangle|00\rangle$ state is robust, remaining for non-zero temperature below a threshold $\bar{n}_{crit} \simeq 0.43$. This gives us a condition for protecting entanglement in this case.

A different sort of issue we have touched on briefly is the role of quantum

correlations between field modes in the entanglement dynamics of the atoms. In the DJC model we compared the resulting entanglement dynamics for fields in a two-mode squeezed state (TMSS) and a thermal state. For appropriate choice of the squeezing parameter, the TMSS has the same reduced density matrix for either mode alone as the thermal state, so in this sense these form a pair of extreme cases to compare, one with strong quantum correlations while the other has none at all. It is necessarily true in the DJC that a thermal state cannot generate entanglement, while a TMSS does. Intuition would also suggest that the local entropy destroys entanglement and leads to qualitative sudden death features, while the entanglement generation we observe in the case of a two-mode squeezed state arises from the field-field entanglement being transferred to the atomic subsystem. The transfer of entanglement from field-field to atoms was analytically verified for a small squeezing approximation of the two-mode squeezed state where one can observe the field-field entanglement going to zero as the atom-atom entanglement builds up. We would expect that the correlations of the TMSS aid in maintaining the entanglement of an initially entangled state, and we find this to generally be the case, although in some cases for brief periods of time a thermal state can actually result in greater atomic entanglement than the corresponding squeezed states.

In SMSC case we have a general result for the class of density matrices that are diagonal in the Fock basis; we conclude that in terms of generating entanglement it is preferable to choose an initial atomic state $|eg\rangle$, which has entanglement being AL or at the least DI, as opposed to $|ee\rangle$ where no entanglement is generated. This had been previously pointed out in the case of Fock states and thermal states [85, 128].

As an interesting result in terms of entanglement protection, we find that a single mode squeezed state interacting with symmetrically coupled atoms initially in the state $|\Phi\rangle$ can be extremely effective in protecting the entanglement. Even for the vacuum, this entangled state is AL, but as squeezing is increased the minimum entanglement rises monotonically toward maximal entanglement. For entanglement generation by a single mode squeezed state in the separable atomic initial states $|ee\rangle$ and $|gg\rangle$, we found that for a sufficient amount of squeezing entanglement is not only generated but remains AL for all future times. Similarly, for a single mode coherent state there is a range of values of the average photon number for which the generated atom-atom entanglement is AL. In these cases, it was observed that $|eg\rangle$ shows sudden death as squeezing or the average photon numbers were increased.

We have chosen in this analysis to try to isolate the effect of atomic separation on entanglement dynamics from the position-dependent effects arising from boundary conditions. For this purpose, we have assumed an atom-field coupling that depends on the coordinate separating the atoms only by a phase factor, as in Eq. (3.2), arising from coupling to two traveling-wave field modes. An experimentally relevant situation in which this form of coupling arises is a toroidal resonator. In this case the two modes of interest would be two resonant, counter-propagating whispering-gallery modes. Here the transformed modes we have considered also have a simple interpretation, as two orthogonal standing wave modes at the same frequency. Because strong coupling between an atom and a whispering-gallery modes of a microtoroidal resonator has been observed experimentally [13], there is the possibility of experimentally probing quite directly the model we have considered.

However, in the experimental system there will be dissipative dynamics arising from emission into other modes outside the resonator as well as scattering that can directly couple the traveling wave modes, so a detailed comparison would require either including these effects in the theoretical model or a restriction to the case of sufficiently strong coupling to the resonator modes and early times that evolution on these longer timescales could be neglected.

Our analysis of special cases of the entanglement dynamics arising in two atoms interacting with two modes suggests a wide variety of different behaviors can arise, with qualitative features of the dynamics changing entirely between the two cases, even with the same initial field state. This suggests that understanding the distance dependence of entanglement dynamics for multiple atoms interacting with a common field will be quite important for predicting even the qualitative features that may arise. Furthermore, if one has the practical goal of dynamically generating entanglement or protecting entanglement once generated, the special cases we have considered suggest that the ability to achieve these goals will be greatly impacted by the positioning of the atoms. We have noted that the special cases we have considered seem to be somewhat exceptional, and our numerical study of the dynamics for other separations suggests that SD is in fact the generic behavior that applies for other separations. The time of sudden death can simply become very long as the special cases are approached.

The model we have used here is comparatively simple, but it is based on a Hamiltonian that employs the RWA, which is integral to deriving the solutions for the time evolution. While we have exactly solved the dynamics under the Hamil-

tonian we are using, the RWA used to derive that Hamiltonian is based on an assumption of weak coupling, so the solution can only really be applied to the physical system in that regime. Moreover, one may wonder what discrepancies may arise through use of the RWA. We pursue precisely this question in Ch. 4. We will comment on the implications for these results in Ch. ch:conclusion.

Chapter 4

Accuracy of the Weak-Coupling and Rotating-Wave Approximations

4.1 Accuracy of Solutions to the Weak-Coupling Master Equation

In Sec. 1.2 we said that in the time-local representation the dynamics of the reduced density matrix of the system can be expressed with a quantum Liouville equation

$$\frac{d}{dt}\boldsymbol{\rho}(t) = \mathcal{L}(t)\boldsymbol{\rho}(t), \quad (4.1)$$

where, despite the apparent time-local form, non-Markovian behavior may be encapsulated in the time dependence of the Liouvillian $\mathcal{L}(t)$. As a perturbative approximation, $\mathcal{L}(t)$ is expanded in powers of the system-environment interaction, scaled here by some parameter g , and truncated to some order.

We will consider the relatively general setting of a perturbative master equations where the Liouvillian $\mathcal{L}(t)$ is time independent at zeroth order and asymptotically constant for late times. We will assume that the perturbative expansion of $\mathcal{L}(t)$ is in even powers of the coupling, because as discussed in Sec. 1.2, this can naturally arise from a microscopic derivation of the open-system dynamics. The expansion of $\mathcal{L}(t)$ will then take the form

$$\mathcal{L}(t) = \sum_{n=0}^{\infty} \mathcal{L}_{[2n]}(t), \quad (4.2)$$

$$\mathcal{L}_{[0]}(t)\boldsymbol{\rho} \equiv [-i\mathbf{H}, \boldsymbol{\rho}], \quad (4.3)$$

where $\mathcal{L}_{[2n]}(t) = \mathcal{O}(g^{2n})$ and to zeroth order the system is driven in a unitary manner by its Hamiltonian \mathbf{H} .

The most well-known perturbative master equation is the second-order master equation, as it can be equivalent to the Redfield and Born-Markov master equations. This is partly due to the fact that in the Markovian limit, the second-order master equation is exact. But equivalence with the previous approximate master equations does not carry to fourth order and there perturbation theory is strictly superior. One might easily assume that solving the second-order master equation defined by the Liouvillian $\mathcal{L}_{[0]} + \mathcal{L}_{[2]}$ would yield a solution that would match the exact solution to the exact master equation up to second order, having error terms of order $\mathcal{O}(g^4)$; however we will show that in general they will differ by second-order terms, so that one can only say they are in perturbative agreement at zeroth order.

One very significant implication of these facts is for positivity. Not being exact, nor generally of Lindblad form [93, 65], a perturbative master equation is not guaranteed to yield a dynamical map with exact complete positivity. Solutions can and should be completely positive to the relevant perturbative order, and as we show in this work that order is not what one might naively expect. Solutions to the second-order master equation can violate positivity by an amount that is $\mathcal{O}(g^2)$. We show that to find solutions good to second-order, canonical perturbation theory generally demands the fourth-order Liouvillian.

4.1.1 Indeterminacy of Solutions

Before determining what the appropriate level of accuracy is for the solutions of perturbative master equations, we will first demonstrate that there is an issue with the naive expectation of order- $2n$ accuracy. This argument is a generalization of one found in Ref. [104], where the discrepancy was noticed for the second-order equilibrium state. Let $\boldsymbol{\rho}_{(2n)}(t)$ be any solution which satisfies the master equation (and is supposedly accurate) to order $2n$, then

$$\frac{d}{dt}\boldsymbol{\rho}_{(2n)}(t) = \mathcal{L}(t)\boldsymbol{\rho}_{(2n)}(t) + \mathcal{O}(g^{2n+2}). \quad (4.4)$$

Furthermore consider the order- $2n$ state

$$\boldsymbol{\rho}'_{(2n)}(t) \equiv \boldsymbol{\rho}_{(2n)}(t) + \boldsymbol{\delta\rho}_{[2n]}(t), \quad (4.5)$$

where $\boldsymbol{\delta\rho}_{[2n]}$ is an order- $2n$ traceless and diagonal (in the energy basis) perturbation for which

$$\boldsymbol{\delta\rho}_{[2n]}(0) = 0, \quad (4.6)$$

$$\frac{d}{dt}\boldsymbol{\delta\rho}_{[2n]}(t) = \mathcal{O}(g^{2n+2}), \quad (4.7)$$

so that both $\boldsymbol{\rho}_{(2n)}(t)$ and $\boldsymbol{\rho}'_{(2n)}(t)$ share the same initial conditions, and the discrepancy $\boldsymbol{\delta\rho}_{[2n]}(t)$ grows slowly with the perturbation as to also satisfy

$$\frac{d}{dt}\boldsymbol{\rho}'_{(2n)}(t) = \mathcal{L}(t)\boldsymbol{\rho}'_{(2n)}(t) + \mathcal{O}(g^{2n+2}), \quad (4.8)$$

since $\mathcal{L}_0\boldsymbol{\delta\rho}_{[2n]}(t) = 0$ by construction. This demonstrates that, for non-perturbative durations of time, there is an order $2n$ ambiguity in the stationary (e.g. diagonal) entries of all solutions if one only compares terms up to order $2n$. This proof also

applies to time-nonlocal master equations, replacing perturbative contributions to the Liouvillian with corresponding memory-kernel operators. Next we will proceed to our main proofs where we show how this issue arises, that this is the full extent of the problem, and precisely how it can be remedied.

4.1.2 Late-time accuracy

It is clear that if Eqs. (4.1) and (4.2) are well defined then for sufficiently short times an order- $2n$ master equation (in which the sum in Eq. (4.2) only includes terms up to order $2n$) can produce a solution that is also accurate to order $2n$. We find that for longer spans of time, and in particular the late-time regime wherein the master equation assumes its stationary limit, solutions to the order- $2n$ master equation are only accurate to order $2n-2$. The reason is an ultimately mundane but slightly subtle result of degenerate perturbation theory. In this section we will address the late-time stationary dynamics, and then in following sections we will address the full-time dynamics, including the crossover from accuracy at the same order to loss of accuracy.

Assuming we have the perturbative expansion of a stationary master equation (i.e., an expansion of \mathcal{L}), we then seek perturbative solutions obtained by applying canonical perturbation theory of the eigenvalue problem, applying the discussion of Sec. 1.2 (based on [53]). So we seek to solve

$$\mathcal{L}\mathbf{o} = f\mathbf{o}, \tag{4.9}$$

for each eigen-operator \mathbf{o} and f is its corresponding eigenvalue. In the appropriate

regime of validity, exact solutions to the perturbative master equation should agree with the perturbative solutions to the exact master equation up to the appropriate order. We have already noted that perturbation theory with master equations is always degenerate perturbation theory, as $\omega_{ii} = \omega_{jj} = 0$. This inevitably-degenerate subspace corresponds to the space of operators that are diagonal in the energy basis of the free system. For simplicity let us assume no other degeneracy in the spectrum of the free Liouvillian (though the possibility of extra degeneracy or near degeneracy arising from resonance can be suitably dealt with).

Perturbation theory tells us that the second-order corrections to all eigenvalues and eigenoperators of \mathcal{L} outside the degenerate subspace (off-diagonal operators) can be computed using only the second-order master equation, as shown in Eqs. (1.26) and (1.27). As noted in Sec. 1.2, to compute corrections to eigen-operators from the degenerate subspace (which all satisfy $\mathcal{L}_{[0]}\mathbf{o}^{[0]} = 0$) we must diagonalize \mathcal{L} in that subspace by solving the associated characteristic equation:

$$\mathbf{W} \vec{\sigma} = f \vec{\sigma}, \quad (4.10)$$

$$[[\vec{\sigma}]]_i \equiv \langle \omega_i | \mathbf{o} | \omega_i \rangle, \quad (4.11)$$

where $\vec{\sigma}$ is the vector that gives the degenerate-subspace projection of \mathbf{o} as the linear combination of the operators $|\omega_i\rangle\langle\omega_i|$ with coefficients $[[\vec{\sigma}]]_i$, and \mathbf{W} is defined

$$[[\mathbf{W}]]_{ij} = \langle \omega_i | \mathcal{L} \{ |\omega_j\rangle\langle\omega_j| \} | \omega_i \rangle, \quad (4.12)$$

which is the degenerate-subspace projection of \mathcal{L} represented as a matrix (giving essentially the Pauli master equation). Therefore Eq. (4.10) must be solved for with

$\mathbf{W}_{[2]}$ exactly, and then the further effects of $\mathbf{W}_{[4]}$, $\mathbf{W}_{[6]}$, etc., can be incorporated via canonical perturbation theory.¹ The eigenvalues obtained in diagonalizing $\mathbf{W}_{[2]}$ give the second-order corrections $f^{[2]}$ to the eigenvalues of \mathcal{L} and the correct zeroth-order eigenoperators $\mathbf{o}^{[0]}$ for the degenerate subspace. Degenerate perturbation theory tells us that in order to calculate each $\vec{o}_i^{[2]}$ for the degenerate subspace, one actually requires $\mathbf{W}_{[4]}$ from the fourth-order master equation; it will contribute the second-order correction

$$\sum_{j \neq i} \frac{\left(\vec{o}_j^{[0]}\right)^{\star} \mathbf{W}_{[4]} \left(\vec{o}_i^{[0]}\right)}{f_i^{[2]} - f_j^{[2]}} \vec{o}_j^{[0]}, \quad (4.13)$$

where \vec{o}_i^{\star} is the left eigen-vector of \mathbf{W} such that $\vec{o}_i^{\star} \mathbf{W} = \vec{o}_i^{\star} f_i$ and $\vec{o}_j^{\star} \vec{o}_i = \delta_{ij}$. In the non-degenerate problem the denominator of Eq. (4.13) would be $f_i^{[0]} - f_j^{[0]}$ and such corrections would be fourth order, but the degeneracy of the free Liouvillian in any perturbative master equation leaves second order as the relevant lowest-order nonvanishing eigenvalue splitting. Without this information from the fourth-order master equation, one cannot generate the complete second-order solution.

Finally note that this requirement must extend even to exact solutions of the perturbative master equation. A perturbative solution to the second-order master equation will be equivalent to solving the full master equation perturbatively and then artificially setting $\mathcal{L}_{[4]}$ and all higher-order contributions to the Liouvillian to vanish. From this and the preceding perturbative analysis we know that the second-order perturbative solutions to the exact and second-order master equations

¹This is slightly more complicated than the canonical perturbation one often sees treated for the Schrödinger equation where the perturbation has only a first order part and no higher-order corrections.

must differ by a term that is $\mathcal{O}(g^2)$. Since the exact solutions to each given master equation must differ from the corresponding second-order perturbative solutions by terms of $\mathcal{O}(g^4)$, we can conclude from our analysis that even the exact solution to the second-order master equation differs from the exact solution to the full master equation by a term of $\mathcal{O}(g^2)$. In Sec. 4.1.5 we use the example of quantum Brownian motion, where an exact solution is available, to show that the second-order corrections arising from the fourth-order Liouvillian are indeed present.

More generally, the same argument can be extended to higher order and tells us that while the short-time accuracy of an order- $2n$ master equation can also be order $2n$, the long-time accuracy can only be order $2n - 2$. To obtain order- $2n$ solutions one requires not only the order- $2n$ master equation but in addition the order- $(2n+2)$ Pauli master equation.

Among the information missing due to the second-order errors of the solution to the second-order master equation are important contributions to the asymptotic state of the system. When coupled to a thermal reservoir the system must asymptote to $\rho \propto e^{-\beta \mathbf{H}}$ for vanishing system-environment coupling (though this may also happen in other, very specific approximations [61]). One often desires to find the additional environmentally induced system-system correlations (and possibly entanglement) provided by perturbative corrections, but these will not be given correctly by directly finding the steady state of the second-order master equation. However, at least for zero-temperature noise, it is still possible to easily construct via other methods the order- $2n$ corrections using only order- $2n$ master equation coefficients and limits thereof [53], as we will see in Ch. 5.

Another important characteristic that is mangled by the second-order master equation is positivity, as was mentioned at the beginning of this section. The second-order inaccuracies that arise from using the second-order master equation imply that the diagonal elements of the density matrix in the (free) energy basis are off by second-order terms. This can lead to second-order violations of positivity. In fact, this is almost guaranteed at low temperature, where any off-diagonal perturbation to the ground state will immediately cause second-order positivity violation, given that the necessary inequality

$$\rho_{ii} \rho_{jj} \geq \rho_{ij} \rho_{ji}, \quad (4.14)$$

cannot be satisfied with the left-hand side vanishing at zeroth-order and not perturbed to the correct second-order values.

4.1.3 Full-time accuracy

In analyzing the full-time accuracy of time-dependent master equations, first we will show that the short-time solutions are accurate to the order of the master equation, and then we will show that longer-time solutions display accuracy loss. The timescale for this transition is determined by the frequency perturbations, e.g. $1/f_{[2]}$.

To analyze the short-time behavior we rotate to the interaction picture defined

$$\underline{\rho}(t) \equiv \mathcal{G}_0^{-1}(t) \rho(t), \quad (4.15)$$

$$\mathcal{G}_0(t) \rho \equiv e^{-i\mathbf{H}t} \rho e^{+i\mathbf{H}t}, \quad (4.16)$$

wherein the master equation is now given by

$$\frac{d}{dt}\underline{\rho}(t) = \underline{\delta\mathcal{L}}(t) \underline{\rho}(t), \quad (4.17)$$

$$\underline{\delta\mathcal{L}}(t) \equiv \mathcal{G}_0^{-1}(t) \delta\mathcal{L}(t) \mathcal{G}_0(t), \quad (4.18)$$

$$\delta\mathcal{L}(t) \equiv \mathcal{L}(t) - \mathcal{L}_0, \quad (4.19)$$

and so the interaction-picture dynamics are strictly perturbative. Short-time solutions can be obtained from the Neumann series

$$\underline{\rho}(t) = \underline{\mathcal{G}}(t) \rho(0), \quad (4.20)$$

$$\underline{\mathcal{G}}(t) = \mathbf{1} + \int_0^t d\tau \underline{\delta\mathcal{L}}(\tau) + \int_0^t d\tau \int_0^\tau d\tau' \underline{\delta\mathcal{L}}(\tau) \underline{\delta\mathcal{L}}(\tau') + \dots, \quad (4.21)$$

where the order- $2n$ solution is fully determined by $\mathcal{L}_{[2n]}(t)$. However, such solutions are inherently secular in time. If $f_{[2]}$ denotes the second-order frequency perturbations, e.g. dissipation and diffusion rates, then the above solutions (at second order) are only good for times $t \ll 1/f_{[2]}$. This is the regime wherein perturbative master equations are ensured to provide matching accuracy in their solutions.

For longer spans of time, one must resort to time-ordered integration for solutions. For weak coupling the master equation can asymptote to its stationary value within timescales much shorter than $1/f_{[2]}$, and so one can apply the stationary master equation and our corresponding proof of accuracy loss. More generally one may consider the behavior of the time-dependent eigen-value equation

$$\mathcal{L}(t) \mathbf{o}(t) = f(t) \mathbf{o}(t), \quad (4.22)$$

so that the time-translation generator may be given by its spectral decomposition

$$\mathcal{L}(t) = \sum_k f_k(t) \mathbf{o}_k(t) \mathbf{o}_k^*(t). \quad (4.23)$$

Again, the order- $2n$ master equation can only determine the perturbatively-stationary eigen-operators $\mathbf{o}(t)$ to within order $2n-2$. Given that the time-dependent basis of the time-translation generator cannot be determined to second order, neither can the solutions.

One might be concerned with how the proof of short-time accuracy is compatible with this proof of full-time accuracy loss. In fact, the short-time accuracy occurs within a span of time $0 < t \ll 1/f_{[2]}$, which is not sufficient enough to accumulate full-order contributions from the perturbation. Therefore the regime of short-time accuracy is a rather trivial result.

4.1.4 Time non-local accuracy

Corresponding to the time-local master equation (4.1) is the time-nonlocal master equation

$$\frac{d}{dt}\boldsymbol{\rho}(t) = \int_0^t d\tau \boldsymbol{\mathcal{K}}(t-\tau) \boldsymbol{\rho}(\tau), \quad (4.24)$$

first derived via the projection-operator formalism of Nakajima [105] and Zwanzig [143]. The two representations are contrasted in Ref. [135, 35, 53]. The nonlocal kernel $\boldsymbol{\mathcal{K}}(t)$ also has a perturbative expansion with zeroth-order dynamics given by

$$\boldsymbol{\mathcal{K}}_{[0]}(t) = 2\delta(t) \boldsymbol{\mathcal{L}}_{[0]}. \quad (4.25)$$

which is time-local and unitary. Solutions are most easily calculated in the Laplace domain wherein one has the kernel

$$\hat{\mathcal{K}}(s) = \int_0^\infty dt e^{-ts} \mathcal{K}(t), \quad (4.26)$$

$$\hat{\mathcal{K}}_{[0]}(s) = \mathcal{L}_{[0]}. \quad (4.27)$$

Perturbative solutions can then be acquired by solving the nonlocal eigen-value equation [53]

$$\hat{\mathcal{K}}(s) \hat{\mathbf{o}}(s) = \hat{k}(s) \hat{\mathbf{o}}(s), \quad (4.28)$$

where from Eq. (4.27) the nonlocal eigen-system must be a perturbation of the free system-energy eigen-system, and therefore our proof of accuracy loss will carry over. The order- $2n$ master equation can only determine the perturbatively-stationary eigen-operators $\hat{\mathbf{o}}(s)$ to within order $2n-2$.

4.1.5 Example: QBM

As an example of an exactly-solvable open system, let us consider the master equation of an oscillator bilinearly coupled (position-position) to an environment of oscillators initially in a thermal state [74]:

$$\frac{d}{dt} \boldsymbol{\rho} = [-i \mathbf{H}_R, \boldsymbol{\rho}] - i \Gamma [\mathbf{x}, \{\mathbf{p}, \boldsymbol{\rho}\}] - MD_{pp} [\mathbf{x}, [\mathbf{x}, \boldsymbol{\rho}]] - D_{xp} [\mathbf{x}, [\mathbf{p}, \boldsymbol{\rho}]], \quad (4.29)$$

where \mathbf{H}_R is the system Hamiltonian but with frequency Ω_R , Γ is the dissipation coefficient, D_{pp} and D_{xp} are the regular and anomalous diffusion coefficients. This master equation describes the dynamics of damped nano-mechanical resonators at low temperature, among other physical systems.

In Ref. [56] exact solutions are given with full time dependence, and it is from this reference that we take all of the following results. Let us consider Ohmic coupling to the bath with damping kernel $\gamma(t) = 2\gamma_0 \delta_\Lambda(t)$, where $\delta_\Lambda(t)$ is a representation of the delta function in the high-frequency cutoff limit $\Lambda \rightarrow \infty$. [The damping kernel, and thus γ_0 , is second order in the system-environment interaction g .] The homogeneous coefficients quickly asymptote to $\Omega_R = \Omega$ and $\Gamma = \gamma_0$ within the cutoff timescale, whereas the diffusion coefficients asymptote to

$$D_{xp} = +\gamma_0 \text{Im}[\mathcal{I}_0] , \quad (4.30)$$

$$D_{pp} = 2\gamma_0 T + \gamma_0 \text{Im} \left[(\gamma_0 + i\tilde{\Omega}) \mathcal{I}_0 \right] , \quad (4.31)$$

$$\mathcal{I}_0 \equiv \frac{2}{\pi} \left(i + \frac{\gamma_0}{\tilde{\Omega}} \right) \left\{ \text{H} \left(\frac{\Lambda}{2\pi T} \right) - \text{H} \left(\frac{\gamma_0 + i\tilde{\Omega}}{2\pi T} \right) \right\} , \quad (4.32)$$

$$\tilde{\Omega} \equiv \sqrt{\Omega^2 - \gamma_0^2} , \quad (4.33)$$

mostly within the system timescale, but also hastened by temperature. In all coefficients we have neglected terms of order $\mathcal{O}(1/\Lambda)$. H here is the harmonic number function, which is asymptotically logarithmic and yet $\text{H}(0) = 0$. Therefore both diffusion coefficients contain logarithmic cutoff sensitivities, though the sensitivity is present in the anomalous diffusion coefficient at second order, whereas it does not appear in the regular diffusion coefficient until fourth order.

In the stationary limit, the system relaxes into a Gaussian state with phase-space covariance

$$\boldsymbol{\sigma}_T = \begin{bmatrix} \frac{1}{M\Omega_R^2} \left(\frac{1}{2\Gamma} D_{pp} - D_{xp} \right) & 0 \\ 0 & \frac{M}{2\Gamma} D_{pp} \end{bmatrix} . \quad (4.34)$$

One can see that for a second-order master equation, the contribution from the regular diffusion D_{pp}/Γ starts at zeroth order, while the contribution from anomalous diffusion D_{xp} starts at second order. The full second-order contribution from the regular diffusion actually requires the fourth-order coefficients.

In the exact calculation, or in any consistent perturbative calculation, the logarithmic cutoff sensitivities present in the diffusion coefficients actually cancel in the position uncertainty. In this sense the anomalous diffusion coefficient acts as an anti-diffusion coefficient and this behavior will also occur for supra-Ohmic couplings. If one were to naively apply the second-order diffusion coefficients, and solve the master equation exactly, then one would obtain a mixed-order result and the logarithmic cutoff sensitivities would not precisely cancel. The position uncertainty would contain a second-order *negative* $\log(\Lambda)$ contribution. For sufficiently large cutoff frequencies, the Heisenberg uncertainty principle would be violated. For even larger frequencies, the covariance would become negative. In any case the second-order master equation would produce a (supposedly) second-order position uncertainty which is an underestimation of the true second-order uncertainty.

4.2 The Rotating-Wave Approximation

The rotating-wave approximation (RWA) is used in many places in the study of open quantum systems, particularly in the fields of quantum optics (see for example [26, 131, 32]) and nuclear magnetic resonance [2], but the validity of the approximation is treated in depth far less often. There are actually two distinct

rotating-wave approximations both in widespread use : 1) the ‘pre-trace’ (preT) RWA, which consists of modifying the interaction Hamiltonian by dropping the so-called counter-rotating terms that are quickly oscillating in the Dirac picture; and 2) the ‘post-trace’ (posT) RWA, which is obtained by neglecting terms in the master equation for the reduced density matrix that are quickly oscillating in the Dirac picture (see, e.g., [131, 32] and [26, 6] respectively). Agarwal examined the RWA [6, 4, 5], differentiating between these two distinct forms and addressing in some respects their validity for atom-field interactions and spontaneous emission processes. More recently, various authors have claimed some features of the RWA that may limit its applicability, which we will now discuss.

The most widely acknowledged problem with the preT RWA seems to be that it yields incorrect frequency shifts in the atomic energy levels, so that it is not suitable for calculating environmentally induced level shifts or induced cooperative frequency shifts [6, 4, 5]. West and Lindenberg [133] found that the reduced system dynamics obtained from the pre-trace RWA do not have a Markovian limit ². Finally, Ford and O’Connell [58] have raised concerns that in general the total Hamiltonian obtained by the preT RWA does not have a spectrum which is bounded below, and they suggest that this limits the applicability of the approximation to first-order transition amplitudes.

Other authors have raised a very different sort of concern about the preT-RWA Hamiltonian for coupling of a localized system to a quantized field, that it

²These authors also claim that there is no fluctuation-dissipation theorem for this model, a statement that the present authors cannot agree with.

may produce spurious causality violation in the calculations. Consider, for example, a two-level atom in the dipole approximation interacting with the electromagnetic field. The Hamiltonian for the interaction is

$$\begin{aligned}
 H &= \vec{d} \cdot \vec{D}(\vec{R}) \\
 &= \sum_{\vec{k}} \sum_{s=1}^2 -i \frac{\Omega}{\sqrt{2\epsilon_0 \epsilon_{\vec{k}} V}} \left(\vec{d} \cdot \vec{e}_{\vec{k},s} \right) \left(\sigma_+ e^{i\omega t} + \sigma_- e^{-i\omega t} \right) \left(\mathbf{a}_{\vec{k},s} e^{-i\epsilon_{\vec{k}} t} - \mathbf{a}_{\vec{k},s}^\dagger e^{i\epsilon_{\vec{k}} t} \right)
 \end{aligned} \tag{4.35}$$

in the Dirac picture, and in the preT RWA the terms with frequency $\Omega + \epsilon_{\vec{k}}$ would be neglected. However, with these terms dropped the interaction can no longer be expressed in terms of the local field variable $\vec{D}(\vec{R})$ [37]. Indeed, a numerical study of a three-atom problem [45] found that noncausal terms appear when the preT RWA is used, unless one makes the *ad hoc* modification of extending frequency integrals to $-\infty$. The preT RWA may then misrepresent the effects of retarded propagation in the electromagnetic field, which suggests problems with causality in the study of multipartite systems.

Moreover, the Glauber detector model [64, 63], long used in photodetection theory and quantum optics, uses the preT RWA, and it might give rise to quantum correlations between spacelike separated events that do not represent the effects of actual entanglement. The effective status of preT RWA in Glauber's theory is debated: some authors have shown that photodetection probabilities at short times appear to violate causality [29, 127], and modifications to Glauber's photodetection theory have been suggested [29, 127, 52], while others indicate that a different form of the RWA in photodetection theory can guarantee causality [102]. Our interest in this problem partly arose from discussion of how the imposition of preT RWA affects

the range of validity of results from the calculation of the entanglement dynamics of two atoms interacting with a common quantum field at large atomic separation [11].

Some form of the RWA is often invoked in the quantum optics and atomic physics literature, in derivations of the Born-Markov master equation for a system weakly coupled to bosonic reservoir. In such derivations, the Born-Markov master equation requires an RWA to render it in *Lindblad form* [26], thus providing a completely-positive dynamical map (for all states at all times) as is useful to assume for many quantum information theory discussions.

With these two distinct RWAs in widespread use while some open questions remain about their limitations and fallacies, we find it useful to carry out a systematic analysis of the consistency and applicability of the RWAs in the modern language of open quantum systems. This is especially needed with researchers now tackling problems beyond those of level population and dissipation rates to deal with more subtle issues such as quantum decoherence and entanglement dynamics and performing more demanding tasks such as quantum state tomography and engineering.

In the analysis that follows, we find that the RWA may be sufficient or insufficient depending on what information is desired about the system. For the perturbative relaxation rates either the pre-trace or post-trace RWA is sufficient. To obtain the environmentally induced shifts in system frequencies, only the post-trace RWA is sufficient. In order to get more detailed information about the evolution of the quantum state, entanglement dynamics, and the asymptotic steady state nei-

ther RWA is sufficient in general. We also find that the pre-trace RWA does not in general have a Markovian limit. Finally, we seek to emphasize the following fact: Even in a system where the underlying environmental noise is colored and dynamics nonlocal, the RWA can yield a Lindblad-form master equation similar to what one might get in the Markovian limit with white noise. However, with the inclusion of multiple systems and any external forces, one cannot obtain the correct dynamics by naively adding together the dissipative terms of the master equations, as would be possible in the Markovian limit. While the master equation obtained by such a naive addition has a mathematically valid form, it does not generally yield the dynamics of the system obtained from a microscopic derivation of the master equation for the combined system (even after the RWA).

However, there are sufficiently simple systems and bath correlations for which a less judicious application of the RWA can nevertheless produce an adequate master equation. Likewise, there are mathematical limits in which the RWA will be exact, and in some cases experiments may work very close to these limits. Finally, we find that finite bandwidth of measurements may mask the inaccuracies produced by the RWA (at least for some measurements).

4.2.1 The rotating-wave approximation in closed systems

We first examine the rotating-wave approximation as ordinarily applied to a closed system consisting of several interacting subsystems. Its wave function $|\psi\rangle$

evolves as

$$\frac{d}{dt} |\psi\rangle = -i \mathbf{H} |\psi\rangle , \quad (4.36)$$

under the total Hamiltonian $\mathbf{H} \equiv \mathbf{H}_0 + \mathbf{H}_1$ where \mathbf{H}_0 represents the sum of all uncoupled subsystems and \mathbf{H}_1 represents the part from the subsystems coupling. One seeks to solve the eigenvalue problem

$$\mathbf{H} |\omega\rangle = \omega |\omega\rangle , \quad (4.37)$$

for eigenstates $|\omega\rangle$ with eigenvalues ω by perturbing off the free eigensystem

$$\omega_i = \omega_i^{(0)} + \delta\omega_i^{(1)} + \dots , \quad (4.38)$$

$$|\omega_i\rangle = |\omega_i^{(0)}\rangle + |\delta\omega_i^{(1)}\rangle + \dots , \quad (4.39)$$

where $\omega_i^{(0)}$ are the eigenvalues of the uncoupled system. The *non-degenerate* first-order corrections are then

$$\delta\omega_i^{(1)} = \langle \omega_i^{(0)} | \mathbf{H}_1 | \omega_i^{(0)} \rangle , \quad (4.40)$$

$$\langle \omega_j^{(0)} | \delta\omega_i^{(1)} \rangle = \frac{\langle \omega_j^{(0)} | \mathbf{H}_1 | \omega_i^{(0)} \rangle}{\omega_i - \omega_j} \quad (\omega_i \neq \omega_j) , \quad (4.41)$$

and for the *degenerate* corrections one must find the correct linear combination of degenerate states $|f\rangle$, which exist solely in the degenerate subspace $|\omega_{d_i}^{(0)}\rangle$ wherein $\mathbf{H}_0 |\omega_{d_i}^{(0)}\rangle = \omega_d |\omega_{d_i}^{(0)}\rangle$. $|f\rangle$ are the eigenstates of the degenerate interaction \mathbf{H}_d

$$\mathbf{H}_d |f\rangle = f |f\rangle , \quad (4.42)$$

which possesses matrix elements

$$(H_d)_{ij} = \langle \omega_{d_i}^{(0)} | \mathbf{H}_1 | \omega_{d_j}^{(0)} \rangle , \quad (4.43)$$

This kind of analysis should also extend to *nearly-degenerate* subspaces where the basis corrections in Eq. (4.41) would nearly diverge.

In the rotating-wave approximation one only considers components of the interaction \mathbf{H}_1 which oscillate least rapidly in the interaction picture. If these terms are stationary, e.g. at resonance, then they will include the correct non-degenerate first-order frequencies, Eq. (4.40), as well as the correct characteristic equation, Eq. (4.43), which determines the degenerate first-order frequencies and zeroth-order energy states. What the RWA generally neglects are the first-order basis corrections, Eq. (4.41). If the RWA terms are non-stationary, then they will include the most nearly-degenerate first-order frequencies and also neglect their first order basis corrections. Therefore the RWA has limited correspondence to perturbation theory as long as all terms that are close to resonance have been retained in the interaction Hamiltonian. If, however, the RWA is made such that there are neglected terms that are near resonance, then the correspondence fails even in the weak coupling regime (because the missing first-order basis corrections become large, and even the first-order eigenvalue corrections are inaccurate). Moreover, for subsystems with a multiplicity of timescales, there may be several near-resonance frequencies which a proper application of RWA would have to take into account.

In the rest of this section we consider open quantum systems and divide our attention between two cases: the post- and pre- trace RWA.

4.2.2 The post-trace rotating-wave approximation

The RWA is an approximation that is employed in the weak-coupling regime. It is a valid question to ask precisely what this approximation is doing by comparing it to the weak coupling dynamics without the RWA. As we will show, the post-trace RWA actually lies between the zeroth-order and second-order master equations. For a system weakly coupled to a reservoir, such open-system master equations can be derived perturbatively, in the system-environment interaction, with a variety of different techniques [81, 25, 122]. All of these are equivalent to no approximations other than ordinary perturbation in the interaction. The second-order perturbative master equation, which we call the weak-coupling master equation, is known to be non-Markovian [81, 25, 122]. While the master equation can assume a Lindblad form in the limit of vanishing coupling, for any actual finite coupling it will generally differ from Lindblad form. The rotating-wave approximation is often introduced, not in a purely perturbatively derived master equation, but in one derived via the Born-Markov approximation. To second order in the system-environment interaction, the Born-Markov approximation is consistent with weak coupling perturbation, even well outside of the Markovian limit. Therefore, given that the RWA will only be applicable to second order, it is of no consequence if one starts from the Born-Markov approximation or a more rigorous perturbative analysis. One only has to keep in mind that RWA has no reliance upon any kind of Markovian approximation.

It may also be useful to note that Davies has derived [40, 41] a Lindblad-form master equation in the weak-coupling regime with the additional requirement

that one take the limit where the coupling λ vanishes and rescale time as $\tau = \lambda^2 t$, effectively taking a simultaneous $t \rightarrow \infty$ limit. Our analysis supposes only weak (but non-vanishing) coupling and can be applied even at early times, although we focus on the late-time dynamics, so in principle we are restricted to neither limit.

The post-trace (posT) RWA effectively consists of only considering the parts of the super-operator $\mathcal{L}_{[2]}$ which commute with the free system propagation super-operator

$$\mathcal{G}_0(t)\{\rho\} = e^{-iHt} \rho e^{+iHt}. \quad (4.44)$$

If we consider evaluating our master equation coefficients in the energy basis, which in pseudo-Lindblad form amounts to resolving

$$\mathcal{D}_{ki;jl} = \sum_{nm} \mathcal{D}_{nm} \langle \omega_k | \mathbf{e}_n | \omega_i \rangle \langle \omega_j | \mathbf{e}_m^\dagger | \omega_l \rangle, \quad (4.45)$$

then the RWA essentially amounts to projecting out the diagonal of this Hermitian matrix, i.e. terms with $\omega_k - \omega_i = \omega_j - \omega_l$ or equivalently $\omega_i - \omega_j = \omega_k - \omega_l$. For the perturbative master equation to second order in the system-environment coupling, which is assumed to be weak, these diagonal entries will settle to positive values and therefore this projection yields a master equation of the Lindblad form. We will refer to the master equation obtained this way as the RWA-Lindblad equation.

Such a Lindblad projection is only reasonable because the system-environment coupling is assumed to be weak and the projection is performed in the energy basis. As we will presently show, the eigen-operators of the Liouvillian have the form $|\omega_j\rangle \langle \omega_k|$ plus corrections at second order in the coupling strength so that the discrepancy introduced by the dropped terms is small for sufficiently weak coupling.

The RWA-Lindblad equation is not fully equivalent to the weak coupling master equation, but it generates an evolution which is close to that of the weak coupling master equation in a perturbative sense.

4.2.2.1 Correspondence with perturbation theory

Recall from Sec. 1.2.3 that the environmentally-induced corrections to the eigenvalues and eigenoperators of the Liouvillian are

$$f_{ij}^{[2]} = \langle \omega_i | \mathcal{L}_{[2]} \{ |\omega_i\rangle\langle\omega_j| \} | \omega_j \rangle, \quad (4.46)$$

$$\langle \omega_{i'} | \mathbf{o}_{ij}^{[2]} | \omega_{j'} \rangle = \frac{\langle \omega_{i'} | \mathcal{L}_{[2]} \{ |\omega_i\rangle\langle\omega_j| \} | \omega_{j'} \rangle}{-i(\omega_{ij} - \omega_{i'j'})} \quad (4.47)$$

when $\omega_i \neq \omega_j$ and $\omega_{ij} \neq \omega_{i'j'}$. From this we see that the perturbative corrections to the eigenvalues are entirely captured by the post-trace RWA, since those terms in the Liouvillian are retained in the RWA. The perturbative basis corrections, however, are entirely neglected. The lack of basis perturbation can lead to discrepancies (with the non-RWA evolution) even at late times, as was seen for example by Haikka and Maniscalco in [68].

We can readily see a late-time discrepancy in the thermal state of the system. The system evolving under the RWA-Lindblad equation will relax into the thermal state described by the Boltzmann density matrix $\boldsymbol{\rho} \propto e^{-\beta \mathbf{H}}$. But this is generally not how most systems would actually thermalize in a Hamiltonian formulation: Given the full system + bath and interaction Hamiltonian, $\mathbf{H} + \mathbf{H}_B + \mathbf{H}_I$, the system is expected to relax into a state described by the reduced density matrix

$\rho \propto \text{Tr}_B [e^{-\beta(\mathbf{H}+\mathbf{H}_B+\mathbf{H}_I)}]$, assuming the bath to be very large³. This state typically only reduces to Boltzmann form in the limit of zero system-bath interaction strength; however, an infinitesimal interaction strength would imply an infinite relaxation time, so we cannot speak self-consistently of the system relaxing to the thermal state the RWA-Lindblad equation predicts.

This property suggests a limitation to the applicability of postT RWA in the study of entanglement dynamics. In a multipartite system with components interacting only through the bath, this precludes the presence of asymptotic residual entanglement. This is in contrast to the asymptotic behavior of bipartite systems in quantum Brownian motion—see, for example [107, 108, 92].

We also remark that if one takes the simultaneous limits of vanishing coupling and $t \rightarrow \infty$ on the second-order master equation such that all $f_{ij}^{[2]}t$ remain finite following Davies [40, 41], then one will similarly obtain a master equation of Lindblad form, which is exactly the RWA-Lindblad equation. Our perturbative approach is not restricted to such a limit, of course, and the difference between the perturbative weak-coupling dynamics and the postT RWA dynamics will also show the difference with the limit of vanishing coupling used by Davies, namely the limit used by Davies removes the lowest order basis corrections.

³That the entire system + environment appears thermalized in its reduction is proven to second order in [53].

4.2.2.2 RWA fails when perturbation theory fails

The second-order master equation should be valid when the second-order corrections provided by $\mathcal{L}_{[2]}$ are small as compared to the unperturbed dynamics generated by \mathcal{L}_0 . Let us denote the strength of the dissipative corrections generically by the frequency γ_D , then the weak coupling condition is

$$\gamma_D \ll \min_{\omega_{ij} \neq 0} |\omega_{ij}|, \quad (4.48)$$

as ω_{ij} corresponds to the eigenvalues of \mathcal{L}_0 (not ω_i which corresponds to the eigenvalues of the unperturbed Schrödinger equation).

The RWA-Lindblad equation does not directly correspond to the second-order master equation, but more correctly to the second-order solutions of said master equation. For the second-order solutions to be valid the coupling must not only be weak in the above sense but also in the following sense

$$\gamma_D \ll \min_{\omega_{ij} \neq \omega_{kl}} |\omega_{ij} - \omega_{kl}|, \quad (4.49)$$

which justifies the perturbative solutions. One cannot have near degeneracy in the energy level splittings or the naive perturbative solutions, which the RWA-Lindblad equation corresponds to, will fail. Perfect degeneracy is acceptable; the RWA-Lindblad equation retains these terms in the Pauli master equation for instance. But near-degeneracy needs to be treated in a manner analogous to degeneracy; the nearly degenerate subspace should be diagonalized. With the second-order master equation this is still possible, but with the RWA-Lindblad equation these terms have been discarded and one is left with an invalid master equation. Thus, there can

be situations where the weak-coupling condition is satisfied while the post-RWA condition is not.

This problem arises, for example, in cavity QED. A two-level atom of frequency Ω coupled to a resonant intracavity field mode will result in an energy spectrum of the composite system that has the form of the harmonic oscillator with each level split in two by the Rabi frequency $\sqrt{n}\Omega_{VR}$ of the dressed states,

$$E_{n,\pm} = (\Omega n \pm \sqrt{n}\Omega_{VR}) .$$

If the intracavity field is coupled to the field outside the cavity, this becomes an open quantum system. If the intracavity field is coupled weakly enough to the atom, then the system will be in the weak-coupling regime of cavity QED and the vacuum Rabi frequency Ω_{VR} will be small compared to γ_D . In this case the post-RWA procedure does not, strictly speaking, apply as was noted by Scala et. al. [117].

In such a case one can still do a partial RWA, neglecting terms that oscillate much faster than γ_D and keeping those that are slower. This still leaves the master equation in pseudo-Lindblad form; however, assuming these timescales are sufficiently slow and the spectrum of environmental noise is sufficiently flat, one may be able to make an effective Markovian approximation for the remaining pseudo-Lindblad terms (even if one might not have been valid for original master equation due to the faster system dynamics that have been ignored in the post-RWA) to recover a Lindblad-form master equation. Scala et. al. argued this is the case for cavity QED with a low-temperature bath [116].

4.2.2.3 Combining RWA-Lindblad Equations

A non-Markovian master equation will exhibit memory in a manner that is not naively apparent in its time-local representation. This is true even of the RWA-Lindblad equation, despite the fact that it is of Lindblad form as one would have in a Markovian limit. Let us consider the master equations for the reduced density matrices of the (open) systems A and B with Hamiltonians $\mathbf{H}_A, \mathbf{H}_B$ each coupled to a dissipative environment of equivalent influence. We then have the open system

$$\frac{d}{dt}\rho_A = -i[\mathbf{H}_A, \rho_A] + \delta\mathcal{L}_A\{\rho_A\}, \quad (4.50)$$

$$\frac{d}{dt}\rho_B = -i[\mathbf{H}_B, \rho_B] + \delta\mathcal{L}_B\{\rho_B\}, \quad (4.51)$$

where the Hamiltonians are those of the free systems and the corrections to the Liouville operator are introduced via interaction with the dissipative environment. In the Hamiltonian formalism one can simply add two Hamiltonians and arrive at another Hamiltonian, though one might be motivated to fix the energy spectrum through renormalization. One cannot do this with non-Markovian Liouville operators. E.g. given some coupling \mathbf{H}_{AB} between subsystems one cannot simply add dissipative terms.

$$\frac{d}{dt}\rho_{A+B} \neq -i[\mathbf{H}_A + \mathbf{H}_B + \mathbf{H}_{AB}, \rho_{A+B}] + \delta\mathcal{L}_A\{\rho_{A+B}\} + \delta\mathcal{L}_B\{\rho_{A+B}\} \quad (4.52)$$

The above (incorrect) master equation is in general completely different from the correct open-system master equation derived from first principles. For non-Markovian processes, the environmental contributions have a nontrivial dependence (due to memory effects) upon the system's dynamics through their couplings. If one changes

the system Hamiltonian then one must also change the environmental contributions to be compatible with the history these new terms will create. This is how memory exhibits itself in a time-local representation. Moreover, one must also take into account whether or not the dissipative environments are separate or shared. If the dissipative environment is shared then the two subsystems can interact via environmental back-reaction. This effect is also missed when simply combining the Liouville operators.

In a general non-Markovian master equation, the problems of the above incorrect master equation would be readily apparent as it would likely violate positivity, uncertainty, etc. Positivity violation will not occur when adding RWA-Lindblad terms, but the mistake has only become more subtle and therefore more dangerous. The master equation might be completely positive, but it does not correspond to the dynamics of the physical system considered. This is the key point.

This issue has already been commented on in the context of cavity QED. The often-used master equation includes the Hamiltonian for the atom, intracavity field, and atom-field interaction, but the dissipator used is exactly that of an empty cavity with dissipation plus that of an atom spontaneously emitting into empty space, so that the situation is just that depicted in Eq. (4.52). And, indeed, if one begins instead with the atom-cavity system and derives the microscopic master equation using the standard technique [26], one finds that the master equation has a different dissipative term [117, 116]. As explained in [116] if the spectrum of environmental noise is sufficiently flat then the difference is suppressed, which explains the success of the standard cavity QED master equation. But this is not true in general, and it

is a point often overlooked.

4.2.2.4 Application to the two-level atom

Here we consider a two-level system with σ_z Hamiltonian and energy level splitting Ω , bilinearly coupled to a thermal reservoir via a σ_x coupling. This would, for example, model a two-level atom coupled to the electromagnetic field in the dipole approximation. Denoting our reduced density matrix

$$\boldsymbol{\rho} = \begin{bmatrix} \rho_{++} & \rho_{+-} \\ \rho_{-+} & \rho_{--} \end{bmatrix}, \quad (4.53)$$

one can compute the second-order master equation [53] and place it into the form

$$\frac{d}{dt} \begin{bmatrix} \rho_{++} \\ \rho_{--} \end{bmatrix} = \frac{\Gamma}{\cosh\left(\frac{\Omega}{2T}\right)} \begin{bmatrix} -e^{+\frac{\Omega}{2T}} & +e^{-\frac{\Omega}{2T}} \\ +e^{+\frac{\Omega}{2T}} & -e^{-\frac{\Omega}{2T}} \end{bmatrix} \begin{bmatrix} \rho_{++} \\ \rho_{--} \end{bmatrix}, \quad (4.54)$$

$$\frac{d}{dt} \begin{bmatrix} \rho_{+-} \\ \rho_{-+} \end{bmatrix} = \begin{bmatrix} -\Gamma - i(\Omega - \delta\Omega) & +\Gamma + i\delta\Omega \\ +\Gamma - i\delta\Omega & -\Gamma + i(\Omega - \delta\Omega) \end{bmatrix} \begin{bmatrix} \rho_{+-} \\ \rho_{-+} \end{bmatrix}, \quad (4.55)$$

with decoherence rate (here also the half thermalization rate) and energy level shift

$$\Gamma \equiv \Gamma(\Omega), \quad (4.56)$$

$$\delta\Omega \equiv \frac{2}{\pi} \int_0^\infty d\varepsilon \mathcal{P} \left[\frac{\Omega}{\varepsilon^2 - \Omega^2} \right] \Gamma(\varepsilon), \quad (4.57)$$

in terms of the phenomenological decoherence rate function $\Gamma(\omega)$. \mathcal{P} denotes the Cauchy principal value which regulates contained poles from contributing to the integral.

This master equation and those that follow are exact to second order, only the coefficients have been allowed to relax to their asymptotic values. The relax-

ation occurs quickly, within the system and bath timescales, as compared to their effect, which occurs in the coupling timescale. Therefore, when considering properly correlated initial states which do not jolt, it is safe to consider this “late-time” regime.

In terms of the microscopically derived damping kernel $\tilde{\gamma}(\omega)$, the anti-derivative of the dissipation kernel, the decoherence rate can be expressed

$$\Gamma(\Omega) = \tilde{\gamma}(\Omega) \Omega \coth\left(\frac{\Omega}{2T}\right). \quad (4.58)$$

Regardless of system-environment coupling, the damping kernel is effectively constant for Ohmic coupling, which along with high temperature is responsible for thermal white noise. For linear coupling to the collective positions of a bath of harmonic oscillators the dissipation kernel has no more temperature dependence than the system-environment coupling itself.

The post-trace RWA here amounts to neglecting the dynamical interaction between ρ_{+-} and ρ_{-+} . To second order in the coupling, the only effect of this is to neglect a perturbative amount of phase information pertaining to their damped oscillations, i.e. the perturbative change of basis. The asymptotic state works out to be exactly the same in either case. Thus under the specific conditions leading to these results the post-trace RWA can be viewed as largely acceptable and somewhat innocuous.

4.2.2.5 Application to quantum Brownian motion

Now we return to the example of Quantum Brownian Motion (QBM), which is of interest since the problem is exactly solvable. The master equation will have a stationary limit if the noise correlation is not excessively widespread in time (e.g. a regulated ohmic coupling is perfectly suitable). To lowest order in the coupling, the late-time expressions for these coefficients can be determined from the weak coupling master equation [53] to be

$$\Gamma = \Gamma(\Omega), \quad (4.59)$$

$$\Omega_{\text{R}} = \Omega - \frac{2}{\pi} \int_0^\infty d\varepsilon \mathcal{P} \left[\frac{\varepsilon^2}{\varepsilon^2 - \Omega^2} \right] \Gamma(\varepsilon), \quad (4.60)$$

$$D_{pp} = \Gamma(\Omega) \Omega \coth\left(\frac{\Omega}{2T}\right), \quad (4.61)$$

$$D_{xp} = +\frac{2}{\pi} \int_0^\infty d\varepsilon \mathcal{P} \left[\frac{1}{\varepsilon^2 - \Omega^2} \right] \Gamma(\varepsilon) \varepsilon \coth\left(\frac{\varepsilon}{2T}\right), \quad (4.62)$$

in terms of the phenomenological dissipation function, which is proportional to the dissipation kernel at second order.

For this problem, the Fokker-Planck equation for the probability distribution function (Wigner function) W in a phase space representation presents a much cleaner picture with simple solutions [56].

$$\frac{d}{dt} W = \left\{ \vec{\nabla}^T \mathbf{H} \vec{q} + \vec{\nabla}^T \mathbf{D} \vec{\nabla} \right\} W, \quad (4.63)$$

$$\vec{q} = [x, p]^T, \quad (4.64)$$

$$\vec{\nabla} = \left[\frac{\partial}{\partial x}, \frac{\partial}{\partial p} \right]^T, \quad (4.65)$$

The matrices \mathbf{H} and \mathbf{D} are the homogeneous and diffusion coefficient matrices

respectively.

$$\mathcal{H} = \begin{bmatrix} 0 & -\frac{1}{M} \\ M\Omega_{\text{R}}^2 & 2\Gamma \end{bmatrix}, \quad (4.66)$$

$$\mathcal{D} = \begin{bmatrix} 0 & -\frac{1}{2}D_{xp} \\ -\frac{1}{2}D_{xp} & M D_{pp} \end{bmatrix}. \quad (4.67)$$

Do not confuse the homogeneous generator with the Hamiltonian; they differ by some frequency renormalization and the dissipation Γ . From hereon we will assume the system frequency to be properly renormalized such that $\Omega_{\text{R}} = \Omega$ in the stationary limit. The diffusion matrix contains two components: the regular diffusion D_{pp} and an anomalous anti-diffusion D_{xp} which keeps the position uncertainty insensitive to high frequency.

If one expresses the QBM master equation in terms of ladder operators, the pseudo-Lindblad coefficient matrix can be calculated to be

$$\mathcal{D} = \frac{1}{\Omega} \begin{bmatrix} D_{pp} - \Gamma \Omega & D_{pp} + iD_{xp} \Omega \\ D_{pp} - iD_{xp} \Omega & D_{pp} + \Gamma \Omega \end{bmatrix}. \quad (4.68)$$

The rotating-wave approximation then constitutes projecting out the diagonal of this matrix, which will be positive definite. Transforming back into the phase space representation, the Fokker-Plank coefficients become

$$\mathcal{H}_{\text{RWA}} = \begin{bmatrix} \Gamma & -\frac{1}{M} \\ M\Omega_{\text{R}}^2 & \Gamma \end{bmatrix}, \quad (4.69)$$

$$\mathcal{D}_{\text{RWA}} = \begin{bmatrix} \frac{D_{pp}}{2M\Omega^2} & 0 \\ 0 & \frac{MD_{pp}}{2} \end{bmatrix}. \quad (4.70)$$

The anomalous diffusion coefficient vanishes entirely while the dissipation and regular diffusion coefficients are both broken in half, with the missing half reappearing as an analogous coefficient of the master equation.

The role of the homogeneous coefficients are to generate the homogeneous propagator $e^{-t\mathcal{H}}$. The RWA homogeneous coefficients are just slightly off in both the oscillation rates and phase; the dissipation rates are entirely correct. Compare the characteristic frequencies of the two matrices

$$h = \Gamma \pm i\sqrt{\Omega^2 - \Gamma^2}, \quad (4.71)$$

$$h_{\text{RWA}} = \Gamma \pm i\Omega. \quad (4.72)$$

The diffusion coefficients are relatively more mangled given that the anomalous coefficient is entirely absent. The effect of diffusion is only present in the second cumulant or covariance of the Wigner function. For this stationary master equation, the evolution of the covariance is simply

$$\boldsymbol{\sigma}(t) = e^{-t\mathcal{H}} [\boldsymbol{\sigma}(0) - \boldsymbol{\sigma}(\infty)] e^{-t\mathcal{H}^T} + \boldsymbol{\sigma}(\infty), \quad (4.73)$$

where the stationary covariance is determined by the Lyapunov equation

$$\mathcal{H}\boldsymbol{\sigma}(\infty) + \boldsymbol{\sigma}(\infty)\mathcal{H}^T = 2\mathbf{D}. \quad (4.74)$$

We can easily compare the stationary covariances.

$$\boldsymbol{\sigma}(\infty) = \begin{bmatrix} \frac{1}{M\Omega^2} \left(\frac{1}{2\Gamma} D_{pp} - D_{xp} \right) & 0 \\ 0 & \frac{M}{2\Gamma} D_{pp} \end{bmatrix}, \quad (4.75)$$

$$\boldsymbol{\sigma}_{\text{RWA}}(\infty) = \begin{bmatrix} \frac{1}{M\Omega^2} \frac{1}{2\Gamma} D_{pp} & 0 \\ 0 & \frac{M}{2\Gamma} D_{pp} \end{bmatrix}. \quad (4.76)$$

Amazingly the only difference in the stationary state will come from the lack of an anomalous diffusion coefficient. This contribution will ultimately be lower order in the coupling, due to the Γ^{-1} prefactor before D_{pp} , and therefore its absence is acceptable perturbatively.

4.2.3 The pre-trace rotating-wave approximation

4.2.3.1 Inconsistency of approximation

Let us consider a bilinear interaction Hamiltonian \mathbf{H}_I between a system observable \mathbf{L} and the collective environment observable \mathbf{l} .

$$\mathbf{H}_I = \mathbf{L} \mathbf{l}, \quad (4.77)$$

For each of these operators, assuming them to be completely non-stationary, there is a *gross* raising and lowering decomposition \mathbf{L}_\pm given by

$$\mathbf{L}_+ = \sum_{i>j} \langle \omega_i | \mathbf{L} | \omega_j \rangle | \omega_i \rangle \langle \omega_j |, \quad (4.78)$$

$$\mathbf{L}_- = \sum_{i<j} \langle \omega_i | \mathbf{L} | \omega_j \rangle | \omega_i \rangle \langle \omega_j |, \quad (4.79)$$

such that

$$\mathbf{L} = \mathbf{L}_+ + \mathbf{L}_-, \quad (4.80)$$

$$\mathbf{J} = i(\mathbf{L}_+ - \mathbf{L}_-), \quad (4.81)$$

$$\mathbf{L}_\pm^\dagger = \mathbf{L}_\mp, \quad (4.82)$$

where \mathbf{L} and \mathbf{J} will be two relevant observables. For position coupling with a harmonic oscillator the decomposition becomes

$$\mathbf{L} = \mathbf{x}, \quad (4.83)$$

$$\mathbf{L}_+ = \frac{1}{\sqrt{2M\Omega}} \mathbf{a}^\dagger, \quad (4.84)$$

$$\mathbf{L}_- = \frac{1}{\sqrt{2M\Omega}} \mathbf{a}, \quad (4.85)$$

$$\mathbf{J} = \frac{1}{M\Omega} \mathbf{p}, \quad (4.86)$$

and for σ_x coupling with a σ_z Hamiltonian (two-level system) we have

$$\mathbf{L} = \sigma_x, \quad (4.87)$$

$$\mathbf{L}_\pm = \frac{1}{2} \sigma_\pm, \quad (4.88)$$

$$\mathbf{J} = -\sigma_y. \quad (4.89)$$

Now consider coupling the system to an environment made of a large number of harmonic oscillators in their collective positions. Let us furthermore assume the system coupling is like that of the above harmonic oscillator or two-level system such that it is characterized by a single frequency Ω .

$$\mathbf{l} = \sum_k c_k \mathbf{x}_k, \quad (4.90)$$

$$\mathbf{H}_I = \sum_k \frac{c_k}{\sqrt{m_k \varepsilon_k}} \left\{ \left(\mathbf{L}_+ \mathbf{a}_k + \mathbf{L}_- \mathbf{a}_k^\dagger \right) + \left(\mathbf{L}_+ \mathbf{a}_k^\dagger + \mathbf{L}_- \mathbf{a}_k \right) \right\}, \quad (4.91)$$

where \mathbf{x}_k is the environment position operator with ladder operator \mathbf{a}_k , energy ε_k and mass m_k . In the interaction picture we have the interaction Hamiltonian

$$\begin{aligned} \mathbf{H}_I(t) = & \sum_k \frac{c_k}{\sqrt{2m_k \varepsilon_k}} \left(\mathbf{L}_+ \mathbf{a}_k e^{+i(\Omega - \varepsilon_k)t} + \mathbf{L}_- \mathbf{a}_k^\dagger e^{-i(\Omega - \varepsilon_k)t} \right) + \\ & \sum_k \frac{c_k}{\sqrt{2m_k \varepsilon_k}} \left(\mathbf{L}_+ \mathbf{a}_k^\dagger e^{+i(\Omega + \varepsilon_k)t} + \mathbf{L}_- \mathbf{a}_k e^{-i(\Omega + \varepsilon_k)t} \right). \end{aligned} \quad (4.92)$$

An often utilized pre-trace rotating-wave approximation (preT RWA) is to neglect the second terms (conventionally referred to as counter-rotating terms) as they are deemed more rapidly oscillating than the first. However, this is only true in a mode-by-mode comparison. Keeping terms of frequency $|\Omega - 2\Omega| = \Omega$ while discarding terms of frequency $|\Omega + 0| = \Omega$ serves no good purpose. There is no a priori sense in which this is an approximation at all, unless the only environment modes which exist are near resonance.

A true bandwidth approximation which does what the preT RWA claims would instead modify the interaction Hamiltonian of Eq. (4.92) (before tracing out the environment) by neglecting all the “rapid” terms that oscillate with a frequency outside some frequency band $\Delta\omega$ in the interaction picture while retaining all the slower terms ⁴. The resulting Hamiltonian would be

$$\begin{aligned} \mathbf{H}_I(t) = & \sum_{\varepsilon_k=0}^{\Delta\omega+\Omega} \frac{c_k}{\sqrt{2m_k\varepsilon_k}} \left(\mathbf{L}_+ \mathbf{a}_k e^{+i(\Omega-\varepsilon_k)t} + \mathbf{L}_- \mathbf{a}_k^\dagger e^{-i(\Omega-\varepsilon_k)t} \right) + \\ & \sum_{\varepsilon_k=0}^{\Delta\omega-\Omega} \frac{c_k}{\sqrt{2m_k\varepsilon_k}} \left(\mathbf{L}_+ \mathbf{a}_k^\dagger e^{+i(\Omega+\varepsilon_k)t} + \mathbf{L}_- \mathbf{a}_k e^{-i(\Omega+\varepsilon_k)t} \right) \end{aligned} \quad (4.93)$$

Note that if $\Delta\omega < \Omega$, then the bandwidth approximated Hamiltonian would have no counter-rotating terms . Furthermore, if the environment were such that all environmental frequencies ε_k lie in a band around resonance with $|\varepsilon_k - \Omega| < \Omega$, then a bandwidth approximation using this band would be equivalent to dropping all counter-rotating terms. However, in the general case the two approximations are

⁴Note that this “bandwidth” Hamiltonian does *not* arise from restricting the field to some bandwidth of modes around the resonance frequency.

inequivalent, and simply dropping all counter-rotating terms is inconsistent.

It is also important to note that if the bandwidth approximation of Eq. (4.93) is performed with $\Delta\omega$ chosen such that all near-degenerate terms are retained, then this is just the sort of RWA we discussed in Sec. 4.2.1. The only difference is that the environment is to be traced out at the end of the calculation. In any case, such a bandwidth approximation would render the problem more difficult to solve than simply calculating a full perturbative solution.

4.2.3.2 Noise and the Markovian limit

The Hamiltonian obtained after RWA is not generally an approximation of the full interaction Hamiltonian for reservoirs. It is nonetheless a linear Hamiltonian interaction with a thermal reservoir and will cause dissipation, decoherence, thermalization, etc. Therefore it still possesses some of the same character as the original model.

Back in terms of observables, the RWA interaction Hamiltonian takes the form

$$\mathbf{H}_I = \frac{1}{2} \mathbf{L} \sum_k c_k \mathbf{x}_k + \frac{1}{2} \mathbf{J} \sum_k c_k \frac{\mathbf{p}_k}{m_k \omega_k}, \quad (4.94)$$

and thus it describes a different but related set of system variables coupled to a different, but related set of bath variables. This results in two quantum noise sources

$$\mathbf{l}_{\text{RWA}} = \frac{1}{2} \sum_k c_k \mathbf{x}_k, \quad (4.95)$$

$$\mathbf{j}_{\text{RWA}} = \frac{1}{2} \sum_k c_k \frac{\mathbf{p}_k}{m_k \omega_k}, \quad (4.96)$$

which have not only autocorrelations in and of themselves but cross-correlations between themselves. Perhaps more clearly, if we consider the original damping

kernel with one \mathbf{L} -coupled source

$$\tilde{\gamma}(\omega) = \tilde{\gamma}(\omega) \begin{bmatrix} 1 & 0 \\ 0 & 0 \end{bmatrix}, \quad (4.97)$$

then the RWA damping kernel with both \mathbf{L} and \mathbf{J} -coupled sources becomes

$$\tilde{\gamma}_{\text{RWA}}(\omega) = \frac{\tilde{\gamma}(\omega)}{4} \begin{bmatrix} 1 & -i \text{sign}(\omega) \\ +i \text{sign}(\omega) & 1 \end{bmatrix}, \quad (4.98)$$

with reference to the original damping kernel $\tilde{\gamma}(\omega)$. The damping kernel, here in Fourier space, is defined (as in [53]) as the anti-derivative of the multivariate dissipation kernel, which is itself the imaginary part of the multivariate noise correlation in the time domain. The diagonal components come from the self-correlations $\langle \mathbf{l}(t) \mathbf{l}(\tau) \rangle_{\text{B}}$ and $\langle \mathbf{j}(t) \mathbf{j}(\tau) \rangle_{\text{B}}$, while the off-diagonal components come from the cross-correlations $\langle \mathbf{l}(t) \mathbf{j}(\tau) \rangle_{\text{B}}$ and $\langle \mathbf{j}(t) \mathbf{l}(\tau) \rangle_{\text{B}}$.

There is a subtle pathology in the cross-correlations of these two noise sources. The RWA interaction is an example of couplings to *different* kinds of bath observables with strong cross-coupling. Such couplings do not always admit a Markovian limit. The reason for this is because in addition to high temperature, the white noise limit also requires a local damping kernel, i.e. one constant in the Fourier domain. This is not a problem with one noise source as one can typically choose an appropriate coupling, e.g. Ohmic, such that the damping kernel will work out to be local. But with multivariate noise one must make all components of the damping tensor local, including new kinds of terms which arise from the cross-correlations. Whether or not this is possible depends in part upon any relation between the self-correlations and the cross-correlations.

For the RWA damping tensor, if we make the diagonal components local with what was Ohmic coupling, then the off-diagonal components will appear highly non-local like $\text{sign}(\omega)$. But if we were to choose a coupling as to make the off-diagonal components local, then the diagonal components will necessarily be highly non-local. There is no choice of coupling which can give us white noise. This problem with the white noise limit of pre-trace RWA has been noted before [133].

4.2.3.3 Correspondence with perturbation theory

The perturbative correspondence between the pre-trace RWA and the original model is a bit more complicated to demonstrate. Let us start with the second-order corrections for our simple separable coupling without any sort of RWA following [53].

$$\begin{aligned}
\langle \omega_k | \mathcal{L}_{[2]} \{ |\omega_i\rangle \langle \omega_j| \} | \omega_l \rangle &= \langle \omega_k | \mathbf{L} | \omega_i \rangle [A(\omega_{ki}) + \bar{A}(\omega_{lj})] \langle \omega_j | \mathbf{L} | \omega_l \rangle \\
&\quad - \delta_{lj} \sum_h \langle \omega_k | \mathbf{L} | \omega_h \rangle A(\omega_{hi}) \langle \omega_h | \mathbf{L} | \omega_i \rangle \\
&\quad - \delta_{ki} \sum_h \langle \omega_j | \mathbf{L} | \omega_h \rangle \bar{A}(\omega_{hj}) \langle \omega_h | \mathbf{L} | \omega_l \rangle , \quad (4.99)
\end{aligned}$$

with late-time master equation coefficients

$$A(\omega) \equiv \frac{1}{2} \tilde{\alpha}(\omega) - \frac{i}{2\pi} \int_{-\infty}^{+\infty} d\varepsilon \mathcal{P} \left[\frac{1}{\omega - \varepsilon} \right] \tilde{\alpha}(\varepsilon), \quad (4.100)$$

$$\alpha(t) \equiv \langle \mathbf{l}(t) \mathbf{l}(0) \rangle_{\text{B}}, \quad (4.101)$$

where α is the quantum noise correlation for our stationary bath. These corrections capture all of the second-order relaxation rates, perturbative frequency shifts, and basis corrections.

As we have discussed, the post-trace RWA essentially considers taking only entries where $\omega_{ki} = \omega_{lj}$, and under appropriate conditions this is sufficient to reproduce all of the perturbative frequency shifts and relaxation rates but not the basis corrections.

$$\begin{aligned}
\langle \omega_i + \omega | \mathcal{L}_{[2]} \{ |\omega_i\rangle \langle \omega_j| \} | \omega_j + \omega \rangle &= \langle \omega_i + \omega | \mathbf{L} | \omega_i \rangle 2 \operatorname{Re}[A(\omega)] \overline{\langle \omega_j + \omega | \mathbf{L} | \omega_j \rangle} \\
&\quad - \delta_{0\omega} \sum_{\omega'} A(\omega') |\langle \omega_i + \omega' | \mathbf{L} | \omega_i \rangle|^2 \\
&\quad - \delta_{0\omega} \sum_{\omega'} \bar{A}(\omega') |\langle \omega_j + \omega' | \mathbf{L} | \omega_j \rangle|^2 . \quad (4.102)
\end{aligned}$$

One can see that the first terms, which directly correspond to the pseudo-Lindblad dissipator, are now only determined by the real part of $A(\omega)$ or the characteristic function of the noise correlation $\tilde{\alpha}(\omega)$. This function is always positive by Bochner's theorem.

The pre-trace RWA master equation has four related sets of terms because of the two correlated noise sources. But as far as these diagonal terms are concerned, which determine the perturbative timescales, one can essentially consider a master equation of the same form but with the modified coefficients

$$A_{\text{RWA}}(\omega) = \frac{1}{2} \tilde{\alpha}(\omega) - \frac{i}{2\pi} \int_{-\infty}^{+\infty} d\varepsilon \frac{1 + \operatorname{sign}(\omega) \operatorname{sign}(\varepsilon)}{2} \mathcal{P} \left[\frac{1}{\omega - \varepsilon} \right] \tilde{\alpha}(\varepsilon) . \quad (4.103)$$

The real part, which determines the relaxation rates, remains unchanged. But the imaginary part, which determines the energy level shifts, is very different. So while the post-trace RWA can correctly produce all of the perturbative timescales, the pre-trace RWA can only produce the relaxation rates, consistent with what has been found in earlier specific cases [6, 4].

4.2.3.4 Non-Markovian nature of the master equation

It is necessary to point out that, although the pre-trace RWA can often produce a master equation of Lindblad form, the coefficients are inherently non-Markovian. Even though the master equation is in a convolutionless form, the coefficients themselves contain integrals over the system's history alongside nonlocal correlations of the noise. As such, they cannot be universally applied to different systems (which would have different histories) even if one only wants the relaxation rates. This was easy to notice for the post-trace RWA as the correctly derived master equation coefficients would come out to be completely different. Here the reason is much the same.

For instance, let us consider an oscillator system with \mathbf{x} coupling to the environment. The accuracy of the pre-trace RWA decay rates stems from a correct \mathbf{a}^\dagger , \mathbf{a} raising and lowering operator decomposition of \mathbf{x} . This leads to a different but related model of environmental interaction with \mathbf{x} and \mathbf{p} -coupled noise. We have proven that the perturbative decay timescales will work out to be equivalent, but only by using the raising and lowering properties. If we couple this oscillator to additional degrees of freedom in some larger system, then \mathbf{a}^\dagger and \mathbf{a} are no longer ensured to be raising and lowering operators for the new energy eigenstates of the system. Once this criterion has been broken, the proof fails to apply and all coefficients of the misapplied master equation will likely be wrong. A correct pre-trace RWA interaction would have to involve a raising and lowering operator decomposition which utilizes the full Hamiltonian of the larger system.

4.2.3.5 Application to the two-level atom

Utilizing the second-order master equation, we find the RWA interaction Hamiltonian yields

$$\frac{d}{dt} \begin{bmatrix} \rho_{++} \\ \rho_{--} \end{bmatrix} = \frac{\Gamma}{\cosh\left(\frac{\Omega}{2T}\right)} \begin{bmatrix} -e^{+\frac{\Omega}{2T}} & +e^{-\frac{\Omega}{2T}} \\ +e^{+\frac{\Omega}{2T}} & -e^{-\frac{\Omega}{2T}} \end{bmatrix} \begin{bmatrix} \rho_{++} \\ \rho_{--} \end{bmatrix}, \quad (4.104)$$

$$\frac{d}{dt} \begin{bmatrix} \rho_{+-} \\ \rho_{-+} \end{bmatrix} = \begin{bmatrix} -\Gamma - i(\Omega - \delta\Omega_*) & +\Gamma + i\delta\Omega_* \\ +\Gamma - i\delta\Omega_* & -\Gamma + i(\Omega - \delta\Omega_*) \end{bmatrix} \begin{bmatrix} \rho_{+-} \\ \rho_{-+} \end{bmatrix}, \quad (4.105)$$

with new energy level shift

$$\delta\Omega_* \equiv \frac{1}{\pi} \int_0^\infty d\varepsilon \mathcal{P} \left[\frac{1}{\varepsilon - \Omega} \right] \Gamma(\varepsilon). \quad (4.106)$$

In addition to differing from the frequency shift without the RWA, it also contains a higher order cutoff sensitivity. For approximately local dissipation, the sensitivity was logarithmic but is now linear.

4.2.3.6 Application to quantum Brownian motion

Again utilizing the second-order master equation, we find the RWA interaction Hamiltonian yields

$$\frac{d}{dt} \boldsymbol{\rho} = -i[\mathbf{H}_R^*, \boldsymbol{\rho}] - i\Gamma[\mathbf{x}, \{\mathbf{p}, \boldsymbol{\rho}\}] - M D_{pp}[\mathbf{x}, [\mathbf{x}, \boldsymbol{\rho}]] - D_{xp}^*[\mathbf{x}, [\mathbf{p}, \boldsymbol{\rho}]] \quad (4.107)$$

with new frequency shift and anomalous diffusion coefficient

$$\Omega_R^* = \Omega - \frac{1}{\pi} \int_0^\infty d\varepsilon \mathcal{P} \left[\frac{\varepsilon}{\varepsilon - \Omega} \right] \Gamma(\varepsilon), \quad (4.108)$$

$$D_{xp}^* = +\frac{1}{\pi} \int_0^\infty d\varepsilon \mathcal{P} \left[\frac{\frac{1}{\Omega}}{\varepsilon - \Omega} \right] \Gamma(\varepsilon) \varepsilon \coth\left(\frac{\varepsilon}{2T}\right). \quad (4.109)$$

For what was Ohmic coupling in the original model, the frequency shift has a different but still linear cutoff sensitivity. However the anomalous diffusion coefficient now also has a linear cutoff sensitivity. If the cutoff is very large, this could be very problematic.

4.2.3.7 A multipartite example

Let us say that we have an array of, otherwise non-interacting, parallel qubits all with σ_z Hamiltonians. A simple dipole interaction can be represented with the bilinear interaction Hamiltonian

$$\mathbf{H}_I = \sum_n \sigma_{x_n} \mathbf{l}_n \quad (4.110)$$

where σ_{x_n} is the x spin component of the n^{th} qubit and \mathbf{l}_n is its corresponding collective environment coupling. The environmental coupling for a qubit at location \vec{r}_n is ⁵

$$\mathbf{l}_n = \sum_{\vec{k}} g_k \left\{ e^{+i\vec{k}\cdot\vec{r}_n} \mathbf{a}_k^\dagger + e^{-i\vec{k}\cdot\vec{r}_n} \mathbf{a}_k \right\}. \quad (4.111)$$

The resultant damping kernel corresponding to the $\langle \mathbf{l}_n(t) \mathbf{l}_m(\tau) \rangle_B$ correlation is

$$\tilde{\gamma}_{nm}(\omega) = \tilde{\gamma}_0 \text{sinc}(r_{nm}\omega), \quad (4.112)$$

where $\vec{r}_{nm} = \vec{r}_n - \vec{r}_m$ and therefore the damping is Ohmic or local for the autocorrelations where $r_{nm} = 0$. The cross-correlations, which are strictly nonlocal, vanish in the limit of large distance separation.

⁵Note that this form of the damping kernel assumes that the coupling is independent of the direction of \vec{k} , which is like an interaction with a scalar field rather than a vector field like the electromagnetic field.

The pre-trace RWA interaction, which was considered for two qubits in [11], introduces the duplication of quantum noise sources

$$\mathbf{l}_n^{\text{RWA}} = \frac{1}{2} \sum_{\vec{k}} g_k \left\{ e^{+i\vec{k}\cdot\vec{r}_n} \mathbf{a}_k^\dagger + e^{-i\vec{k}\cdot\vec{r}_n} \mathbf{a}_k \right\}, \quad (4.113)$$

$$\mathbf{j}_n^{\text{RWA}} = \frac{i}{2} \sum_{\vec{k}} g_k \left\{ e^{+i\vec{k}\cdot\vec{r}_n} \mathbf{a}_k^\dagger - e^{-i\vec{k}\cdot\vec{r}_n} \mathbf{a}_k \right\}, \quad (4.114)$$

and one must now consider the correlations between all such operators. The resultant damping kernels can be organized

$$\begin{bmatrix} \tilde{\gamma}_{l_n l_m}^{\text{RWA}}(\omega) & \tilde{\gamma}_{l_n j_m}^{\text{RWA}}(\omega) \\ \tilde{\gamma}_{j_n l_m}^{\text{RWA}}(\omega) & \tilde{\gamma}_{j_n j_m}^{\text{RWA}}(\omega) \end{bmatrix} = \frac{\tilde{\gamma}_{nm}(\omega)}{4} \begin{bmatrix} 1 & -i \text{sign}(\omega) \\ +i \text{sign}(\omega) & 1 \end{bmatrix}, \quad (4.115)$$

with reference to the original damping kernel $\tilde{\gamma}_{nm}(\omega)$. The scenario is much the same. The damping rates will be correct, while the frequency shifts and basis corrections (including asymptotic entanglement) will be incorrect. There is no longer a white noise limit, even when the qubits are distantly separated.

However this remains a fairly reasonable physical theory, as the RWA interaction itself was fairly reasonable. The cross-correlations between *different* qubits still vanishes for large separations. The second-order master equation, being determined by the second-order cumulants or two-time correlations, will therefore reduce to that of qubits coupled to independent environments in the large separation limit.

4.2.4 The Effect of Finite Bandwidth

The discussion so far has examined the discrepancies between the mathematical solutions with and without the RWA. However, in a physical experiment one does not have access to the pure mathematical solution. In fact, measurements in

a laboratory must be made using instruments with finite response or integration times, i.e. finite bandwidth. We will see that measurements under this constraint obscure some of the inaccuracies introduced by the RWA.

Consider the expectation of an observable O measured with some apparatus with a finite bandwidth described in the time domain by the function $h(t)$. Assuming that O is time independent in the Schrödinger picture,

$$\langle O \rangle = \text{Tr} [O(\boldsymbol{\rho} * h)(t)] \quad (4.116)$$

in terms of the convolution $\boldsymbol{\rho} * h$. We know that the solution to the weak coupling equation has the form of Eq. (1.31), which gives

$$(\boldsymbol{\rho} * h)(t) = \sum_{ij} c_{ij} \mathbf{o}_{ij} (h * e^{f_{ij}t}). \quad (4.117)$$

In the Fourier domain $(\boldsymbol{\rho} * h)(t)$ becomes $\tilde{\boldsymbol{\rho}}(\omega)\tilde{h}(\omega)$ with

$$\tilde{\boldsymbol{\rho}}(\omega) = -\frac{1}{\sqrt{2\pi}} \sum_{ij} c_{ij} \mathbf{o}_{ij} \frac{i(\omega - \omega'_{ij}) + \text{Re} [f_{ij}^{[2]}]}{(\omega - \omega'_{ij})^2 + \text{Re} [f_{ij}^{[2]}]^2}, \quad (4.118)$$

where $\omega'_{ij} = \omega_{ij} + \text{Im} [f_{ij}^{[2]}]$ and we have implicitly multiplied $\boldsymbol{\rho}(t)$ by a step function for convenience (which will be irrelevant for later times assuming $h(t)$ has compact support). Thus, assuming that $\tilde{h}(\omega)$ falls off quickly with frequency, all the terms with large values of ω'_{ij} will be greatly attenuated, and the contributions from $\mathbf{o}_{ij}^{[2]}$ may easily become negligible.

For example, let us suppose that the finite bandwidth of the measuring apparatus results in taking a running average of observables with averaging time τ_a . In that case, the measured expectation of an observable will be $\langle O \rangle = \text{Tr} [O\bar{\boldsymbol{\rho}}(t)]$ with

$$\bar{\boldsymbol{\rho}}(t) = \frac{1}{\tau_a} \int_{-\frac{\tau_a}{2}}^{\frac{\tau_a}{2}} \boldsymbol{\rho}(t + \tau) d\tau. \quad (4.119)$$

Using the weak coupling solution we obtain

$$\bar{\rho}(t) = \sum_{ij} c_{ij} \mathbf{o}_{ij} e^{f_{ij}t} \frac{2 \sinh(f_{ij}\tau_a/2)}{f_{ij}\tau_a}. \quad (4.120)$$

If we assume that there is some smallest non-zero frequency Ω for the values of ω'_{ij} , largest value γ for $\text{Re} [f_{ij}^{[2]}]$, and that $\Omega \gg \frac{1}{\tau_a} \gg \gamma$, then we have two small scales in the problem

$$1 \gg \frac{1}{\Omega\tau_a} \gg \frac{\gamma}{\Omega}. \quad (4.121)$$

Any term in Eq. (4.120) for which $\omega_{ij} \neq 0$ will be attenuated by $\frac{1}{\Omega\tau_a}$, making the contribution of the second-order basis corrections $\mathbf{o}_{ij}^{[2]}$ much smaller. Based on the assumption of weak coupling, these basis corrections must necessarily be small, but with this extra attenuation they may easily become negligible (even if they were not previously). Thus, the discrepancies introduced by using the RWA can be hidden somewhat when making single-time measurements with finite bandwidth. However, it should be noted that the terms with $\omega_{ij} = 0$ will be relatively unaffected by the finite bandwidth (since they are slowly evolving). So, for example, $\mathbf{o}_{ii}^{[2]}$ will in general have corrections with off-diagonal elements (terms proportional to $|\omega_l\rangle \langle \omega_m|$) that would be neglected by the RWA, and these are not significantly attenuated by finite measurement bandwidth. The other issue is that we have only looked at single-time measurements, and it is not clear without further study to what degree finite bandwidth would effect the apparent accuracy of the RWA for measurements of multi-time correlations.

4.3 Discussion

In this chapter we have examined the effect of two widely used approximations, the RWA and the weak coupling approximation (i.e., use of the perturbative master equation). We have found that each approximation introduces inaccuracies in the predicted lowest-order corrections to the system dynamics, and we have characterized the source and size of the discrepancies. We have also noted that in the context of some experiments these errors may be too small to be detected. On a theoretical level, however, this sheds significant new light on problems of positivity and may have some implications for entanglement dynamics.

We have shown that even when provided with a stationary master equation describing dynamics that are amenable to perturbative solution, the solutions to an order- $2n$ perturbative master equation are, in general, only accurate to order- $(2n-2)$, a step down from that of the master equation itself. This has a wide range of implications upon the common use of second-order master equations and related master equations derived from second-order dynamics: the Redfield, Born-Markov, and many Lindblad equations. Moreover, not even a nonlocal representation, such as with the Nakajima-Zwanzig master equation can avoid this effect. This is to be expected as a thorough analysis of time-local and nonlocal dynamics shows their asymptotics to be perturbatively the same [53].

To be more specific, the second-order master equation can provide all second-order timescales and off-diagonal density matrix elements (in the free energy basis). However it can only provide the diagonal matrix elements with zeroth-order

accuracy, and the missing information is the most relevant to positivity in the low-temperature regime. Therefore the second-order master equation can produce second-order positivity violations, whereas the full second-order solutions are positive to second-order. Likewise, the steady state of the second-order master equation may only agree with the steady state of the full master equation to zeroth order. Without knowledge of the accuracy limitations we have discussed, this violation of positivity could easily be mistaken as a problem with the physics of the master equation.

More generally, the predicted expectation of observables will typically be off by a second-order amount, except if an observable O anticommutes with the Hamiltonian. Certainly the energy or other quantities that were conserved at zeroth order will have such discrepancies, as will any quantities involving the diagonal elements of the density matrix. We have shown that this inaccuracy manifests itself in the case of quantum Brownian motion (where an exact solution is available for verification) through an underestimation of the position uncertainty stationary limit. As we will see in Ch. 5, these same inaccuracies affect predictions about the dynamics of entanglement in bipartite systems, and the complete second-order solution is required to make meaningful predictions about the sudden death of entanglement.

We have also systematically examined the rotating-wave approximation by using the weak-coupling master equation. There are, in fact, two distinct rotating-wave approximations: The pre-trace RWA is an approximation performed on the interaction Hamiltonian before the environment is traced out which yields a somewhat modified Hamiltonian dynamics from which the reduced dynamics can be derived.

The post-trace RWA is performed on the master equation for the reduced density matrix after the environment has already been traced out. Using the general framework of [31], we have compared the master equation describing the dynamics of this open system under the pre and post-trace RWA to the dynamics without making such an approximation. We have specifically addressed the master equations for a two-level system and for a linear oscillator, two models in which the RWA is often invoked.

We find the post-trace RWA to be more innocuous than the pre-trace RWA. It can be seen as an approximation in which the full weak-coupling Liouvillian (which is time-local and of pseudo-Lindblad form) is projected onto a Lindblad-form Liouvillian. We call the resulting master equation the RWA-Lindblad equation. We find that for a general open quantum system the post-trace RWA will yield exactly the same timescales as perturbative solutions of the weak-coupling master equation. The perturbative corrections to eigen-operators of the Liouvillian are neglected in the RWA-Lindblad equation, so the details of the predicted quantum state will differ. In particular, the steady state solution of the RWA-Lindblad master equation will differ from the true steady state by an amount that is perturbative in the coupling, adding to discrepancies already present from using the weak coupling approximation. Our results are consistent with what Agarwal found [6, 4, 5] for the two-level atom and the linear oscillator in the Born-Markov approximation. One context in which the discrepancy in the steady state could be important is examining the late-time behavior of entanglement dynamics at low temperature. When the system is bipartite and the ground state is separable, the RWA-Lindblad

equation will give an asymptotically separable state, whereas the weak-coupling master equation leaves open the possibility of asymptotic entanglement. In view of our findings, we can say that generally the post-trace RWA is suitable if one only wants the perturbative timescales of the dynamics, but it may not be appropriate if one wants more detailed information about the quantum state of the system, as it misses some corrections introduced by the coupling to the environment, and it will also not be appropriate when perturbative timescales fail, i.e. for near-resonance in the energy level splittings.

We find the pre-trace RWA to be more problematic. When the environment contains many frequencies with a spread comparable to the frequencies of the system, then the pre-trace RWA in general does not provide a faithful representation of the true solution. We also find that the pre-trace RWA results in two strongly correlated sources of environmental noise that together have no Markovian limit. The cross-correlations between the noise sources are such that if the autocorrelations are white then the cross-correlations are strongly colored. This issue has been noticed before [133]. Finally, we have shown that, unlike the post-trace RWA, the pre-trace RWA in general does not correctly obtain all perturbative timescales for the dynamics, yielding incorrect frequency shifts. This finding based on a more extended theoretical framework agrees with results obtained for specific cases studied before for the two-level atom [6, 4, 5]. In use, this problem may be obscured if the renormalized system frequencies are simply determined phenomenologically. It is worth noting that Klimov *et al.* have developed a different, algebraic way of analyzing the pre-trace RWA [86].

We caution that the way the RWA is applied also matters. For Markovian processes in closed and open systems, certain liberties can be taken with the master equation; dissipation terms can be simply added together to find their collective effect and the interplay between the system Hamiltonian and dissipator coefficients is absent. A Markovian process will generally produce a master equation of Markovian (i.e. time-local) representation and Lindblad form. The RWA can also produce a master equation of Markovian representation and Lindblad form, and therefore one might assume that the master equations can be treated in the same cavalier fashion as those for Markovian processes. But this is not the case, as the underlying stochastic process remains non-Markovian and the master equation coefficients contain memory despite their Markovian representation. A haphazard construction of RWA-Lindblad master equations for multipartite systems, or those with external forcings, can produce an evolution which is completely positive and yet totally unphysical.

A single two-level atom is clearly a particularly simple quantum system. As such, some of the shortcomings of the RWA are obscured in this case. We find that the post-trace RWA gives the correct equilibrium state for a thermal environment in this case, in addition to the correct timescales, though it does miss some of the corrections to the transient quantum evolution that can be obtained from the weak-coupling master equation without the RWA. Thus, if one's theoretical investigations are limited to those features that it captures correctly, then the post-trace RWA may be a suitable approach.

To summarize the total effect of both approximations it is useful to think about

the elements of the density matrix ρ_{ij} in the energy basis. We have said that using weak coupling approximation (i.e. solving the second-order master equation) yields $\mathcal{O}(\gamma/\Omega)$ errors (if there is a characteristic system frequency Ω and dissipation rate γ) in the diagonal elements of the density matrix. Introducing the post RWA introduces additional $\mathcal{O}(\gamma/\Omega)$ errors in all the elements of the density matrix. Even with both these approximations, the timescales calculated will be correct to $\mathcal{O}(\gamma)$. Using the pre RWA will additionally introduce errors in the environmentally-induced frequency shifts (as well as seemingly destroying the Markovian limit).

There are three mathematical limits in which these approximations will still give solutions accurate to second order: The first is early times, where t is small compared to any of the second-order damping time scales. The second is the Markovian limit, because in this limit the second-order master equation is exact and of Lindblad form. The third is the limit employed by Davies [40] where one rewrites the master equation in terms of the rescaled time parameter $\tau = g^2 t$ and then takes the limit $g \rightarrow 0$ (for $\tau \neq 0$ this effectively amounts to taking a simultaneous $t \rightarrow \infty$ limit). In this limit all corrections to the eigenoperators of the Liouvillian vanish, and the only effect of the environment is to introduce damping rates through corrections to the eigenvalues, which are correctly captured by the perturbative master equation and post RWA. Thus, the inaccuracies introduced by these approximations may be sufficiently suppressed (even at late times) if a physical system is sufficiently close to being described by one of these limits.

Reading about the inaccuracies present in the predicted lowest-order corrections under the weak-coupling approximation and RWA, one might easily question

the apparent success of their ubiquitous application in atomic physics and the literature on open quantum systems more generally. In atomic physics, the answer is often simply that the coupling is so small that one is essentially in the limit used by Davies. The lowest-order dissipation rates (decoherence and population decay) introduced by the environment will always become important at sufficiently late times, when $t \gtrsim 1/\gamma$. Lowest-order corrections to the eigenoperators contribute only $\mathcal{O}(\gamma/\Omega)$ to the state at all times. But in an optical-frequency atomic system, for example, one can have $\gamma/\Omega \sim 10^{-9}$, so that these corrections will be too small to be noticed unless one were doing a very high precision experiment with extraordinarily low noise.

If one is concerned with predicting the values of observables measured at a single time in an experiment with finite temporal resolution (characterized by timescale τ_a that is long compared to system timescales and short compared to dissipation timescales), then many of the terms in the weak coupling solution (specifically those with $\omega_{ij} \neq 0$) will be suppressed by an additional factor of $\mathcal{O}((\Omega\tau_a)^{-1})$. This could easily make terms arising from $\mathbf{o}_{ij}^{[2]}$ that were small but measurable become negligible. However, there will still be off-diagonal corrections from the terms with $\omega_{ij} = 0$ that will not be suppressed by finite measurement bandwidth.

The practical applicability of these results will then depend on precisely how small γ/Ω is, the accuracy with which measurements are made, and the temporal resolution of the measurements. Our results should be most heeded in the non-Markovian regime of low temperature or long-ranged correlations in contexts where $\mathcal{O}(\gamma/\Omega)$ discrepancies are not negligible. We will see in Ch. 5 that these considera-

tions do have an impact on theoretical examination of entanglement dynamics in low temperature environments. Also, we have not addressed the question of multi-time correlation measurements in the non-Markovian regime, where these approximations could potentially be more problematic.

Chapter 5

Entanglement Dynamics Beyond the Rotating-Wave Approximation

In this chapter we apply the results of Ch. 4 to understand entanglement dynamics in weakly coupled open quantum systems. We explore the effects of the weak coupling approximation and rotating-wave approximation (RWA) on our predictions for asymptotic entanglement dynamics at late time for a general bipartite system where interaction between the subsystems happens only through the environment. Specifically, we focus on the issue of sudden death. We then proceed to apply the weak-coupling master equation to a specific such system, namely two atoms sharing a common field. Using that approach we find the dynamics of the system without invoking the RWA. We then examine the entanglement dynamics and its relationship to atomic separation for this case.

5.1 Weak Coupling, the Rotating-Wave Approximation, and Asymptotic Entanglement Dynamics

We have already said in Sec. 4.1 that in any calculation using the second-order master equation, we know that there will be second-order inaccuracies in the diagonals of the density matrix, and this will generally lead to discrepancies in the value of entanglement obtained. The addition of the post-trace RWA adds further errors of the same size. However, so long as the weak coupling approximation is good,

these errors will be small; thus, the qualitative picture of entanglement, including generation, sudden birth, sudden death, and revival, should be much the same, except in specific cases where such a small discrepancy would make a qualitative difference. The question of SD focuses on whether or not entanglement will decay to zero asymptotically, however, so if one understands the late time behavior one may be able to make broader statements about SD.

5.1.1 Asymptotic State for Weak Coupling and a Thermal Reservoir

We have assumed a bipartite system with interaction between the two occurring only through the environment which is thermal and weakly coupled to the system. To zeroth order in the system-environment interaction, the asymptotic steady state is Boltzmann, which can be expressed

$$\rho_T = \prod_n \rho_{T_n}, \quad (5.1)$$

$$\rho_{T_n} \equiv e^{-\mathbf{H}_n/T} / \text{Tr} [e^{-\mathbf{H}_n/T}] \quad (5.2)$$

and is uncorrelated. The asymptotic state of the second-order master equation is consistent with this result and can additionally provide some of the second-order corrections $\delta\rho_T$ via the constraint

$$\mathcal{L}_{[0]}\{\delta\rho_T\} + \mathcal{L}_{[2]}\{\rho_T\} = 0. \quad (5.3)$$

These will specifically be the off-diagonal or non-stationary perturbations. In general, to find the second-order corrections to the diagonal elements of the density matrix one needs to compute contributions from the fourth-order Liouvillian as discussed in Sec. 4.1.

It has been shown [104, 53] that for non-vanishing interaction with the environment the off-diagonal elements of the asymptotic state match reduced thermal state

$$\boldsymbol{\rho}_\beta \equiv \frac{1}{Z_C(\beta)} \text{Tr}_E [e^{-\beta(\mathbf{H}+\mathbf{H}_E+\mathbf{H}_I)}] , \quad (5.4)$$

where $Z_C(\beta)$ is the partition function of the system and environment with non-vanishing interaction. We will refer to $\boldsymbol{\rho}_\beta$ as the thermal Green's function; this function can be expanded perturbatively in the system-environment coupling as

$$\boldsymbol{\rho}_\beta = \frac{1}{Z_0(\beta)} e^{-\beta \mathbf{H}} + \boldsymbol{\delta\rho}_\beta + \dots , \quad (5.5)$$

where $Z_0(\beta)$ is the partition function of the free system. These coefficients agree perturbatively with those from Eq. (5.3). Because such an expansion is inherently secular in β , it is valid only at a sufficiently high temperature such that the perturbations are small compared to the smallest Boltzmann weight,

$$\frac{\gamma}{\Omega} \ll e^{-\beta(\Omega_n+\Omega_m)} = \left(\frac{\bar{n}(\Omega_n, T)}{\bar{n}(\Omega_n, T)+1} \right) \left(\frac{\bar{n}(\Omega_m, T)}{\bar{n}(\Omega_m, T)+1} \right) , \quad (5.6)$$

where Ω is the smallest positive system frequency splitting (i.e., a characteristic system frequency) and γ is the largest dissipation rate. The expansion does not apply at lower temperatures, and $\bar{n}(\Omega_n, T)$ is the thermal average photon number in a bosonic mode with frequency Ω_n and temperature T . Reliability of the expansion at higher temperature suggests that the diagonal corrections to the asymptotic state must be suppressed in that regime.

Since neither the second-order master equation nor the perturbative expansion of the thermal Green's function can give the full low-temperature solution, including

diagonal corrections, it appears that in general this will require the fourth-order master equation coefficients. However, at zero temperature the thermal state is simply the ground state of the total system-environment Hamiltonian. This ground state can be calculated perturbatively from the Hamiltonian as usual in a closed system, and the zero-temperature reduced thermal state follows directly. All three of these formalisms are fully consistent as shown in Ref. [53]. It is unclear how to compute the complete second-order corrections to the asymptotic state for low positive temperatures.

5.1.2 Late-time Entanglement Dynamics of Two Qubits

Let us consider two qubits labeled n and m with frequencies Ω_n and Ω_m , and let γ and Ω still the largest dissipation rate and smallest positive frequency splitting, respectively. To quantify the bipartite entanglement we will use Wootters' concurrence function [134], which we have said is a monotone with a one-to-one relationship to the *entanglement of formation* for two qubits. The concurrence is defined in Eq. (1.47), but it will be useful to rewrite it in terms of what we will call the unmaximized concurrence \underline{C} as

$$C(\boldsymbol{\rho}) = \max\{0, \underline{C}(\boldsymbol{\rho})\} \quad (5.7)$$

$$\underline{C}(\boldsymbol{\rho}) = \sqrt{\lambda_1} - \sqrt{\lambda_2} - \sqrt{\lambda_3} - \sqrt{\lambda_4}. \quad (5.8)$$

A two-qubit state is entangled if and only if $\underline{C} > 0$. It is important to note that $\underline{C}(\boldsymbol{\rho})$ is a continuous function of the matrix elements of $\boldsymbol{\rho}$ (since the eigenvalues of a matrix can be written as a continuous function of the matrix elements [121]);

this then implies that any density matrix with $\underline{C} < 0$ lies in the interior of the set of separable states (with every sufficiently nearby state also separable), while states with $\underline{C} > 0$ lie in the interior of the set of entangled states. States with $\underline{C} = 0$ are separable but include states that lie on the boundary between the two sets, infinitesimally close to both entangled states and the interior of the separable states. Any separable pure state lies on this boundary [73].

Given the late-time asymptotic state of the two qubits ρ_{nm} , one can easily compute the asymptotic entanglement from $\underline{C}(\rho_{nm})$. Based on the preceding paragraph, however, we know that this will also tell us something qualitatively about the late-time entanglement dynamics. Assuming only continuous evolution in state space, if $\underline{C}(\rho_{nm}) < 0$ then every initial state must become separable at some finite time as it crosses into the set of separable states. Likewise, if $\underline{C}(\rho_{nm}) > 0$ then all initial states lead to entanglement at sufficiently late time, any sudden death of entanglement must be followed by revival, and any initially separable state must become entangled. In models that have a unique asymptotic state, it is only when $\underline{C}(\rho_{nm}) = 0$ that this qualitative feature of the late-time behavior will depend on the initial state, with some entangled states remaining separable forever after some finite time and others becoming disentangled only asymptotically in the limit $t \rightarrow \infty$ as in [138, 49]. Previous work has pointed out that the late-time entanglement dynamics can be determined by the character of the asymptotic state [139, 39], with Yu and Eberly [140] discussing the role of \underline{C} in predicting sudden death. In Refs. [140, 39] the authors consider models with multiple steady states, a situation which introduces additional dependence on initial conditions. The previous work, however, was

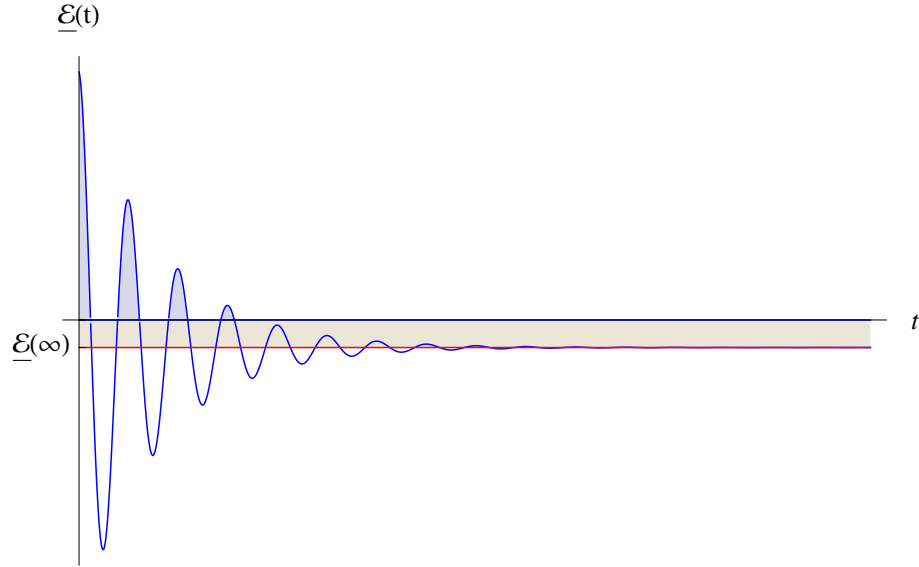


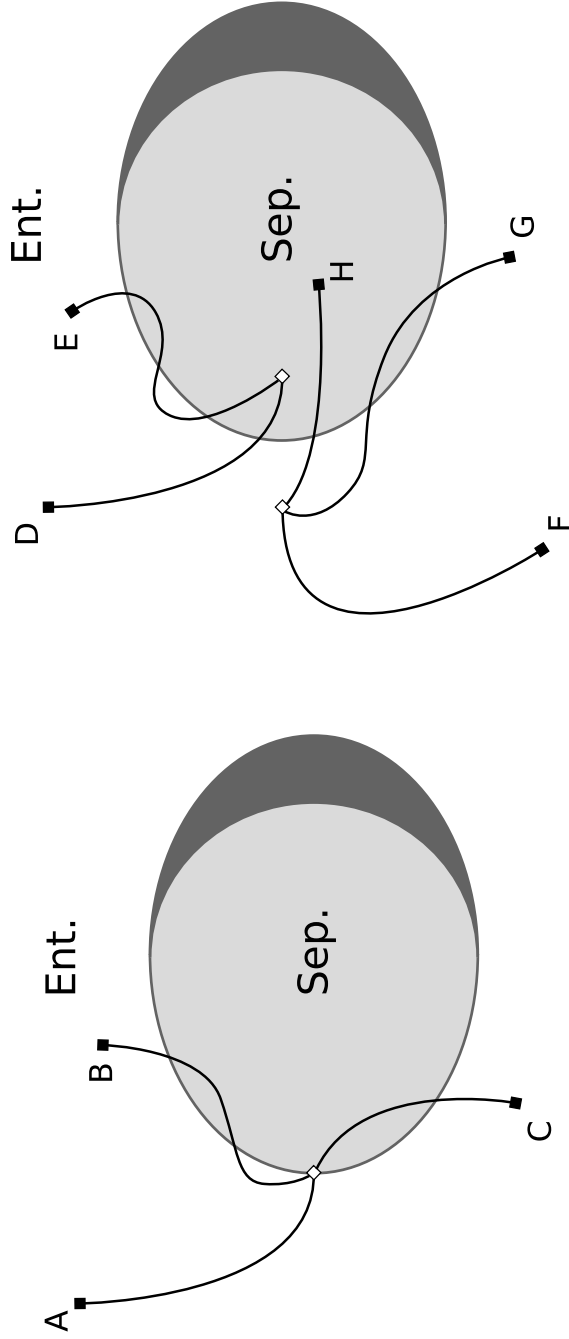
Figure 5.1: Qualitative plot of an (unmaximized) entanglement function showing dynamics including entanglement sudden death, revival, and asymptotic separability.

based upon perturbative master equations using the RWA (where microscopic models were used); in that case the asymptotic state is just the separable Boltzmann state. We will see that the correct second-order asymptotic state is necessary to make predictions about SD at low temperature.

It can be seen that none of the foregoing discussion is specific to the concurrence; it would apply to any continuous function of the density matrix that takes on negative values for some separable states and is an entanglement monotone when non-negative. If we have such an unmaximized entanglement function $\underline{\mathcal{E}}$ from which an entanglement monotone can be defined by $\mathcal{E} = \max\{0, \underline{\mathcal{E}}\}$, then we can use it just as we have discussed using $\underline{\mathcal{C}}$ above. As illustrated qualitatively in Fig. 5.1, entanglement sudden death occurs because the unmaximized entanglement function

asymptotes towards a negative value, whereas any entanglement monotone (derived from $\underline{\mathcal{E}}$ or otherwise) cannot go below zero, leading to an abrupt sudden death of entanglement when $\underline{\mathcal{E}}$ becomes negative.

An important point arises from the facts we have noted about $\underline{\mathcal{C}}$ and separability: At sufficiently low temperature the $\mathcal{O}(\gamma/\Omega)$ corrections to the asymptotic state are required to calculate the sign of $\underline{\mathcal{C}}(\rho_{nm})$ and, therefore, the qualitative features of late-time entanglement dynamics. At zero temperature, the zeroth-order asymptotic state is simply the ground state of the system, assuming no degeneracy at the ground energy, according to Eq. (5.1). Thus the zeroth-order asymptotic state is a pure separable state. This means that it lies on the boundary between the entangled and separable states, and in general some initial states will suffer sudden death while others will not, as depicted in Fig. 5.2(a). But any non-zero perturbation, however small, can lead to asymptotic entanglement or can place the asymptotic state in the interior of the separable states, implying sudden death for all initial conditions. Fig. 5.2(b) shows each of these situations. Thus, knowing only the zeroth-order asymptotic state one can make no meaningful prediction about late-time entanglement dynamics, and this will always be the case when working with a perturbative master equation and using the rotating-wave approximation, because the second-order corrections to the asymptotic state are neglected as we saw in Ch. 4. This makes calculations such as [49] incapable of correctly predicting whether SD is universal or there is asymptotic entanglement at late times.



(a) Pure Asymptotic State

(b) Mixed Asymptotic State

Figure 5.2: A schematic representation of the evolution in state space. The white area represents entangled states ($\underline{C} > 0$), while the gray areas represent separable states $\underline{C} \leq 0$ with the dark gray representing states with $\underline{C} = 0$. The asymptotic state is represented by \diamond , while initial states are represented by \blacksquare . In (a) we have the asymptotic state on the boundary as in the zeroth-order at $T = 0$. In (b) two scenarios are shown that can arise from a small perturbation moving the asymptotic state off the boundary, into the interior of one of the two sets. This illustrates how such a perturbation qualitatively changes the late-time entanglement dynamics.

At positive temperature the zeroth-order asymptotic state is simply the Boltzmann state ρ_T , which lies in the interior of the set of separable states [139], and

$$\rho_T \tilde{\rho}_T = \frac{e^{-(\Omega_n + \Omega_m)/T}}{Z_0(T)^2} \mathbf{1}, \quad (5.9)$$

so that $\underline{C}(\rho_T) = -2e^{-(\Omega_n + \Omega_m)/(2T)}/Z_0(T)$. The $\mathcal{O}(\gamma/\Omega)$ corrections to ρ_{nm} will yield order $\mathcal{O}(\gamma/\Omega)$ corrections to $\rho_{nm} \tilde{\rho}_{nm}$. Then simply from the definition of \underline{C} we know that so long as the temperature is sufficiently high that Eq. (5.6) is satisfied the corrections to ρ_{nm} will cause at most $\mathcal{O}(\gamma/\Omega)$ corrections to $\underline{C}(\rho_{nm})$ so that it must remain negative. Consequently, the second-order asymptotic state still lies in the interior of the separable states, and all initial states will suffer entanglement sudden death at sufficiently late times. For lower temperatures it does not appear that the sign of $\underline{C}(\rho_{nm})$ can be generically predicted, and one must find the late-time asymptotic state for the specific system in question which generally requires terms from the fourth-order master equation.

5.2 Two Atoms in a Field Common Field

A common setting for theoretical discussion of SD is atomic systems interacting with the electromagnetic field [138, 136, 137, 49, 11, 12], serving as an environment in the quantum open system perspective. All of this work has been performed in the RWA, and most [138, 136, 137, 49] under the BMA. A fully non-Markovian treatment of multiple two-level atoms in a common quantum field has yet to be carried out in a manner which can predict entanglement evolution fully and address critical issues such as sudden death of entanglement. As discussed in Sec. 5.1, perturbative

master equations (which BMA master equations are equivalent to) derived under the RWA are unsuitable for examining asymptotic entanglement dynamics and SD, due to inaccuracies in the predicted asymptotic state. Additionally, use of the RWA makes proper consideration of near resonance (as additional near-stationary terms are needed in the Dirac picture)¹. The existence of a subradiant *dark state* generically requires the resonance condition, but determining how critical this is requires some analysis of the near-resonance regime.

Rather than employing the BMA or RWA, we use the weak coupling master equation. We make careful and justified use of the second-order master equation for the dynamics, paying attention to the expected accuracy of the solutions. We use the alternative (but compatible) means of calculating the late-time asymptotics from the system+environment ground state. In this way we are able to show that the two atoms in a single field are not asymptotically entangled, even when near resonance and very close together — which is the criterion for a dark state. This asymptotic behavior turns out to be the opposite of what one finds with two oscillators in a field, which can be asymptotically entangled [92]. In fact, we find that the entanglement of any pair of atoms will always undergo sudden death, regardless of the initial state. We also find that coherence can be long lived amongst the ground state and dark states, and we proceed to describe all relevant timescales of the atom-field system. We explore what conditions are required for sub- and super-radiance in terms of proximity, tuning, and dissipation. In brief, to achieve dark and bright states one

¹Near resonant terms can be preserved in implementing the RWA, but this will then lead to a master equation not of Lindblad-form as in [116].

requires proximity better than the resonant wavelength and tuning better than the ordinary dissipation rates. Temperature only appears to change the nature of these states and does not diminish their existence (other than increasing any positive decay rates linearly).

In physical terms the sub- and super-radiance of the dark and bright states are ultimately a result of *interference* among the multiple noise processes provided by the field modes evaluated at different locations. As such, one cannot simply add the emission rates of two isolated atoms. Some special mention should also be given to our treatment of renormalization. Previous works have only considered renormalization of the atoms individually, which is sufficient if the atoms are far apart, and also simultaneous in time, which is sufficient in the late-time regime. Here we “dress” the joint system in its entirety, which gives rise to an immersed dynamics more similar to the free system and also more well behaved. Our counter terms are also introduced along the light cone, which keeps the full-time theory causal, and not across all of space simultaneously.

5.2.1 Second-order master equation

5.2.1.1 System-environment coupling and correlations

We wish to investigate the properties of multiple atoms with frequencies Ω_n interacting with a common electromagnetic field in free space, which serves as the environment in the open quantum system description. As before we will use the two-level approximation to describe the atoms, so that they are an array of otherwise

non-interacting qubits. It will be convenient to write the interaction Hamiltonian of our system with the environment as

$$\mathbf{H}_I = \sum_n \boldsymbol{\sigma}_{x_n} \mathbf{l}_n \quad (5.10)$$

where $\boldsymbol{\sigma}_{x_n}$ is the x spin component of the n^{th} qubit and \mathbf{l}_n is its corresponding collective environment coupling. The environmental coupling for an atom at location \vec{r}_n with dipole moment \vec{d}_n is

$$\mathbf{l}_n = \sum_{\vec{k},s} i \frac{b}{\sqrt{k}} \left(\vec{d}_n \cdot \vec{\epsilon}_{\vec{k},s} \right) \left\{ e^{+i\vec{k} \cdot \vec{r}_n} \mathbf{a}_{\vec{k},s} - e^{-i\vec{k} \cdot \vec{r}_n} \mathbf{a}_{\vec{k},s}^\dagger \right\}, \quad (5.11)$$

with b a constant and where $\vec{\epsilon}_{\vec{k},s}$ denote the polarization vectors perpendicular to \vec{k} for an electro-magnetic field environment such as discussed in Ref. [4, 131, 10] and Sec. 1.3. For a scalar field environment one can simply neglect the dot product.

We calculate the resultant damping kernels corresponding to the correlation functions of the scalar field $\alpha_{nm}(t, \tau) = \text{Tr}_E [\mathbf{l}_n(t) \mathbf{l}_m(\tau)]$ to be

$$\tilde{\gamma}_{nm}(\omega) = \tilde{\gamma}_0 \text{sinc}(r_{nm}\omega), \quad (5.12)$$

and for the electromagnetic field,

$$\tilde{\gamma}_0 \left\{ \text{FS}_1(r_{nm}\omega) \left(\hat{d}_n \cdot \hat{d}_m \right) - \frac{1}{2} \text{FS}_0(r_{nm}\omega) \left(\hat{d}_n^\parallel \cdot \hat{d}_m^\parallel \right) \right\}, \quad (5.13)$$

in the Fourier domain. Here $\vec{r}_{nm} = \vec{r}_n - \vec{r}_m$ is the separation vector and \hat{d}^\parallel denotes the component of the dipole unit vector parallel to \vec{r}_{nm} , with the entire functions

$$\text{FS}_1(z) \equiv \frac{3(z^2 - 1) \sin(z) + z \cos(z)}{z^3}, \quad (5.14)$$

$$\text{FS}_0(z) \equiv 3 \frac{(z^2 - 3) \sin(z) + 3z \cos(z)}{z^3}. \quad (5.15)$$

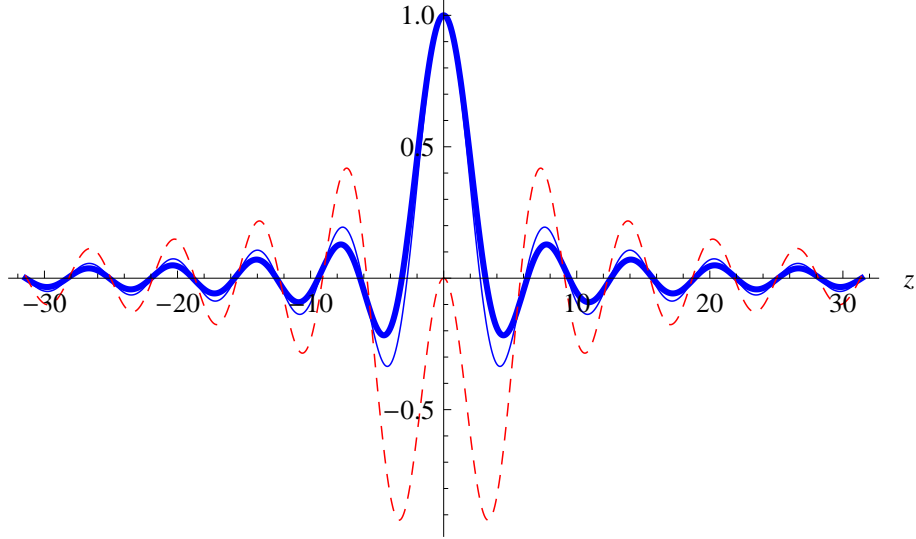


Figure 5.3: Comparison of sinc (bold), FS_1 , and FS_0 (dashed). Sinc and FS_1 are extremely qualitatively similar, both being unity at zero whereas FS_0 vanishes at zero.

In Fig. 5.3 we compare these functions. One can see that the scalar-field correlations are very similar to that of the electromagnetic field when $\vec{d}_n \parallel \vec{d}_m \perp \vec{r}_{nm}$. Under this condition, one can also see that the cross correlations, which are very nonlocal, are maximized when the dipoles are very close. Whereas when the dipoles are very far apart, the cross correlations always vanish and thus all noise can be treated independently. As we will wish to maximize cross correlations, we will primarily work with the scalar-field correlations, which one can think of as being very similar to the parallel dipoles.

Our theory will be manifestly causal (as long as our renormalization and state preparation is causal) given that our field correlations are inherently causal. Note

for instance the temporal representation of the scalar-field damping kernel

$$\gamma_{nm}(t) = \frac{\tilde{\gamma}_0}{2} \delta_{r_{nm}}(t), \quad (5.16)$$

$$\delta_r(t) \equiv \frac{\theta(r-|t|)}{2r}, \quad (5.17)$$

where θ is the Heaviside step function. This kernel strictly adheres to the light cone.

The fluctuation-dissipation relation allows us to express the environmental correlations in terms of the damping kernel as

$$\tilde{\alpha}(\omega) = \tilde{\gamma}(\omega) \frac{\omega}{\sinh\left(\frac{\omega}{2T}\right)} e^{-\frac{\omega}{2T}}, \quad (5.18)$$

$$= 2 \tilde{\gamma}(\omega) \omega [\bar{n}(|\omega|, T) + \theta(-\omega)], \quad (5.19)$$

and also noise kernel as

$$\tilde{\nu}(\omega) = \tilde{\gamma}(\omega) \omega \coth\left(\frac{\omega}{2T}\right), \quad (5.20)$$

$$= \tilde{\gamma}(\omega) |\omega| [\bar{n}(|\omega|, T) + 1], \quad (5.21)$$

where $\bar{n}(\omega, T)$ is the thermal average photon number in a mode of frequency ω . The damping kernel $\tilde{\gamma}(\omega)$ characterizes dissipation, the noise kernel $\tilde{\nu}(\omega)$ characterizes diffusion, and the full quantum correlation $\tilde{\alpha}(\omega)$ can be thought to characterize decoherence [54]. For two very close and parallel dipoles the off-diagonal entries of the kernels approach the diagonal values, and in doing so an eigen-value must also vanish. At resonance this damping and decoherence deficit can give rise to a “dark state” as we explain more thoroughly in Sec. 5.2.2.2.

5.2.1.2 Master equation form and coefficients

We will find the dynamics of the reduced density matrix of the atoms using the weak-coupling master equation Eq. (1.17). In this case

$$\mathcal{L}_{[2]} \rho = \sum_{nm} [\sigma_{x_n}, \rho (\mathbf{a}_{nm} \diamond \sigma_{x_m})^\dagger - (\mathbf{a}_{nm} \diamond \sigma_{x_m}) \rho] , \quad (5.22)$$

with the second-order operator most easily represented by the ladder operators as

$$(\mathbf{a}_{nm} \diamond \sigma_{x_m}) = A_{nm}(+\Omega_m) \sigma_{+m} + A_{nm}(-\Omega_m) \sigma_{-m} , \quad (5.23)$$

and the second-order coefficients being related to the correlation function as

$$A_{nm}(\omega) = \frac{1}{2} \tilde{\alpha}_{nm}(\omega) - i \mathcal{P} \left[\frac{1}{\omega} \right] * \tilde{\alpha}_{nm}(\omega) , \quad (5.24)$$

here in the late-time limit (as compared to system and cutoff timescales), where \mathcal{P} denotes the Cauchy principal value.

The first portion of the second-order coefficient, or Hermitian part (here real), is immediately given by Eq. (5.19). Whereas the second term, or anti-Hermitian part (here imaginary), must be evaluated via the convolution

$$\text{Im}[A_{nm}(\omega)] = -\frac{1}{2\pi} \int_{-\infty}^{+\infty} d\varepsilon \mathcal{P} \left[\frac{1}{\omega - \varepsilon} \right] \tilde{\alpha}_{nm}(\varepsilon) , \quad (5.25)$$

and together they form a causal response function. These are the coefficients which often require regularization and renormalization. For now let us simply evaluate the bare coefficients for non-vanishing r . For finite temperatures, the coefficients exactly evaluate to

$$\begin{aligned} \text{Im}[A_{nm}(\omega)] = & + \frac{\tilde{\gamma}_0}{r_{nm}} \frac{1}{\pi} \text{Im} \left[\Phi_1 \left(\frac{i\omega}{2\pi T}; 2\pi T r_{nm} \right) \right] \\ & - \frac{\tilde{\gamma}_0}{r_{nm}} \left\{ \frac{T}{\omega} - \frac{1}{2} \left[\coth \left(\frac{\omega}{2T} \right) - 1 \right] \cos(r_{nm}\omega) \right\} , \end{aligned} \quad (5.26)$$

in terms of the Lerch Φ_1 function

$$\Phi_1(z; \lambda) \equiv \sum_{k=1}^{\infty} \frac{e^{-k\lambda}}{k+z}. \quad (5.27)$$

This functional representation is exact, though best for positive temperature. Conversely, one also has the low-temperature expansion

$$\begin{aligned} \text{Im}[A_{nm}(\omega)] &= \frac{\tilde{\gamma}_0}{r_{nm}} \frac{\text{sign}(\omega)}{\pi} \sum_{k=1}^{\infty} S_k \\ &- \frac{\tilde{\gamma}_0}{r_{nm}} \frac{1}{\pi} [\sin(r_{nm}\omega) \text{ci}(|r_{nm}\omega|) - \cos(r_{nm}\omega) \text{si}(r_{nm}\omega)], \end{aligned} \quad (5.28)$$

in terms of the summand

$$S_k = \frac{\text{Ei}[(+k\beta + i r_{nm})|\omega|]}{e^{(+k\beta + i r_{nm})|\omega|}} + \frac{\text{Ei}[-k\beta + i r_{nm})|\omega|] - i\pi}{e^{(-k\beta + i r_{nm})|\omega|}}, \quad (5.29)$$

and where the trigonometric integrals are defined

$$\text{si}(z) \equiv - \int_z^{\infty} dz' \frac{\sin(z')}{z'}, \quad (5.30)$$

$$\text{ci}(z) \equiv - \int_z^{\infty} dz' \frac{\cos(z')}{z'}, \quad (5.31)$$

$$\text{Ei}(z) \equiv - \int_{-z}^{\infty} dz' \mathcal{P} \left[\frac{e^{-z'}}{z'} \right], \quad (5.32)$$

however, for positive temperatures this expansion is not well behaved for small energy differences. For zero temperature, the exact relation (the second term on the right-hand side in (5.28)) is well behaved and matches perfectly to the zero-temperature limit of Eq. (5.26).

At resonance it may be useful to cast Eq. (5.22) in a somewhat more familiar form as

$$\frac{d}{dt} \boldsymbol{\rho} = -i [\mathbf{H} + \mathbf{V}_{\text{RW}} + \mathbf{V}_{\text{NRW}}, \boldsymbol{\rho}] + \mathcal{D}_{\text{RW}} \{\boldsymbol{\rho}\} + \mathcal{D}_{\text{NRW}} \{\boldsymbol{\rho}\}, \quad (5.33)$$

with the Hermitian generators

$$\begin{aligned} \mathbf{V}_{\text{RW}} \equiv & + \sum_{nm} \text{Im}[A_{nm}(-\Omega)] \boldsymbol{\sigma}_{+n} \boldsymbol{\sigma}_{-m} \\ & + \sum_{nm} \text{Im}[A_{nm}(+\Omega)] \boldsymbol{\sigma}_{-n} \boldsymbol{\sigma}_{+m}, \end{aligned} \quad (5.34)$$

$$\begin{aligned} \mathbf{V}_{\text{NRW}} \equiv & + \sum_{nm} \frac{A_{nm}(+\Omega) - A_{nm}^*(-\Omega)}{2i} \boldsymbol{\sigma}_{+n} \boldsymbol{\sigma}_{+m} \\ & + \sum_{nm} \frac{A_{nm}(-\Omega) - A_{nm}^*(+\Omega)}{2i} \boldsymbol{\sigma}_{-n} \boldsymbol{\sigma}_{-m}, \end{aligned} \quad (5.35)$$

and (pseudo) Lindblad-form dissipators

$$\begin{aligned} \mathcal{D}_{\text{RW}}\{\boldsymbol{\rho}\} \equiv & \sum_{nm} \Gamma_{nm} (\bar{n}(\Omega, T) + 1) (2 \boldsymbol{\sigma}_{-n} \boldsymbol{\rho} \boldsymbol{\sigma}_{+m} - \{\boldsymbol{\sigma}_{+m} \boldsymbol{\sigma}_{-n}, \boldsymbol{\rho}\}) \\ & + \sum_{nm} \Gamma_{nm} \bar{n}(\Omega, T) (2 \boldsymbol{\sigma}_{+n} \boldsymbol{\rho} \boldsymbol{\sigma}_{-m} - \{\boldsymbol{\sigma}_{-m} \boldsymbol{\sigma}_{+n}, \boldsymbol{\rho}\}), \end{aligned} \quad (5.36)$$

$$\begin{aligned} \mathcal{D}_{\text{NRW}}\{\boldsymbol{\rho}\} \equiv & \sum_{nm} \frac{A_{nm}^*(-\Omega) + A_{nm}(+\Omega)}{2} (2 \boldsymbol{\sigma}_{+n} \boldsymbol{\rho} \boldsymbol{\sigma}_{+m} - \{\boldsymbol{\sigma}_{+m} \boldsymbol{\sigma}_{+n}, \boldsymbol{\rho}\}) \\ & + \sum_{nm} \frac{A_{nm}^*(+\Omega) + A_{nm}(-\Omega)}{2} (2 \boldsymbol{\sigma}_{-n} \boldsymbol{\rho} \boldsymbol{\sigma}_{-m} - \{\boldsymbol{\sigma}_{-m} \boldsymbol{\sigma}_{-n}, \boldsymbol{\rho}\}), \end{aligned} \quad (5.37)$$

where $\Gamma_{nm} = \Omega \tilde{\gamma}_{nm}(\Omega)$ is the zero-temperature value of $\text{Re}[A_{nm}(-\Omega)]$. The RW terms are among those preserved in the rotating-wave approximation RWA, which results in a Lindblad master equation even outside of the Markovian regime as discussed in Sec. 4.2. At zero temperature these terms coincide with the form of the master equation in Ref. [49] and their expression for the distances dependence of Γ_{nm} . The NRW terms are the so-called ‘‘counter-rotating’’ terms that are neglected in the RWA (though not necessarily \mathbf{V}_{NRW}).

Note that $\text{sinc}(\omega/\Lambda)$ is a high frequency regulator: $\text{sinc}(z) : [0, \infty) \rightarrow [1, 0)$ sufficiently fast for all of our integrals to converge. Therefore we do not need to

consider any additional regularization in our damping kernel if we do not evaluate $\text{sinc}(r\omega)$ for vanishing r . Instead of allowing r to vanish for self-correlations, we impose a high frequency cutoff $r_0 = \Lambda^{-1}$, perhaps motivated by the non-vanishing physical size of the dipole. The more common alternative is to introduce cutoff regularization directly into the field coupling \mathbf{l}_n in Eq. (5.11), often by treating the coupling strength b as a form factor with some gradual \vec{k} -dependence. Different choices of cutoff regulators will yield the same results to highest order in Λ , and the theory should be somewhat insensitive to these details in the end.

Given some form of regularization, the coefficients are then bounded yet also cutoff sensitive. The remaining cutoff sensitivity is reduced through a renormalization scheme. The typical scheme in quantum open systems is to subtract off the zero-energy correction

$$\text{Im}[A_{nm}(0)] = -\frac{\tilde{\gamma}_0}{2r_{nm}}. \quad (5.38)$$

This is equivalent to the quadratic $\sigma_{x_n}\sigma_{x_m}$ counter-term which arises from moving the bilinear system-environment interaction into the square of the harmonic potential for the environment. There are numerous reasons for this choice of renormalization. Most importantly it is the minimal renormalization which ensures a lower bound in the energy spectrum of the interacting system + environment Hamiltonian for all strengths of interaction [53].

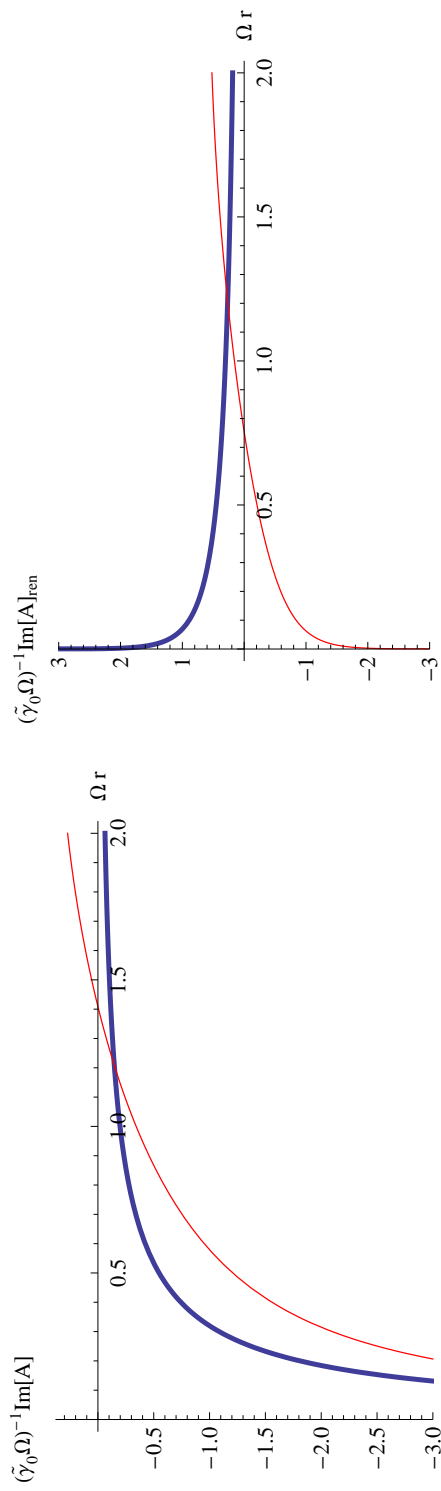


Figure 5.4: Separation dependence of asymptotic coefficients $\text{Im}[A_r(\pm\Omega)]$ for (left) the bare coefficients and (right) the renormalized coefficients, where the bold curve denotes evaluation at $+\Omega$ and the other $-\Omega$.

The bare coefficients contain linear cutoff sensitivity while the renormalized coefficients are only logarithmically cutoff sensitive. As depicted in Fig. 5.4, this cutoff sensitivity only appears for small r as $\text{sinc}(r\omega)$ acts as a natural cutoff regulator regardless of any cutoff regulation we might put in by hand. Small r divergence appears in the coefficients, and thus the induced frequency shifts, of other works [91, 50, 49, 11], which may arise if one has not considered regularization of the full influence of the environment, including all cross terms. Here we have chosen to regularize and renormalize all coefficients $A_{nm}(\omega)$ and not simply the auto-coefficients $A_{nn}(\omega)$.

Putting aside the previous arguments, one might consider renormalization to be a choice of model. However one is not free to choose any form of joint regularization. In previous works, when the cross terms were left unregularized, the implication is that the environment correlation function $\alpha(\omega)$ (5.19) and related influence kernels are not positive definite for large ω . Their environment correlation therefore does not strictly correspond to any microscopic model and there can potentially be some pathology associated with this.

Finally we question the physical implications of renormalization or the lack thereof in its entirety. Without full renormalization of cross terms, one has a theory where *neutral* atoms have $1/r$ potential interactions at *close range*. This does not appeal to physical expectations.

For the full-time evolution of initially uncorrelated states, one must apply the

full-time coefficients

$$A_{nm}(\omega; t) = \int_0^t d\tau e^{-i\omega\tau} \alpha_{nm}(\tau), \quad (5.39)$$

which must exhibit causal behavior as the field correlations are causal. At zero temperature there is a $(r - t)^{-1}$ pole in the integrand which can be encapsulated by contour integrals for $t > r$. The encapsulation of this pole produces an activation *jolt* in the master equation coefficients precisely at $t = r$ which we plot in Fig. 5.5.

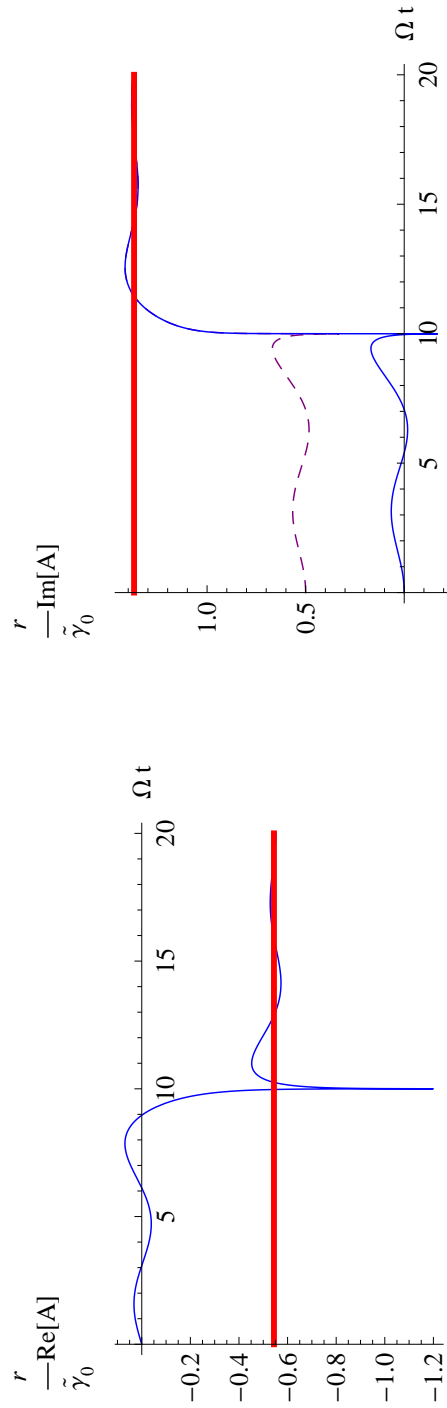


Figure 5.5: $\text{Re}[A_{nm}(-\Omega_m; t)]$ (left) and renormalized $\text{Im}[A_{nm}(-\Omega_m; t)]$ (right) for a zero temperature reservoir at $r_{nm} = 10/\Omega_m$. The bold line denotes the asymptotic coefficients. For the latter plot, the dashed curve is the result of simultaneous renormalization and is acausal.

Prior to the jolt, the master equation coefficients are roughly zero; whereas after the jolt, the coefficients are roughly their asymptotic value. For positive temperatures there is an infinite series of poles increasingly attenuated by the rising temperature.

With the consideration of renormalization, one becomes even more directly confronted with causality. If renormalization is applied to the entire system simultaneously, e.g.

$$\text{Im}[A_{nm}(\omega; t)] \rightarrow \text{Im}[A_{nm}(\omega; t)] - \text{Im}[A_{nm}(0; \infty)], \quad (5.40)$$

then the renormalization will be felt instantaneously over finite distances. Effectively such an acausal renormalization is introducing a counter term into the Hamiltonian at $t = 0$ for which there is nothing to counter until $t > r$. Whereas if renormalization is applied at a retarded time, e.g.

$$\text{Im}[A_{nm}(\omega; t)] \rightarrow \text{Im}[A_{nm}(\omega; t)] - \theta(t - r_{nm}) \text{Im}[A_{nm}(0; \infty)], \quad (5.41)$$

where $\theta(z)$ denotes the unit-step function, then the renormalized theory will be as causal in its behavior as the non-renormalized theory. Renormalization (and any state preparation [55]) must be performed in a causal manner (along the light cone) if one desires causal evolution. Improper renormalization, in the context of a factorized initial state of the system and environment, will create (apparently) mediated interactions between the atoms which are activated before mediation can actually occur. Such a theory is Hamiltonian, but not causal.

5.2.2 Second-order solutions

From an analysis of the full-time coefficients (see Fig. 5.5), one can see that each coefficient jolts on at $t = r$.² So for $t < r$ the atoms roughly evolve independently (equivalent to $r \rightarrow \infty$) and then for $t > r$ the atoms become aware of each other's presence and evolve jointly. If there is any acausal behavior, such as creation of entanglement outside of the light cone, then it would have to be very small.

Because the master equation coefficients mostly asymptote to constant values quite quickly here in the weak-coupling regime, as can be seen in Fig. 5.5, it is sufficient to consider a sequence of constant Liouvillians [55]. E.g. for two atoms

$$\mathcal{L}_{[r]}(t) \approx \begin{cases} \mathcal{L}_{[\infty]}(\infty) & t < r \\ \mathcal{L}_{[r]}(\infty) & t > r, \end{cases} \quad (5.42)$$

and therefore the full-time propagator can be sufficiently approximated by a chain of exponential propagators, here

$$\mathcal{G}_{[r]}(t) \approx \begin{cases} e^{t\mathcal{L}_{[\infty]}(\infty)} & t < r \\ e^{t\mathcal{L}_{[r]}(\infty)} e^{r\mathcal{L}_{[\infty]}(\infty)} & t > r. \end{cases} \quad (5.43)$$

A more accurate full-time treatment would be sensitive to initial conditions, and our factorized initial conditions are not reasonable enough to warrant that level of scrutiny for any physical applications. For the remainder of the chapter, we will be interested in the $t \gg r$ regime. The challenge then lies in calculating the evolution due to $e^{t\mathcal{L}_{[r]}(\infty)}$.

²The jolting (here logarithmic divergence) is a result of the factorized initial conditions and would become a more smooth activation upon considering properly correlated initial states or switching on the interaction gradually.

5.2.2.1 Dynamics

The open-system dynamics are described approximately by the time-independent Liouvillian $\mathcal{L}_{[r]}(\infty)$, which we will now write simply as \mathcal{L} . The time evolution is then approximately $e^{t\mathcal{L}}$, and we will compute it from the solutions of the eigen-value problem

$$\mathcal{L}\mathbf{o} = f\mathbf{o} \quad (5.44)$$

as in Sec. 1.2.3, where f is an eigenvalue and \mathbf{o} a right eigen-operator (super-vector). In principle this can be performed numerically with the super-matrix operators, but when confronted with numerical instability we resorted to a careful application of canonical perturbation theory, discussed in Sec. 1.2.3. The perturbative corrections to the eigenvalues will give us environmentally-induced frequency shifts and dissipation rates, while the eigen-operators will determine the details of the evolution of the quantum state. As always, we know that this perturbative problem is degenerate at zeroth order.

As our system coupling is non-stationary (the coupling operator anti-commutes with the Hamiltonian), with no additional degeneracies the cross-coupling will have no effect upon the second-order frequencies of the perturbed off-diagonal operators, and the f_{ij} corresponding to $|\omega_i\rangle\langle\omega_j|$ for $i \neq j$ are given by

$$f_{ij} = -i\omega_{ij} + \langle\omega_i|\mathcal{L}_{[2]}\{|\omega_i\rangle\langle\omega_j|\}\omega_j\rangle, \quad (5.45)$$

which reference no cross-correlations. Second-order corrections to the eigen-operators \mathbf{o} (and thus the states) can then be found by perturbative consistency with the master equation. Dynamics of the diagonal operators and any other degenerate (and

near-degenerate) subspaces must be treated much more carefully with degenerate perturbation theory. For the energy states, their second-order dynamics are encapsulated by a Pauli master equation. This gives rise to their second-order relaxation rates and zeroth-order eigen-operators. Due to inherent degeneracy, $\omega_{ii} = \omega_{jj} = 0$ and any resonant frequencies, their second-order operator perturbations require the fourth-order Pauli master equation as discussed in Sec. 4.1. In Sec. 5.2.2.3 we use the alternative method of Sec. 5.1.1 to calculate corrections to the asymptotic or reduced thermal state using only the second-order coefficients. Based on the results of Ch. 4, in general the matrix elements of the solution $\rho(t)$ expressed in the (free) energy basis will be accurate to $\mathcal{O}(\gamma/\Omega)$ off the diagonal but only to $\mathcal{O}(1)$ on the diagonal. Timescales are known to $\mathcal{O}(\gamma)$. If we had used the RWA, however, *all* matrix elements are only good to $\mathcal{O}(1)$.

In Figs. 5.6–5.7 we plot all relaxation rates associated with the two-atom system as a function of proximity, where γ is specifically the decoherence rate of a single isolated atom. For large separation the decay rates for $|\Psi_{\pm}\rangle \equiv (|0,1\rangle \pm |1,0\rangle)/\sqrt{2}$ are $1 + 1$ times γ (which would be $N\gamma$ for N atoms), as the noise processes are independent and the decay rates are additive. Whereas at proximity they become 0 and N^2 times γ for $|\Psi_{-}\rangle$ and $|\Psi_{+}\rangle$ respectively, as the noise processes are maximally correlated and display destructive and constructive interference. In Fig. 5.8 we plot all non-stationary decoherence rates associated with the two-atom system as a function of detuning. To achieve a dark state, the tuning of the two atoms must be much better than the dissipation, $\delta\Omega \ll \gamma$, which counter-intuitively implies that weak-dissipation is not always desirable to preserve coherence. However, this con-

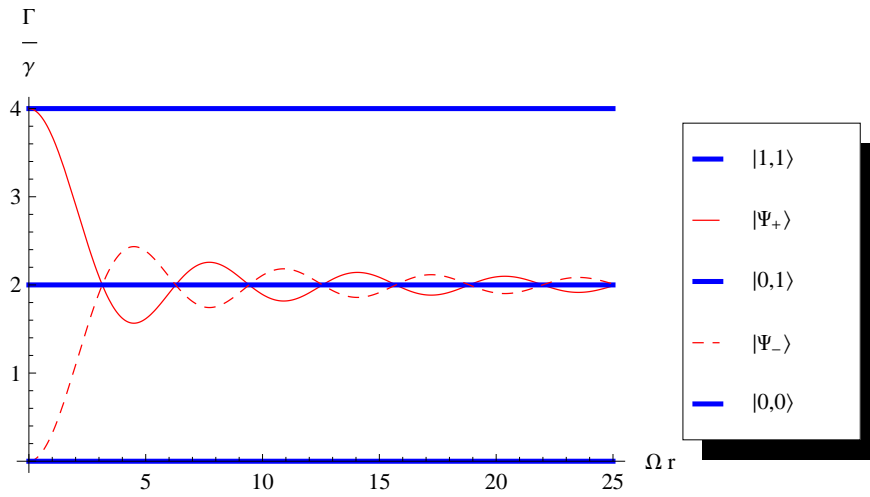


Figure 5.6: Decay rates of the (zeroth-order) stationary operators for two resonant atoms in a zero-temperature environment at varying separation distance. The legend indicates the pure states the curves approximately correspond to in the order they occur at the vertical axis.

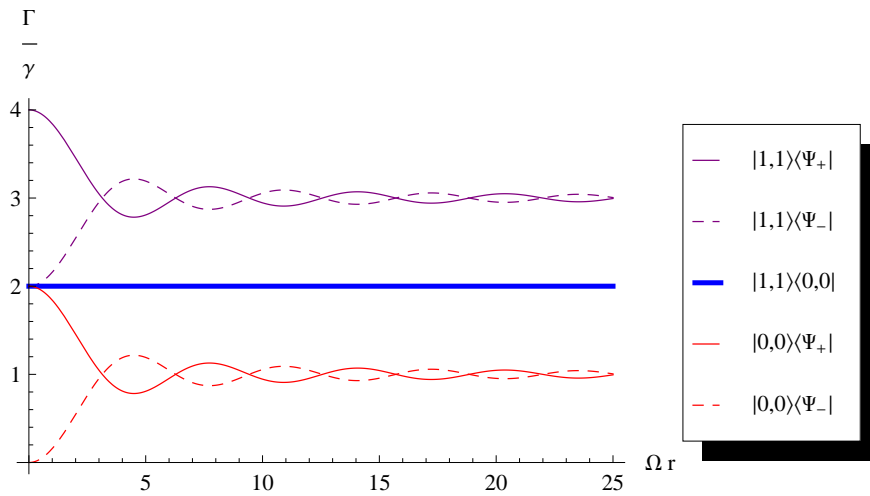


Figure 5.7: Decoherence rates of the (zeroth-order) non-stationary operators for two resonant atoms in a zero-temperature environment at varying separation distance. The legend indicates the matrix elements the curves correspond to in the order they occur at the vertical axis.

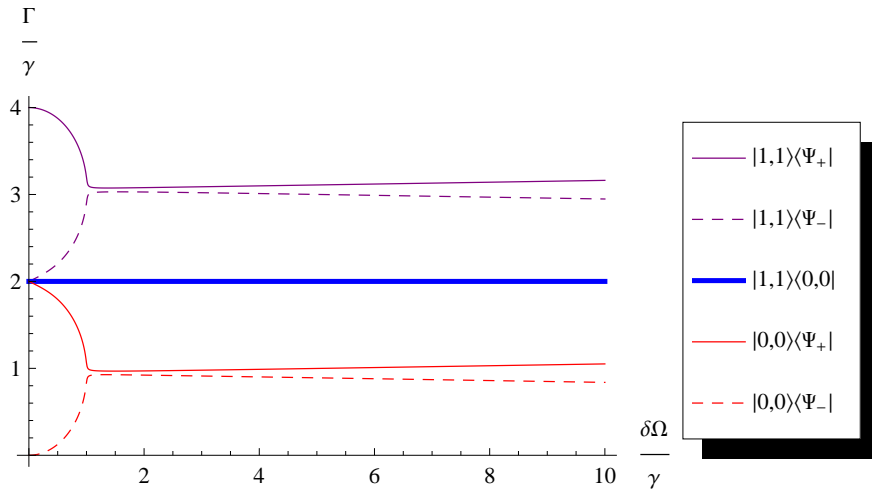


Figure 5.8: Decoherence rates of the (zeroth-order) non-stationary operators for two atoms in a zero-temperature environment at varying detuning and vanishing separation, $r_{12} \ll \Omega_1, \Omega_2$, with $\gamma = \langle \Omega \rangle / 100$. The legend indicates the matrix elements the curves approximately correspond to for small detunings (in the order they occur at the vertical axis) as to compare with Fig. 5.7.

dition makes more sense if thought of in another way: The dark state arises from the destructive interference of the emission from the two atoms. If the emission from each atom is characterized by center frequency Ω_n and an emission line width γ , then the condition $\delta\Omega \ll \gamma$ simply specifies that the emission lines of the atoms must overlap enough that their emissions are not distinguishable from one another. This allows the required destructive interference.

One behavior which is qualitatively different from the closed-system evolution is the damped oscillations between the singly-excited states. More specifically for any initial state of the form

$$\rho_0 = \begin{array}{c} |0,1\rangle \\ |1,0\rangle \end{array} \begin{bmatrix} a + \delta & +i b \\ -i b & a - \delta \end{bmatrix} \begin{array}{c} \langle 0,1| \\ \langle 1,0| \end{array}, \quad (5.46)$$

with all positive coefficients, in addition to the Bell state decay one will also have damped oscillations of the form

$$\begin{aligned} & [\delta \cos(f_1 t) - b \sin(f_1 t)] e^{-\gamma_1 t} (|0,1\rangle\langle 0,1| - |1,0\rangle\langle 1,0|) \\ & + i [b \cos(f_1 t) + \delta \sin(f_1 t)] e^{-\gamma_1 t} (|0,1\rangle\langle 1,0| - |1,0\rangle\langle 0,1|) \end{aligned} \quad (5.47)$$

which can oscillate from one excited state to the other excited state. But this happens very slowly, with the frequency

$$f_1 = 2\tilde{\gamma}_0 \frac{1 - \cos(\Omega r)}{r}, \quad (5.48)$$

for all temperatures. The oscillation arises from the master equation term defined in Eq. (5.34), and should be present in conventional calculations using the RWA. This particular frequency vanishes for small separation; without our choice of regularization and renormalization, as detailed in Sec. 5.2.1.2, it would diverge.

5.2.2.2 Subradiance

All stationary (and thus decoherence-free) states ρ_D of the open-system must satisfy the relation

$$\mathcal{L} \rho_D = 0, \quad (5.49)$$

and are thus right eigen-supervectors of the Liouvillian with eigenvalue 0. As the Liouvillian is not Hermitian, there is no trivial correspondence between the left and right eigen-supervectors. The super-adjoint of the master equation [26] time-evolves system observables and for closed systems can be contrasted

$$\mathcal{L}_{[0]} \rho = -i[\mathbf{H}, \rho], \quad (5.50)$$

$$\mathcal{L}_{[0]}^\dagger \mathbf{S} = +i[\mathbf{H}, \mathbf{S}]. \quad (5.51)$$

The left eigen-supervector \mathbf{S}_D^\dagger corresponding to ρ_D must therefore satisfy

$$\mathcal{L}^\dagger \mathbf{S}_D = 0. \quad (5.52)$$

So for every stationary or decoherence-free state ρ_D there is a symmetry operator \mathbf{S}_D whose expectation value is a constant of the motion. The thermal state or reduced thermal state is such a state. In the limit of vanishing coupling strength, this state is the familiar Boltzmann thermal state. One can check that the symmetry operator in this case is proportional to the identity and corresponds to $\text{Tr}[\rho]$ being a constant of the motion.

For two resonant dipoles, with $\Omega_n = \Omega$, there is another stationary state in the limit of vanishing separation $r_{12} = r$. Because of degeneracy, any superposition

of states

$$|\Psi\rangle = a_1 |1,0\rangle + a_2 |0,1\rangle , \quad (5.53)$$

is also an energy state and therefore annihilated by both $\mathcal{L}_{[0]}$ and $\mathcal{L}_{[0]}^\dagger$. Further note that for vanishing separation, the noise processes $\mathbf{l}_n(t)$ become exactly correlated and identical. Their contributions to the interaction Hamiltonian can then be collected into

$$\mathbf{H}_{I_1} + \mathbf{H}_{I_2} = (\sigma_{x_1} + \sigma_{x_2}) \mathbf{l}_n = \sigma_x \mathbf{l}_n . \quad (5.54)$$

Next we note the equality

$$\sigma_x |1,0\rangle = \sigma_x |0,1\rangle , \quad (5.55)$$

so that for the Bell states

$$|\Psi_\pm\rangle \equiv \frac{1}{\sqrt{2}} \{|1,0\rangle \pm |0,1\rangle\} , \quad (5.56)$$

the noise adds destructively for $|\Psi_-\rangle$ and constructively for $|\Psi_+\rangle$. Therefore $|\Psi_-\rangle$ is a decoherence-free state (dark state) of the open system for vanishing separation and at resonance, regardless of coupling strength or temperature. And whereas $|\Psi_-\rangle$ appears dark (subradiant), $|\Psi_+\rangle$ appears bright (superradiant) [44]. Note that for anti-parallel dipoles, these roles will be reversed due to the anti-correlated noise.

In this particular case the left and right eigen-supervectors are equivalent, and so it is the dark-state component $\langle\Psi_-|\rho|\Psi_-\rangle$ which is a constant of the motion. However, unlike the thermal state, if the separation is no longer vanishing then this is not some perturbative limit of a stationary state but of a very long-lived state.

The final constant of motion, which we have validated by analyzing the eigen-system of \mathcal{L} , corresponds to the coherence between the ground state and the dark state or $\langle 0,0 | \rho | \Psi_- \rangle$. Using these constants of motion, for two very close dipoles in a zero-temperature environment with initial state ρ_0 , the system will relax into the state

$$\rho_1 = (1 - b) |0,0\rangle\langle 0,0| + b |\Psi_-\rangle\langle \Psi_-| + c |0,0\rangle\langle \Psi_-| + c^* |\Psi_-\rangle\langle 0,0| , \quad (5.57)$$

$$b \equiv \langle \Psi_- | \rho_0 | \Psi_- \rangle , \quad (5.58)$$

$$c \equiv \langle 0,0 | \rho_0 | \Psi_- \rangle , \quad (5.59)$$

to zeroth order in the system-environment coupling, whereupon the system has bipartite entanglement b .

While our (regularized) model is well behaved in the mathematical limit $r \rightarrow 0$, it is important to remember that physically the model is no longer valid for sufficiently small r . At small enough r other terms would come into play, including electrostatic interaction, and eventually the atoms would cease to even be distinct. We are assuming that this scale is much smaller than all other scales in our model (except perhaps the cutoff). This means that we can sensibly consider cases where r is small compared to the other parameters, but r cannot vanish completely.

Since the coefficients of our master equation are continuous in r , it is useful to consider $r = 0$ to understand the limiting behavior as r becomes small. The existence of the dark state we have discussed at $r = 0$ means that this state will be almost completely dark when r is small; thus, any initial state ρ_0 will first relax approximately into the state given in Eq. (5.57) within the ordinary relaxation timescale γ , and then on a much longer relaxation timescale τ , where roughly $1/\tau \approx \gamma(\Omega r)^2$ for

small r , the system will fully thermalize. However, this expression for the dark state is only to zeroth-order in the system-environment coupling. In order to understand the subsequent final state of decay one needs the second-order asymptotics that we discuss in Sec. 5.2.2.3.

Finally we would note that this “dark state” is a very general feature of resonant multipartite systems with similar linear couplings to a shared environment. One can rather easily work out that for a pair of resonant linear oscillators with these same noise correlations the sum mode is thermalized, and the difference mode is decoherence free for vanishing separation. The separation dependence of the entanglement dynamics of two resonant oscillators was considered in Ref. [92], while that of (effectively) two very close oscillators was considered in Ref. [107, 108].

The subradiant dark state achieves destructive interference in the environmental noise (and thus little-to-no emission) while the bright state achieves constructive interference in the noise (and thus near-maximal emission). For the superradiant bright state one essentially couples the system to N copies of the same noise process $\mathbf{l}_n(t)$ and therefore the superradiant emission rate *can* be proportional to N^2 [44]. An N^2 dependence does appear the case as we demonstrate in Fig. 5.9. The emission rate is (perturbatively) determined by the noise correlation (the square of the noise process). Both results differ having from N independent noise processes where one can simply add the N independent noise correlations which results in an emission rate at most proportional to N .

Following the previous approach, we define a *proper dark state* as an atomic state annihilated by $\mathcal{L}_{[0]}$ and \mathbf{H}_I regardless of the state of the environment. Let us

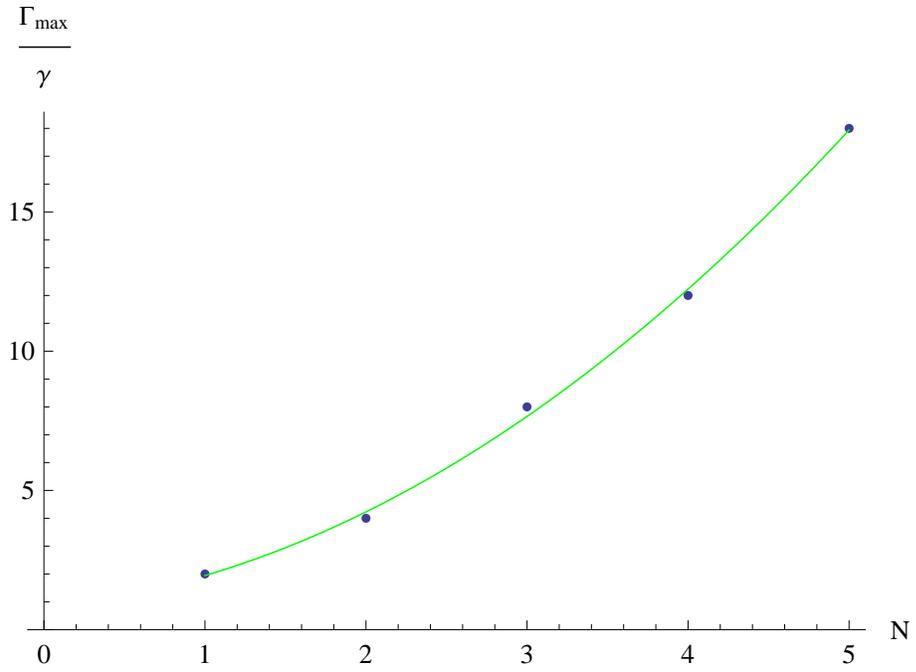


Figure 5.9: Maximal (over states) second-order decay rates as a function of the number of atoms N , at zero temperature and in close proximity. The solid curve denotes the best quadratic fit and has a corresponding p-value of 2.4%, which is fairly significant in corroborating an N^2 dependence.

consider an assembly of N resonant dipoles at close proximity. We first note that the superposition

$$|\Psi\rangle = \sum_{\sum s_n=S} a_{s_1, s_2, \dots, s_N} |s_1, s_2, \dots, s_N\rangle, \quad (5.60)$$

of energy states with the same total excitement S is also an energy state and therefore annihilated by $\mathcal{L}_{[0]}$. Defining the collective spin operator

$$\boldsymbol{\sigma}_x = \sum_n \boldsymbol{\sigma}_{x_n}, \quad (5.61)$$

such that the interaction Hamiltonian can be expressed

$$\mathbf{H}_I = \boldsymbol{\sigma}_x \mathbf{l}_n; \quad (5.62)$$

a proper dark state must then satisfy $\boldsymbol{\sigma}_x |\Psi_-\rangle = 0$ and will be decoherence free. For $N = 2$ this is the familiar Bell state that we've already labeled $|\Psi_-\rangle$.

In considering large N the structure is essentially just what was studied by Dicke [44], so following that approach we define collective y and z spin operators $\boldsymbol{\sigma}_y$ and $\boldsymbol{\sigma}_z$ as well as raising and lowering operators $\boldsymbol{\sigma}_+$ and $\boldsymbol{\sigma}_-$, analogously to Eq. (5.61), as well as $\boldsymbol{\sigma}^2 = \boldsymbol{\sigma}_x^2 + \boldsymbol{\sigma}_y^2 + \boldsymbol{\sigma}_z^2$. And we can note that the free Hamiltonian for the atoms only differs from $\boldsymbol{\sigma}_z$ by a multiple of the identity, so all the eigenstates of that Hamiltonian are also eigenstates of $\boldsymbol{\sigma}_z$. A basis for the Hilbert space of the system can be specified by the eigenstates of $\boldsymbol{\sigma}^2$ with eigenvalues $j(j+1)$ and $\boldsymbol{\sigma}_z$ with eigenvalues m (though for $N > 2$ there will be degeneracy, so that additional quantum numbers are needed to identify a specific state). The dark state we seek must then satisfy $\boldsymbol{\sigma}_z |\Psi_-\rangle = m |\Psi_-\rangle$ and $\boldsymbol{\sigma}_x |\Psi_-\rangle = 0$. As the discussion in [44] implies, only states with $j = 0$ and $m = 0$ can satisfy these requirements

simultaneously. Such states only occur when N is even, and that set of states has dimension $N! / [(N/2 + 1)!(N/2)!]$. These are also the dark states in the RWA, as they are in the null space of both σ_+ and σ_- . For $N = 4$ these states take the form

$$|\Psi_-\rangle = a_1(|0,0,1,1\rangle + |1,1,0,0\rangle) + a_2(|0,1,0,1\rangle + |1,0,1,0\rangle) \\ + a_3(|0,1,1,0\rangle + |1,0,0,1\rangle), \quad (5.63)$$

$$0 = \sum_n a_n, \quad (5.64)$$

where every pair in parenthesis is spin-flip symmetric. One can easily check that any such state is annihilated by σ_x .

More generally we define an *improper dark state* as one only annihilated by \mathcal{L} and not \mathbf{H}_I (i.e., stationary in the coarse-grained open-system dynamics but not in the full closed system dynamics), thus being dependent upon the state of the environment and even the coupling strength. In the simplest case we can consider the zero-temperature environment. For the second-order dynamics, upward transitions are automatically ruled out from the lack of thermal activation. The only term that could lead to population of higher excitation states is the second term in Eq. (5.36), which vanishes at $T = 0$. Rather than investigating the master equation, we can then simply demand that the lowest-order decay transitions are vanishing, meaning that if $|\Psi_-^S\rangle$ has total excitation S , then $\langle S' | \sigma_x | \Psi_-^S \rangle = 0$ for all $S' \leq S$ lesser and equally excited states. We can also state this in terms of the collective spin operators we have defined, by saying that we demand that $|\Psi_-\rangle$ is an eigenstate of σ_z with eigenvalue m , and that all matrix elements onto states with lower m' values must vanish. Since $\sigma_x = \frac{1}{2}(\sigma_+ + \sigma_-)$, we know that there will be non-

vanishing matrix elements onto states with $m' = m - 1$ unless $m = -j$. So any state with $m = -j$ is an imperfect dark state at zero temperature, and there are $N!(2j + 1)/[(N/2 + j + 1)!(N/2 - j)!]$ such states [44]. Interestingly, in the RWA such states (when combined with a vacuum field) are also stationary states but of the closed-system dynamics. For $N = 3$ and at zero temperature, all such dark states can be expressed

$$|\Psi_{-}\rangle = a_1 |1,0,0\rangle + a_2 |0,1,0\rangle + a_3 |0,0,1\rangle, \quad (5.65)$$

$$0 = \sum_n a_n, \quad (5.66)$$

for weak coupling to the field. These dark states also exist for positive temperature, but they take on a different form.

5.2.2.3 The Asymptotic State

In order to get a proper picture of the asymptotic behavior, we now apply the results of Sec. 5.1.1 to find the correct late-time steady state. To zeroth order in the system-environment interaction, the asymptotic steady state is the Boltzmann state

$$\rho_T = \prod_n \rho_{T_n}, \quad (5.67)$$

$$\rho_{T_n} \equiv \frac{1}{2} \left[1 - \tanh\left(\frac{\Omega_n}{2T}\right) \sigma_{z_n} \right], \quad (5.68)$$

in terms of Pauli matrices. For high temperatures, we can use the perturbative expansion of Eq. (5.3) [or Eq. (5.5)] to find the second-order corrections, which are

given by

$$\langle \omega_i | \delta \rho_\beta | \omega_j \rangle = \sum_{nmk} \frac{R_{ijk}^{nm}}{Z_0(\beta)} \langle \omega_i | \sigma_{x_m} | \omega_k \rangle \langle \omega_k | \sigma_{x_n} | \omega_j \rangle . \quad (5.69)$$

All terms with $\omega_i = \omega_j$ are zero, so that this expression gives no correction to the diagonal elements of the density matrix. Otherwise, the (non-resonant) off-diagonal coefficients are given by

$$R_{ijk}^{nm} |_{\omega_i \neq \omega_j} \equiv \text{Im} \left[e^{-\beta \omega_k} \frac{A_{nm}(\omega_{ik}) - A_{nm}(\omega_{jk})}{\omega_i - \omega_j} \right] + \text{Im} \left[\frac{e^{-\beta \omega_i} A_{mn}(\omega_{ki}) - e^{-\beta \omega_j} A_{mn}(\omega_{kj})}{\omega_i - \omega_j} \right] , \quad (5.70)$$

with the free ground-state energy set to zero. At zero temperature we can use the perturbative ground state for the system+environment to find that the off-diagonal second-order corrections to the asymptotic state are still of the form given in Eqs. (5.69) and (5.70), with the coefficients evaluated in the limit $\beta \rightarrow \infty$. The diagonal (and resonant) perturbations are given by

$$\lim_{\beta \rightarrow \infty} R_{ijk}^{nm} |_{\omega_i = \omega_j} = \lim_{\beta \rightarrow \infty} \text{Im} \left[e^{-\beta \omega_k} \frac{d}{d\omega_i} A_{nm}(\omega_{ik}) + e^{-\beta \omega_i} \frac{d}{d\omega_i} A_{mn}(\omega_{ki}) \right] , \quad (5.71)$$

where only a handful of terms are non-vanishing. We note that the expression inside the limit in Eq. (5.71) has both the correct low and high-temperature limits, so it may be roughly correct for all temperatures, but we have yet to fully investigate the fourth-order master equation.

For most regimes the second-order thermal state can now be expressed entirely in terms of the second-order master equation coefficients and limits thereof, therefore we can say that the environmentally induced correlations do vanish for large separations with a power-law decay like $1/r$ and $1/r^2$.

5.2.2.4 Entanglement of Two Atoms and Sudden Death

Now we will consider the bipartite entanglement between any two atoms, labeled n and m , in a system of N atoms in a common quantum field. If the second-order corrections to the eigen-operators of the Liouvillian are neglected, our solution becomes identical to previous solutions using the RWA (e.g., [49]), thus the small corrections introduced will not generally have a significant impact on the qualitative features of entanglement dynamics at early times. However, in examining late-time dynamics and the approach to equilibrium the corrections we calculate are quite important in looking for asymptotic entanglement and SD. We will apply the results of Sec. 5.1.2 and the asymptotic state we have derived for this system to compute the reduced density matrix for the asymptotic state ρ_{nm} and derive the asymptotic value of entanglement between these two atoms. This computation will show that all entangled initial states become disentangled at a finite time.

From Eq. (5.69) it can be readily seen that the atoms are correlated in the asymptotic state at all temperatures, and from our second-order coefficients these correlations experience power-law decay with separation. However, we find based on Eqs. (5.5), (5.69), and (5.70) that when the high-temperature expansion is valid (according to Eq. (5.6)) the asymptotic state has $\underline{C}(\rho_{nm}) < 0$. At zero temperature, Eqs. (5.70) and (5.71) also give $\underline{C}(\rho_{nm}) < 0$. In both cases the asymptotic state lies in the interior of the separable states, and all initial states become separable permanently after some finite time. With this property upheld for zero and high temperatures, we suspect this to be true at all temperatures, making entanglement

sudden death a generic feature which happens in every case in this model. Of course, as discussed in Sec. 5.2.2.2, for closely spaced atoms there can be a dark state, so that entanglement persists over a long timescale before eventually succumbing to sudden death. It should also be noted that, while this examination of the asymptotic behavior tells us that entanglement always remains zero after some finite time, we do find $\mathcal{O}(1)$ sudden death and revival of entanglement at earlier times for some initial states (similar to [49]).

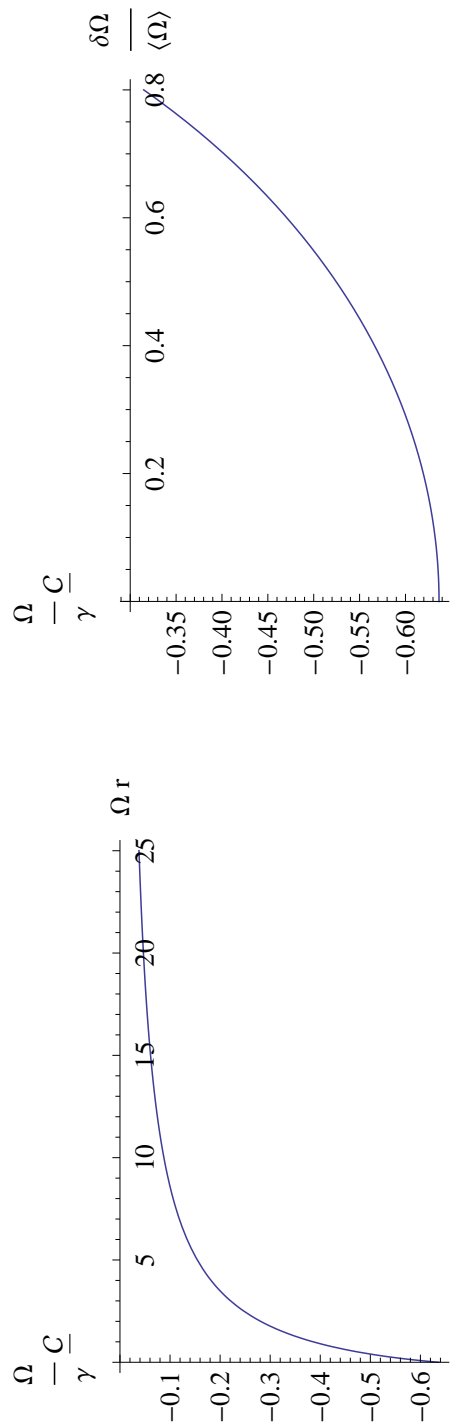


Figure 5.10: Unmaximized concurrence for two resonant atoms at various separation distances (left) and two close atoms at various frequency detunings (right) at zero temperature and for $\gamma = \langle\Omega\rangle/100$.

In Fig. 5.10 we plot \underline{C} as it varies with separation distance and frequency detuning. As a consistency check we also calculated the logarithmic negativity and found it to be consistent with the concurrence to second order. The behavior of the entanglement is markedly different from that of two oscillators in a field. The separation dependence of two resonant oscillators was considered in Ref. [92] and the more general solution will be given in Ref. [57]. For two oscillators, there can be asymptotic entanglement if they are held very close and near enough to resonance with each other. Separation and detuning then causes the entanglement monotonically to decay away. For the two-atom case studied here asymptotic entanglement does not exist, and resonant tuning with proximity will only exacerbate the problem. Permanent sudden death of entanglement occurs because the unmaximized entanglement functions can trend below zero within a finite amount of time and without the need of any asymptotic limit. We would finally note that while the concurrence function does appear to be increasing for large detuning, the parameters drift outside of the weak-coupling regime as one of the frequencies becomes very small.

5.2.3 Discussion

In this chapter we have derived the dynamics of a collection of two-level atoms under a dipole approximation interacting with a common quantized electromagnetic field assuming only weak coupling and not the Born-Markov approximation (BMA) or rotating-wave approximation (RWA). Most prior studies of such systems have assumed the RWA, and the solution we have derived here therefore yields greater

accuracy by going beyond the RWA. We have also presented a method of finding the zero-temperature asymptotic state to higher accuracy than is possible directly with a second-order master equation. We have used this to show that even at zero temperature the bipartite entanglement between any pair of atoms will undergo sudden death for all initial atomic states, in contrast to the predictions of previous theoretical treatments [49] under BMA or RWA. Finally, we have characterized the various decay rates that are present in this solution without the RWA and the sub- and super-radiant states that exist.

Based on the findings of Ch. 4, we know that in the RWA there can be inaccuracies in all entries of the density matrix that are $\mathcal{O}(\gamma/\Omega)$. By contrast, when represented in the (free) energy basis the solution we have derived here will have off-diagonal elements that are accurate at second-order, having $\mathcal{O}((\gamma/\Omega)^2)$ errors. Even in this solution diagonal matrix elements (and matrix elements between any two degenerate energy states) can still have $\mathcal{O}(\gamma/\Omega)$ errors, due to a fundamental limitation of any weak-coupling master equation. However, the expectation of any operator that anti-commutes with the Hamiltonian (including atomic dipole operators), will have only $\mathcal{O}((\gamma/\Omega)^2)$ errors. Moreover, unlike some other methods of solution, our solution can be applied when the atoms have distinct frequencies.

More generally, we have focused on the fact that features of the late-time entanglement dynamics such as SD can often be determined simply by examining the asymptotic state. Sec. 5.1.1 showed how to find the corrections to that asymptotic state, which are missed by direct application of a perturbative master equation and the RWA, at high temperature and zero temperature. At sufficiently high temper-

ature, characterized by Eq. (5.6), the asymptotic state is sufficiently deep in the interior of the set of separable states that all initial states are predicted to undergo SD, with or without the corrections to asymptotic state. At lower temperatures, however, these corrections can move the asymptotic state across the boundary between separable and entangled states, changing the qualitative behavior entirely and potentially allowing asymptotic entanglement or universal SD. Specifically, we find that the RWA constrains the zero temperature asymptotic state to lie exactly on the boundary of the separable states, leading to the appearance of SD depending on the initial state; this is simply an artifact of the approximation, and the proper second-order corrections will generally perturb the asymptotic state such that either SD or asymptotic entanglement is universal. In the specific case of the atoms interacting with a common field, we find that the asymptotic state moves to the interior of the separable states and SD occurs for all initial states.

As discussed in Ch. `ch:approx`, in many experimental contexts the second-order corrections we discuss can be quite small. Though lowest order corrections to the timescales cannot be ignored (as they are responsible for the presence of dissipation), corrections of this size to the values of the density matrix elements at any instant can easily be considered negligible. However, in the case of a theoretical study of entanglement sudden death, where one wishes to distinguish asymptotic decay to zero from vanishing in finite time, small perturbations can become vitally important, as they do at low temperature. In optical frequency atomic systems, for example, γ/Ω might be on the order of 10^{-9} , but at room temperature the thermal-average photon number will be sufficiently small that it places the system into what

we are considering the low-temperature regime for entanglement dynamics.

Chapter 6

Conclusion

Quantum entanglement is a phenomenon that is of great theoretical and practical importance. In this work we have examined the dynamics of entanglement in the context of atom-field interactions, and we will begin this section with an overview of the results.

To begin our examination, we have taken the usual approximated Hamiltonian — subject to the two-level, dipole, and rotating-wave approximations¹— and derived an exact solution of the entanglement dynamics between the atom and field for that Hamiltonian, going beyond previous calculations limited to weak coupling or early times.

For the most part, however, we have focused on the role of atomic separation in shaping the time evolution of entanglement between two atoms interacting with a common field. We seek to characterize important qualitative features that may arise, such as the dynamical generation of entanglement, the protection of pre-existing entanglement, and the phenomenon of entanglement sudden death (SD), which is both theoretically intriguing and potentially a serious practical concern for quantum information processing. Using a model with two field modes, we see the role of atomic separation in its simplest form and find this is sufficient to exhibit a large variety of

¹In fact the form of the rotating-wave approximation that we use in Ch. 2 and 3 is what we identify in Ch. 4 specifically as the pre-trace form.

qualitative behaviors. This encompasses and extends previous results, which treated certain sub-cases [136, 137, 33, 85, 128]. We find that the choice of atomic separation and initial field state can determine whether a state undergoes SD or avoids it, but we find that SD seems to be the generic behavior for most scenarios. We have used the weak-coupling master equation to consider the dynamics of two atoms interacting with the free field, going beyond the rotating-wave approximation (RWA) unlike most previous treatments [6, 26, 131, 32, 11, 12, 138, 141, 136, 137, 50, 49, 51]. We avoid the problems arising from the approximations used by previous work and derive the perturbatively correct steady state of the system for zero temperature and show that, although close spacing of the atoms can cause a long-lived sub-radiant state, all initial atomic states will undergo entanglement sudden death, in contrast to previous predictions [138, 49, 51].

Addressing the more general issues contained in these problems, we have examined the accuracy of perturbative master equations and found that they will yield unexpectedly large errors. This effect does not seem to be accounted for in the literature, and among other consequences it precludes finding the lowest-order corrections to the system's steady state. Perturbative master equations are extremely prevalent in atomic and optical physics and beyond (see e.g., [32, 26]), so the applicability of this result is quite broad. Similarly, we have used the weak-coupling master equation to make a detailed and general evaluation of the discrepancies introduced by using the RWA, where previous analyses had focused on particular sorts of observables or Hamiltonians or particular models [6, 4, 5, 37, 45, 29, 127]. We have shown that while the RWA can obtain the lowest-order corrections to dissipation timescales, it

will give inaccurate lowest-order corrections to the quantum state itself. Finally, we have found that the inaccuracies arising from both of these approximations make the master equations that use them inadequate for making meaningful predictions about the asymptotic late-time behavior of entanglement in general. We have found that the weak-coupling master equation (without RWA) will be sufficient at high temperature and that there is an alternative method of deriving the correct behavior at zero temperature, which we apply to the two-atom problem. However, we have shown that the initial-state dependence of SD featured in many previous calculations (e.g., [138, 49, 141]) is simply an artifact created by the use of the RWA.

We now discuss these results in more detail, beginning with what we have found about the effect of approximations. In Ch. 4 we examined the effect of the weak-coupling and RWA on the predicted dynamics of an open quantum system. Perturbative master equations, including the Born-Markov and Redfield equations, are very commonly used in the study of open quantum systems [81, 32, 25, 26, 122]. It would seem natural that perturbative master equations which are accurate to second-order in the system environment coupling should give solutions accurate to second order; however, we have found in Sec. 4.1 that there will be second-order inaccuracies in the solutions obtained from second-order master equations. The RWA (in one of the two forms we've identified) is widely used in the study of atom-field interactions (and other systems with similar interaction Hamiltonians) [26, 131, 32]. While the RWA has been evaluated previously, such general results about its accuracy have been lacking. Using solutions to the weak-coupling master equation, we have shown that the RWA will introduce additional second-order errors in solu-

tions. If the system has a characteristic frequency Ω and dissipation rate γ , second order terms can be said to be $\mathcal{O}(\gamma/\Omega)$ in terms of those more physically relevant quantities. If the density matrix is expressed in the energy basis, the solution of a second-order perturbative master equations has inaccuracies of $\mathcal{O}(\gamma/\Omega)$ in the diagonal elements and use of the RWA introduces additional inaccuracies of the same order in all elements of the density matrix. Our analysis of the dynamics through the eigen-decomposition of the Liouvillian proves useful in addition, because it illustrates that all timescales can be obtained correctly to second order (having only $\mathcal{O}(\gamma^2/\Omega)$ errors), and it is only the elements of the density matrix at an instant that have the larger errors. Because these approximations are so widely used, it is incumbent upon us to explore why they have met with apparent success in many contexts despite these shortcomings.

In terms of mathematics, we have identified three limits in which these discrepancies vanish: 1) At early times $t \ll 1/\gamma$ the errors will be higher order. If one solves using the eigen-decomposition, the solution is correct by construction at $t = 0$, and the effect of the $\mathcal{O}(\gamma/\Omega)$ errors in the eigenvectors does not become significant until $t \gtrsim 1/\gamma$. 2) In the Markovian limit, where the environment is delta-correlated, the second-order master equation is the exact master equation and of Lindblad form, so the errors introduced by using the perturbative master equation and the post RWA vanish. Issues with the preT RWA, such as the incorrect frequency shifts, may still remain, but they would not be noticed if one is using the master equation phenomenologically. 3) If one rescales the time variable as $\tau = g^2 t$ (where $g = \mathcal{O}(\sqrt{\gamma})$ scales the system-environment coupling) and takes the limit

$g \rightarrow 0$, then in terms of τ again one obtains a second-order master equation of Lindblad form as the exact master equation of the system, which effectively describes the late-time dynamics with vanishing coupling. This will then correspond to the perturbative RWA solution in the same fashion as the previous case.

In actual experiment, then, the RWA and perturbative master equations will make valid predictions as long as the situation is well described by one of the above limits. In most cases where perturbative master equations using the RWA are successful, the relevant limit is probably the third, simply because γ/Ω is extremely small. As we have said, in optical-frequency atomic physics this could be on the order of 10^{-9} . Moreover, we have noted that the timescales are predicted correctly, so in order to uncover these effects one would need to make very high accuracy measurements depending on the details of the density matrix at late times. In other systems, it could be that the environmental temperature is sufficiently high that the dynamics is approximately Markovian and the second mathematical limit above applies. Thus, one can expect these inaccuracies to be of practical importance at low temperature when γ/Ω is still small but measurements are sufficiently precise to resolve $\mathcal{O}(\gamma/\Omega)$ differences. Even in situations where the errors arising from these approximations turn out not to be of direct relevance, there is the benefit that they now are clearly characterized and can be predicted. Furthermore, we have found that they do inform theoretical discussions about the phenomenon of SD.

Having examined the RWA, it is sensible to return to the subject matter of Ch. 2 and 3. In both chapters we use an atom-field interaction Hamiltonian that includes the preT RWA. Because this Hamiltonian is so widely used, it is of some

interest simply to understand the dynamics it generates more completely, as we have sought to do by exploring entanglement dynamics arising from exact solutions with that Hamiltonian. However, one should be cautious applying such solutions to the physical system. As we have noted, the RWA is inherently an approximation useful for weak atom-field coupling. Thus, while the behavior of the exact solutions for large coupling may be of mathematical interest, we do not expect them to make accurate predictions for a physical system which has been approximated using the RWA.

More specifically, we have said that if the constant g scales the atom-field coupling then the RWA misses lowest-order corrections to the state of the closed system that are $\mathcal{O}(g/\Omega)$, while for the open system dynamics the RWA misses lowest order corrections that are $\mathcal{O}(g^2) = \mathcal{O}(\gamma/\Omega)$. This suggests that the new corrections we see in Ch. 2 from using an exact solution will not be larger than the errors introduced by the RWA, and thus the results will not be predictive for a physical atom-field system. Any higher order corrections arising from the use of exact solutions in Ch. 3 would suffer the same fate; however, our interest in that section was in the qualitative features of the entanglement dynamics, which should not be significantly altered. We will not see the large qualitative impact on entanglement dynamics that we saw in Ch. 5, because here there is no relaxation to a steady state and small corrections will not cause qualitative changes.

It should be noted that exact results for the RWA Hamiltonian may be of interest if an interaction of the form given by the RWA arises naturally, rather than as an approximation of weak bilinear coupling of observables. This happens

in the case of the Gardiner-Collett Hamiltonian [59] used to model the coupling between the intracavity field of a high-finesse electromagnetic cavity and external field modes, which takes the form of quantum Brownian motion in the pre-trace RWA. The form of the Gardiner-Collett Hamiltonian is not the result of a RWA and can be derived [46] from a “modes-of-the-universe” approach for a cavity with a partially transmitting mirror in the limit that transmission is weak. So in this case the pre-trace RWA Hamiltonian corresponds to the physical Hamiltonian of an actual system, and the solutions of the master equation have relevance directly, rather than as an approximation.

In both Ch. 3 and 5 we turned to the question of entanglement dynamics of two atoms interacting with a common field. The two-mode model of Ch. 3 represents the most basic model possible in which to examine the effect of atomic separation (since it has no meaningful effect distinct from scaling the coupling with only one mode), yet in examining a number of typical initial conditions we find a great variety of qualitative behavior is possible. In this model some states will undergo SD, while others can maintain entanglement at all times (given the correct atomic spacing). Altering the atomic separation, however, can entirely change these behaviors, and initial conditions for which entanglement was preserved now undergo SD. Indeed, for the classes of initial states we have considered, SD seems to be the generic behavior, with other behaviors only arising for very particular parameter values (i.e., on a set of measure zero in parameter space). Still, at the least it appears that the time at which SD occurs can be strongly influenced through atomic positioning. While the model of Ch. 3 is basic, some aspects of understanding the dynamics are more

complicated, because the lack of irreversible dissipation means that the system does not settle down into any steady state that can then be used to derive late-time behavior.

In Sec. 5.2 we use the weak-coupling master equation to examine the same sort of model with a continuum of field modes, but we improve on all previous examinations insofar as we do not use the RWA. We find results that are in many respects similar to the previous results found using a perturbative master equation and the posT RWA [6, 50, 49], except that our solution includes off-diagonal elements correct to second order, which is not possible with the RWA. We verify, though, that the dynamics seem to be causal in this model and become independent at large separations. For the study of entanglement, however, going beyond the RWA is important. The earlier solutions find that at zero temperature there will be some states that undergo SD while others do not [138, 49, 141]. We derive the correct asymptotic state including contributions neglected in the RWA and find that, in fact, all states experience SD, though closely spaced atoms have a sub-radiant state and entanglement can be quite long lived. At high temperature SD will also be universal. We have primarily characterized the asymptotic late-time entanglement dynamics, since the transient dynamics at earlier times will be quite similar to the RWA model (where the second-order discrepancies won't lead to qualitatively important differences in general). For closely spaced atoms the sub-radiant state has a small dissipation rate that is $\mathcal{O}(\gamma(\Omega r)^2)$, and this can easily lead to entanglement in an intermediate time regime, where other terms have already decayed but sudden death has not occurred.

In fact, we find more generally in Sec. 5.1 that for any two qubit system where interaction occurs only through the environment, using a perturbative master equation with the RWA and a thermal environment will give predictions for the late-time entanglement dynamics that are not correct, even qualitatively. The asymptotic state under those assumptions is constrained to be a Boltzmann state, which is separable and uncorrelated. As a result, such calculations will always predict that SD is universal for any positive temperature [140, 139], and at zero temperature they will predict that SD occurs only for some initial states [138, 49, 141]. We find that the prediction of universal SD at sufficiently high temperature is correct, but at lower temperature these predictions are generally speaking incorrect. The zero-temperature prediction of SD conditional on the initial state is simply an artifact of the approximations used, and this behavior should seemingly occur very rarely in the exact dynamics.

Using the results of [31], we show that the full second-order asymptotic state can be derived for high temperature and zero temperature. At high temperature that state will always be in the interior of the set of separable states, leading to a prediction that all initial states experience SD. At low temperature the asymptotic state could lie either in the entangled states or the interior of the separable states, depending on the details of the particular system, and this would lead to asymptotic entanglement or SD, respectively, for all initial states. Unfortunately, it is unclear how to calculate the asymptotic state at low temperature, except in the special case

that $T = 0$. We find that the condition defining high temperature is

$$\frac{\gamma}{\Omega} \ll \bar{n}(\Omega_n, T)\bar{n}(\Omega_m, T) \quad (6.1)$$

in terms of the thermal average photon number $\bar{n}(\Omega_m, T)$ for an oscillator with the qubit frequency Ω_m (assuming \bar{n} is small in both cases). Note that for optical frequencies $\bar{n} \lesssim 10^{-9}$, placing it in what we are considering here the low temperature regime. Our result that SD is universal at zero temperature for all non-zero separations also adds to the understanding of entanglement dynamics in that it contrasts with the result for linear oscillators [92] where there is asymptotic entanglement when the spacing is small enough.

A number of potential extensions of this work present themselves. The most obvious of these is seeking experimental contexts in which the effects discussed in Ch. 4 and 5 play a larger role. Many optical frequency experiments have long lifetimes so that the corrections we have discussed are very small. In experiments with shorter lifetimes and lower frequencies these corrections would become more important, provided measurements can be made with sufficient precision. Our calculated corrections to, e.g., the steady state, rely on an accurate understanding of the system-environment interaction, so application to other models would rely on these interactions being sufficiently well characterized.

The calculations performed in Sec. 5.2 focused mainly on the situation of two atoms, but the approach (and, indeed, some of the calculation) applies to systems with larger numbers of atoms. It could be applied there to examine superradiance in more detail. With more atoms, one could consider a number of questions related

to the evolution of various sorts of entanglement, entanglement between various possible bi-partitions of the system or higher-order multipartite entanglement, as well as dynamical transfer of entanglement between constituents.

We have focused throughout on the master equation for the density matrix, which allows one to calculate expectations of observables at a single time. In the Markovian limit, all multi-time correlations can be calculated from the master equation using the quantum regression theorem, but in non-Markovian dynamics this is not the case, and the quantum regression theorem will have corrections. One could apply the weak-coupling approach of [31] to that problem and evaluate the effect of the weak-coupling and RWA on predictions for these correlations, which could potentially be considerably different in the non-Markovian case.

Finally, we have used the second-order master equation to derive our results. While we have supplemented it with an alternate derivation of the late-time steady state, our predictions of the transient behavior are still plagued by the second-order inaccuracies we found in the diagonal elements of the density matrix, and we have not found a method of calculating the steady state for low positive temperatures. We have said that fourth-order Liouvillian is required in order to obtain the full second order solution, so another useful extension of this work would be to attempt to derive the necessary matrix elements of the fourth order Liouvillian for weak coupling in order to have a full second order solution for the dynamics.

Bibliography

- [1] A. Einstein, B. Podolsky, and N. Rosen. *Phys. Rev.*, 47:777, 1935.
- [2] A. Abragam. *The principles of nuclear magnetism*. International series of monographs on physics. Clarendon Press, 1961.
- [3] L. Accardi, Y. G. Lu, and I. V. Volovich. *Quantum Theory and Its Stochastic Limit*. Springer, 2002.
- [4] G. S. Agarwal. Rotating-wave approximation and spontaneous emission. *Phys. Rev. A*, 4(5):1778–1781, Nov 1971.
- [5] G. S. Agarwal. Rotating-wave approximation and spontaneous emission. *Phys. Rev. A*, 7(3):1195–1197, Mar 1973.
- [6] G. S. Agarwal. *Quantum statistical theories of spontaneous emission and their relation to other approaches*, volume 70 of *Springer Tracts in Modern Physics*. Springer Berlin / Heidelberg, 1974.
- [7] R. Alicki and K. Lendi. *Quantum Dynamical Semigroups and Applications*. Springer, 2007.
- [8] M. P. Almeida, F. de Melo, M. Hor-Meyll, A. Salles, S. P. Walborn, P. H. Souto Ribeiro, and L. Davidovich. Environment-Induced sudden death of entanglement. *Science*, 316(5824):579–582, April 2007.
- [9] Luigi Amico, Rosario Fazio, Andreas Osterloh, and Vlatko Vedral. Entanglement in many-body systems. *Reviews of Modern Physics*, 80(2):517–60, April 2008.
- [10] C. Anastopoulos and B. L. Hu. Two-level atom-field interaction: Exact master equations for non-markovian dynamics, decoherence, and relaxation. *Phys. Rev. A*, 62(3):033821, Aug 2000.
- [11] C. Anastopoulos, S. Shresta, and B. L. Hu. Quantum entanglement under non-markovian dynamics of two qubits interacting with a common electromagnetic field. 2006.
- [12] C. Anastopoulos, S. Shresta, and B. L. Hu. Non-markovian entanglement dynamics of two qubits interacting with a common electromagnetic field. *Quan. Inf. Proc.*, 8:549–563, 2009.
- [13] Takao Aoki, Barak Dayan, E. Wilcut, W. P. Bowen, A. S. Parkins, T. J. Kippenberg, K. J. Vahala, and H. J. Kimble. Observation of strong coupling between one atom and a monolithic microresonator. *Nature*, 443(7112):671–674, October 2006.

- [14] S. Attal, A. Joye, and C.-A. Pillet. *Open Quantum Systems II: The Markovian Approach*. Springer, 2006.
- [15] I. Bengtsson and K. Życzkowski. *Geometry of Quantum States: An Introduction to Quantum Entanglement*. Cambridge University Press, 2006.
- [16] C.H. Bennett, F. Bessette, G. Brassard, L. Salvail, and J. Smolin. Experimental quantum cryptography. *Journal of cryptology*, 5(1):3–28, 1992.
- [17] C.H. Bennett, G. Brassard, C. Crépeau, R. Jozsa, A. Peres, and W.K. Wootters. Teleporting an unknown quantum state via dual classical and Einstein-Podolsky-Rosen channels. *Phys. Rev. Lett.*, 70(13):1895–1899, 1993.
- [18] C.H. Bennett, G. Brassard, et al. Quantum cryptography: Public key distribution and coin tossing. In *Proceedings of IEEE International Conference on Computers, Systems and Signal Processing*, volume 175. Bangalore, India, 1984.
- [19] B. B. Blinov, D. L. Moehring, L.-M. Duan, and C. Monroe. Observation of entanglement between a single trapped atom and a single photon. *Nature*, 428(6979):153–157, March 2004.
- [20] A. D. Boozer, A. Boca, R. Miller, T. E. Northup, and H. J. Kimble. Reversible state transfer between light and a single trapped atom. *Physical Review Letters*, 98(19):193601, 2007.
- [21] AD Boozer, A Boca, R Miller, TE Northup, and HJ Kimble. Reversible state transfer between light and a single trapped atom. *PHYSICAL REVIEW LETTERS*, 98(19), May 2007.
- [22] S. Bose, I. Fuentes-Guridi, P. L. Knight, and V. Vedral. Subsystem purity as an enforcer of entanglement. *Phys. Rev. Lett.*, 87(5):050401, Jul 2001.
- [23] D. Bouwmeester, J.W. Pan, K. Mattle, M. Eibl, H. Weinfurter, and A. Zeilinger. Experimental quantum teleportation. *Nature*, 390(6660):575–579, 1997.
- [24] H. P. Breuer, D. Burgarth, and F. Petruccione. Non-markovian dynamics in a spin star system: Exact solution and approximation techniques. *Phys. Rev. B*, 70(4):045323, Jul 2004.
- [25] H. P. Breuer and F. Petruccione. Destruction of quantum coherence through emission of bremsstrahlung. *Phys. Rev. A*, 63(3):032102, Feb 2001.
- [26] H. P. Breuer and F. Petruccione. *The Theory of Open Quantum Systems*. Oxford University Press, Oxford, 2002.

- [27] K.-A. Brickman, P. C. Haljan, P. J. Lee, M. Acton, L. Deslauriers, and C. Monroe. Implementation of grover’s quantum search algorithm in a scalable system. *Physical Review A (Atomic, Molecular, and Optical Physics)*, 72(5):050306–4, November 2005.
- [28] V. Buzek, H. Moya-Cessa, P. L. Knight, and S. J. D. Phoenix. Schrödinger-cat states in the resonant jaynes-cummings model: Collapse and revival of oscillations of the photon-number distribution. *Phys. Rev. A*, 45(11):8190–8203, Jun 1992.
- [29] V. P. Bykov and V. I. Tatarskii. Causality violation in the glauber theory of photodetection. *Phys. Lett. A*, 136(1-2):77 – 80, 1989.
- [30] C. Cohen-Tannoudji, J. Dupont-Roc, and G. Grynberg. *Atom-Photon Interactions: Basic Processes and Applications*. Wiley-Interscience, 1992.
- [31] C. H. Fleming. *Non-Markovian Dynamics of Open Quantum Systems*. PhD thesis, University of Maryland, College Park, 2011. in preparation.
- [32] H. J. Carmichael. *Statistical methods in quantum optics I*. Springer, New York, 1999.
- [33] Stanley Chan, M. D. Reid, and Z. Ficek. Entanglement evolution of two remote and non-identical Jaynes-Cummings atoms. *Journal of Physics B: Atomic, Molecular and Optical Physics*, 42(6):065507, 2009.
- [34] Man-Duen Choi. Completely positive linear maps on complex matrices. *Linear Algebra and its Applications*, 10(3):285 – 290, 1975.
- [35] D. Chruściński and A. Kossakowski. Non-markovian quantum dynamics: Local versus nonlocal. *Phys. Rev. Lett.*, 104(7):070406, Feb 2010.
- [36] J. I. Cirac and P. Zoller. Quantum computations with cold trapped ions. *Phys. Rev. Lett.*, 74(20):4091–4094, May 1995.
- [37] A. Clerk and J. Sipe. Nonlocality and the rotating wave approximation. *Foundations of Physics*, 28:639–651, 1998.
- [38] G. Compagno, R. Passante, and F. Persico. *Atom-field interactions and dressed atoms*. Cambridge Univ Press, 1995.
- [39] M. T. Cunha. The geometry of entanglement sudden death. *New J. Phys.*, 9(7):237, 2007.
- [40] E. B. Davies. Markovian master equations. *Comm. Math. Phys.*, 39:91–110, 1974.
- [41] E. B. Davies. Markovian master equations II. *Math. Ann.*, 219:147–158, 1976.

- [42] E. B. Davies. Quantum dynamical semigroups and the neutron diffusion equation. *Rep. Math. Phys.*, 11(2):169 – 188, 1977.
- [43] I. de Vega and D. Alonso. Non-markovian reduced propagator, multiple-time correlation functions, and master equations with general initial conditions in the weak-coupling limit. *Phys. Rev. A*, 73(2):022102, Feb 2006.
- [44] R. H. Dicke. Coherence in spontaneous radiation processes. *Phys. Rev.*, 93(1):99, Jan 1954.
- [45] I. Dolce, R. Passante, and F. Persico. The limits of the rotating wave approximation in electromagnetic field propagation in a cavity. *Phys. Lett. A*, 355(2):152 – 155, 2006.
- [46] S. M. Dutra and G. Nienhuis. Derivation of a hamiltonian for photon decay in a cavity. *Journal of Optics B: Quantum and Semiclassical Optics*, 2(5):584, 2000.
- [47] S.M. Dutra. *Cavity quantum electrodynamics: the strange theory of light in a box*. Wiley-Interscience, 2005.
- [48] D Felinto, CW Chou, J Laurat, EW Schomburg, H De Riedmatten, and HJ Kimble. Conditional control of the quantum states of remote atomic memories for quantum networking. *NATURE PHYSICS*, 2(12):844–848, December 2006.
- [49] Z. Ficek and R. Tanaś. Dark periods and revivals of entanglement in a two-qubit system. *Phys. Rev. A*, 74(2):024304, Aug 2006.
- [50] Z. Ficek and R. Tanas. Entangled states and collective nonclassical effects in two-atom systems. *Phys. Rep.*, 372(5):369 – 443, 2002.
- [51] Zbigniew Ficek and Ryszard Tanas. Delayed sudden birth of entanglement. *Physical Review A (Atomic, Molecular, and Optical Physics)*, 77(5):054301–4, May 2008.
- [52] M. Fleischhauer. Quantum-theory of photodetection without the rotating wave approximation. *J. Phys. A*, 31(2):453, 1998.
- [53] C. H. Fleming and B. L. Hu. The evolution of general systems in non-markovian environments. *in preparation*, 2011.
- [54] C. H. Fleming, B. L. Hu, and A. Roura. Decoherence strength of multiple non-markovian environments. *submitted to Phys. Rev. E*, 2010.
- [55] C. H. Fleming, B. L. Hu, and A. Roura. Initial state preparation with dynamically generated system-environment correlations. 2011.
- [56] C. H. Fleming, A. Roura, and B. L. Hu. Exact analytical solutions to the master equation of quantum brownian motion for a general environment. *accepted for publication, Ann. Phys. (NY)*, 2010.

- [57] C. H. Fleming, A. Roura, and B. L. Hu. Quantum brownian motion of multipartite systems with entanglement dynamics. *in preparation*, 2011.
- [58] G. W. Ford and R. F. O’Connell. The rotating wave approximation (rwa) of quantum optics: serious defect. *Physica A*, 243(3-4):377 – 381, 1997.
- [59] C. W. Gardiner and M. J. Collett. Input and output in damped quantum systems: Quantum stochastic differential equations and the master equation. *Phys. Rev. A*, 31(6):3761–3774, Jun 1985.
- [60] C.C. Gerry and P. L. Knight. *Introductory Quantum Optics*. Cambridge University Press, 2005.
- [61] E. Geva, E. Rosenman, and D. Tannor. On the second-order corrections to the quantum canonical equilibrium density matrix. *J. Chem. Phys.*, 113(4):1380, 2000.
- [62] D. Giulini, E. Joos, C. Kiefer, J. Kupsch, L. O. Stamatescu, and H. D. Zeh. *Decoherence and the Appearance of a Classical World in Quantum Theory*. Springer-Verlag, Berlin, 1996.
- [63] R. J. Glauber. Coherent and incoherent states of the radiation field. *Phys. Rev.*, 131(6):2766–2788, Sep 1963.
- [64] R. J. Glauber. The quantum theory of optical coherence. *Phys. Rev.*, 130(6):2529–2539, Jun 1963.
- [65] V. Gorini, A. Kossakowski, and E. C. G. Sudarshan. Completely positive dynamical semigroups of n-level systems. *J. Math. Phys.*, 17(5):821–825, 1976.
- [66] L.K. Grover. Quantum mechanics helps in searching for a needle in a haystack. *Physical review letters*, 79(2):325–328, 1997.
- [67] L. Gurvits. Classical deterministic complexity of Edmonds’ Problem and quantum entanglement. In *Proceedings of the thirty-fifth annual ACM symposium on Theory of computing*, pages 10–19. ACM, 2003.
- [68] P. Haikka and S. Maniscalco. Non-Markovian dynamics of a damped driven two-state system. *Phys. Rev. A*, 81(5):052103, May 2010.
- [69] K. Hammerer, M. Wallquist, C. Genes, M. Ludwig, F. Marquardt, P. Treutlein, P. Zoller, J. Ye, and H. J. Kimble. Strong coupling of a mechanical oscillator and a single atom. *Physical Review Letters*, 103(6):063005, 2009.
- [70] S. Haroche and J.M. Raimond. *Exploring the quantum: atoms, cavities and photons*. Oxford graduate texts in mathematics. Oxford University Press, 2006.

- [71] Michal Horodecki, Pawel Horodecki, and Ryszard Horodecki. Separability of mixed states: necessary and sufficient conditions. *Phys. Lett. A*, 223(1-2):1–8, November 1996.
- [72] Pawel Horodecki. Separability criterion and inseparable mixed states with positive partial transposition. *Phys. Lett. A*, 232(5):333–339, August 1997.
- [73] R. Horodecki, P. Horodecki, M. Horodecki, and K. Horodecki. Quantum entanglement. *Rev. Mod. Phys.*, 81(2):865–942, Jun 2009.
- [74] B. L. Hu, J. P. Paz, and Y. Zhang. Quantum brownian motion in a general environment: Exact master equation with nonlocal dissipation and colored noise. *Phys. Rev. D*, 45(8):2843–2861, Apr 1992.
- [75] K. Życzkowski, P. Horodecki, M. Horodecki, and R. Horodecki. Dynamics of quantum entanglement. *Phys. Rev. A*, 65(1):012101, Dec 2001.
- [76] R. S. Ingarden, A. Kossakowski, and M. Ohya. *Information Dynamics and Open Systems: Classical and Quantum Approach*. Kluwer Academic, Dordrecht, 1997.
- [77] J. Gea-Banacloche. *Phys. Rev. Lett.*, 65:3385, 1990.
- [78] J. Gea-Banacloche. *Phys. Rev. A*, 47:2221, 1993. 44, 5913 (1991).
- [79] J. S. Bell. *Physics*, 1:195–200, 1964.
- [80] Jun Jing, Zhi-Guo Lu, and Zbigniew Ficek. Breakdown of the rotating-wave approximation in the description of entanglement of spin-anticorrelated states. *Physical Review A (Atomic, Molecular, and Optical Physics)*, 79(4):044305–4, April 2009.
- [81] N. Kampen and I. Oppenheim. Langevin and master equation in quantum mechanics. *J. Stat. Phys.*, 87:1325–1334, 1997.
- [82] N. G. Van Kampen. *Adv. Chem. Phys.*, 34:245–309, 2007.
- [83] M. Keller, B. Lange, K. Hayasaka, W. Lange, and H. Walther. Deterministic coupling of single ions to an optical cavity. *Applied Physics B: Lasers and Optics*, 76(2):125–128, February 2003.
- [84] Matthias Keller, Birgit Lange, Kazuhiro Hayasaka, Wolfgang Lange, and Herbert Walther. Continuous generation of single photons with controlled waveform in an ion-trap cavity system. *Nature*, 431(7012):1075–1078, October 2004.
- [85] M. S. Kim, Jinhyoung Lee, D. Ahn, and P. L. Knight. Entanglement induced by a single-mode heat environment. *Physical Review A*, 65(4):040101, April 2002.

- [86] A. B. Klimov, I. Sainz, and S. M. Chumakov. Resonance expansion versus the rotating-wave approximation. *Physical Review A*, 68(6):063811, December 2003.
- [87] A. Kossakowski. On quantum statistical mechanics of non-hamiltonian systems. *Rep. Math. Phys.*, 3(4):247 – 274, 1972.
- [88] T. D. Ladd, F. Jelezko, R. Laflamme, Y. Nakamura, C. Monroe, and J. L. O’Brien. Quantum computers. *Nature*, 464(7285):45–53, March 2010.
- [89] J. Laurat, K. S. Choi, H. Deng, C. W. Chou, and H. J. Kimble. Heralded entanglement between atomic ensembles: Preparation, decoherence, and scaling. *Physical Review Letters*, 99(18):180504, November 2007.
- [90] M. Lax. Formal theory of quantum fluctuations from a driven state. *Phys. Rev.*, 129(5):2342, 1963.
- [91] R. H. Lehmborg. Radiation from an n -atom system. i. general formalism. *Phys. Rev. A*, 2(3):883–888, Sep 1970.
- [92] S. Y. Lin and B. L. Hu. Temporal and spatial dependence of quantum entanglement from a field theory perspective. *Phys. Rev. D*, 79(8):085020, Apr 2009.
- [93] G. Lindblad. On the generators of quantum dynamical semigroups. *Comm. Math. Phys.*, 48:119–130, 1976.
- [94] G. Lindblad. *Non-Equilibrium Entropy and Irreversibility*. D. Reidel, Dordrecht, 1983.
- [95] M. A. Nielsen and I. L. Chuang. *Quantum Computation and Quantum Information*. Cambridge University Press, Cambridge, England, 2000.
- [96] H. Mabuchi and H. J. Kimble. Atom galleries for whispering atoms: binding atoms in stable orbits around an optical resonator. *Optics Letters*, 19(10):749–751, May 1994.
- [97] Sabrina Maniscalco, Francesco Francica, Rosa L. Zaffino, Nicola Lo Gullo, and Francesco Plastina. Protecting entanglement via the quantum zeno effect. *Physical Review Letters*, 100(9):090503–4, March 2008.
- [98] P. Maunz, T. Puppe, I. Schuster, N. Syassen, P. W. H. Pinkse, and G. Rempe. Normal-mode spectroscopy of a single-bound-atom-cavity system. *Phys. Rev. Lett.*, 94(3):033002, 2005.
- [99] P. Maunz, T. Puppe, I. Schuster, N. Syassen, P.W.H. Pinkse, and G. Rempe. Cavity cooling of a single atom. *Nature*, 428:50–52, 2004.

- [100] J. McKeever, A. Boca, A. D. Boozer, J. R. Buck, and H. J. Kimble. Experimental realization of a one-atom laser in the regime of strong coupling. *Nature*, 425(6955):268271, 2003.
- [101] J. McKeever, A. Boca, AD Boozer, JR Buck, and HJ Kimble. Experimental realization of a one-atom laser in the regime of strong coupling. *Nature*, 425(6955):268–271, 2003.
- [102] P. W. Milonni, D. F. V. James, and H. Fearn. Photodetection and causality in quantum optics. *Phys. Rev. A*, 52(2):1525–1537, Aug 1995.
- [103] D. L. Moehring, P. Maunz, S. Olmschenk, K. C. Younge, D. N. Matsukevich, L.-M. Duan, and C. Monroe. Entanglement of single-atom quantum bits at a distance. *Nature*, 449(7158):68–71, 2007.
- [104] T. Mori and S. Miyashita. Dynamics of the density matrix in contact with a thermal bath and the quantum master equation. *J. Phys. Soc. Jap.*, 77(12):124005, 2008.
- [105] S. Nakajima. On quantum theory of transport phenomena. *Prog. Theo. Phys.*, 20(6):948–959, 1958.
- [106] Stefan Nussmann, Markus Hijlkema, Bernhard Weber, Felix Rohde, Gerhard Rempe, and Axel Kuhn. Submicron positioning of single atoms in a microcavity. *Phys. Rev. Lett.*, 95(17):173602, 2005.
- [107] J. P. Paz and A. J. Roncaglia. Dynamics of the entanglement between two oscillators in the same environment. *Phys. Rev. Lett.*, 100(22):220401, Jun 2008.
- [108] J. P. Paz and A. J. Roncaglia. Dynamical phases for the evolution of the entanglement between two oscillators coupled to the same environment. *Phys. Rev. A*, 79(3):032102, Mar 2009.
- [109] Asher Peres. Separability criterion for density matrices. *Phys. Rev. Lett.*, 77(8):1413, 1996.
- [110] M. B. Plenio. Logarithmic negativity: A full entanglement monotone that is not convex. *Physical Review Letters*, 95(9):090503, 2005.
- [111] M. B. Plenio and S. Virmani. An introduction to entanglement measures. 2005.
- [112] W. T. Pollard, A. K. Felts, and R. A. Friesner. The redfield equation in condensed-phase quantum dynamics. *Adv. Chem. Phys.*, 93:77–134, 1997.
- [113] J. M. Raimond, M. Brune, and S. Haroche. Manipulating quantum entanglement with atoms and photons in a cavity. *Rev. Mod. Phys.*, 73(3):565–582, Aug 2001.

- [114] A. K. Rajagopal and R. W. Rendell. Decoherence, correlation, and entanglement in a pair of coupled quantum dissipative oscillators. *Physical Review A*, 63(2):022116, January 2001.
- [115] S. J. D. Phoenix and P. L. Knight. *Phys. Rev. A*, 44:6023, 1991. *Phys. Rev. Lett.* 66, 2833 (1991).
- [116] M. Scala, B. Militello, A. Messina, S. Maniscalco, J. Piilo, and K. A. Suominen. Cavity losses for the dissipative jaynes–cummings hamiltonian beyond rotating wave approximation. *J. Phys. A*, 40(48):14527, 2007.
- [117] M. Scala, B. Militello, A. Messina, J. Piilo, and S. Maniscalco. Microscopic derivation of the jaynes-cummings model with cavity losses. *Phys. Rev. A*, 75(1):013811, Jan 2007.
- [118] E. Schrödinger. Die gegenwärtige Situation in der Quantenmechanik. *Naturwissenschaften*, 23(49):823–828, 1935.
- [119] P.W. Shor. Algorithms for quantum computation: discrete logarithms and factoring. In *Foundations of Computer Science, 1994 Proceedings., 35th Annual Symposium on*, pages 124–134. IEEE, 1994.
- [120] W. P. Smith, J. E. Reiner, L. A. Orozco, S. Kuhr, and H. M. Wiseman. Capture and release of a conditional state of a cavity QED system by quantum feedback. *Physical Review Letters*, 89(13):133601, 2002.
- [121] G. W. Stewart. *Matrix Algorithms: Eigensystems*. SIAM, 2001.
- [122] W. T. Strunz and T. Yu. Convolutionless non-markovian master equations and quantum trajectories: Brownian motion. *Phys. Rev. A*, 69(5):052115, May 2004.
- [123] S. Swain. Master equation derivation of quantum regression theorem. *J. Phys. A*, 14(10):2577, 1981.
- [124] R Tanas and Z Ficek. Entangling two atoms via spontaneous emission. *Journal of Optics B: Quantum and Semiclassical Optics*, 6(3):S90–S97, 2004.
- [125] R Tanas and Z Ficek. Stationary two-atom entanglement induced by nonclassical two-photon correlations. *Journal of Optics B: Quantum and Semiclassical Optics*, 6(6):S610–S617, 2004.
- [126] Takashi Taneichi and Takayoshi Kobayashi. Enhanced entanglement of two atoms confined in a multi-mode optical cavity. *Chemical Physics Letters*, 378(5-6):576–581, September 2003.
- [127] V. I. Tatarskii. Corrections to the theory of photocounting. *Phys. Lett. A*, 144(8-9):491 – 499, 1990.

- [128] T. E. Tessier, I. H. Deutsch, A. Delgado, and I. Fuentes-Guridi. Entanglement sharing in the two-atom Tavis-Cummings model. *Physical Review A*, 68(6):062316, December 2003. Copyright (C) 2009 The American Physical Society; Please report any problems to prola@aps.org.
- [129] G. Vidal and R. F. Werner. Computable measure of entanglement. *Phys. Rev. A*, 65(3):032314, Feb 2002.
- [130] M. Wallquist, K. Hammerer, P. Zoller, C. Genes, M. Ludwig, F. Marquardt, P. Treutlein, J. Ye, and H. J. Kimble. Single-atom cavity QED and optomechanics. *Physical Review A*, 81(2):023816, February 2010.
- [131] D. F. Walls and G. J. Milburn. *Quantum Optics*. Springer-Verlag, Berlin Heidelberg, 1995.
- [132] U. Weiss. *Quantum Dissipative Systems*. World Scientific, Singapore, 1993.
- [133] B. J. West and K. Lindenberg. On the rotating wave approximation. *Phys. Lett. A*, 102(4):189 – 193, 1984.
- [134] W. K. Wootters. Entanglement of formation of an arbitrary state of two qubits. *Phys. Rev. Lett.*, 80(10):2245–2248, Mar 1998.
- [135] Y. J. Yan and R. X. Xu. Quantum mechanics of dissipative systems. *Ann. Rev. Phys. Chem.*, 56(1):187–219, 2005.
- [136] M. Yönaç, T. Yu, and J. H. Eberly. Sudden death of entanglement of two jaynes–cummings atoms. *J. Phys. B*, 39(15):S621, 2006.
- [137] M. Yönaç, T. Yu, and J. H. Eberly. Pairwise concurrence dynamics: a four-qubit model. *J. Phys. B*, 40(9):S45, 2007.
- [138] T. Yu and J. H. Eberly. Finite-time disentanglement via spontaneous emission. *Phys. Rev. Lett.*, 93(14):140404, Sep 2004.
- [139] T. Yu and J. H. Eberly. Many-Body separability of warm qubits. July 2007.
- [140] T. Yu and J. H. Eberly. Negative entanglement measure, and what it implies. *J. Mod. Opt.*, 54(13-15):2289–2296, 2007.
- [141] T. Yu and J. H. Eberly. Sudden Death of Entanglement. *Science*, 323(5914):598–601, 2009.
- [142] W. H. Zurek. Decoherence, einselection, and the quantum origins of the classical. *Rev. Mod. Phys.*, 75(3):715–775, May 2003.
- [143] R. Zwanzig. Ensemble method in the theory of irreversibility. *J. Chem. Phys.*, 33(5):1338–1341, 1960.
- [144] R. Zwanzig. *Nonequilibrium Statistical Mechanics*. Oxford University Press, Oxford, 2001.